IONIZATION IN OXYGEN

being a thesis on

the measurement of ionization and attachment coefficients in low pressure oxygen discharges

by

Anna Thevarthundiyil Thomas M.A.

and

submitted to the University of Keele in candidature for the degree of Ph.D.

Department of Physics,
University of Keele.

May 1966

TEXT CUT OFF IN THE ORIGINAL

ACKNOWLEDGEMENTS

I wish to express my gratitude to

Professor D. J. E. Ingram for the use of the laboratories and research facilities,

Dr D. Elwyn Davies for his helpful guidance and useful discussions at all stages of this work,

All my colleagues in the Physics Department for friendly and helpful discussions,

Dr B. P. Betts for assistance at all stages of this work,

Dr H. H. Greenwood, Mr J. Tharu and Mrs J. Hollis for advice and help with computation,

Mr S. Thomas for kindly preparing some diagrams,

The technical staff of the Physics Department for their valuable assistance, especially in the photographic work,

Miss Kay B. Davies for kindly helping with the preparation of this thesis,

My parents but for whose encouragement my course at Keele would not have been possible,

The University of Keele for the award of a Research Studentship and the British Council for a Travel Grant.

SYNOPSIS

Ionization processes in oxygen have been studied using a Townsend type apparatus using electron swarms of mean energy of about a few electron volts. From a measurement of currents and gap distances the ionization and attachment coefficients have been calculated using the steady state current growth equation, while breakdown voltage measurements have enabled the evaluation of the secondary coefficient.

As it is well known that the ionization coefficients depend very much on the gas used and that even traces of another gas can lead to quite erroneous values of the coefficients, an ultrahigh vacuum system was designed and constructed in glass. The background pressures were less than 10^{-8} torr in the experimental tube while the experimental gas pressures were of the order of a few torr. The oxygen was initially produced from the electrolysis of $Ba(OH)_2$ in distilled water, but since the silver diffusion tube meant to be used in conjunction with it to purify the oxygen was found to be almost inoperable, spectroscopically pure oxygen supplied by BOC Ltd. was used for most of the work after further purification in freezing traps cooled by liquid nitrogen.

The experimental tubes were all made of glass while the electrodes were evaporated gold films on glass substrates in the first four tubes and solid platinum in the final tube. The gap distance could be altered magnetically from the outside by means of iron slugs fixed to the electrode assembly, and a guard ring around the cathode

ensured uniform field conditions..

Vibron and Keithly electrometers were used to measure the currents of the order of 10^{-11} A, while the pressure was measured on an oil manometer and the gap distance could be measured accurately by means of a travelling microscope. A bank of 120 V dry batteries supplied the stable voltage necessary and an accurate potentiometer was used in conjunction with a resistance chain to measure it to 0·1 V.

An analysis was formulated to determine the ionization and attachment coefficients, α and η, from current growth equations and an IBM 1620 computer was used to simplify the calculations.

α/p values have been obtained for $50 < E/p < 250$ V/cm torr and compared with other available values; the agreement is reasonably good being approximately 10% lower than the previous values. η/p is found to reduce to practically zero at about 80 V/cm torr which could indicate the presence of a photodetachment process. The breakdown voltages and the corresponding secondary coefficients have also been measured in the range $0{\cdot}1 < pd < 5$ cm torr.

CONTENTS

CHAPTER 1

FUNDAMENTAL PROCESSES IN GAS DISCHARGES

1.1 Introduction

A gas is an almost perfect insulator under normal conditions, but its insulating properties break down under large enough electric stresses. The transition of a gas from an insulating to an almost perfectly conducting state and allied phenomena, are of great interest to the physicist as well as the electrical engineer.

The passage of electricity through gases is best explained by assuming that oppositely charged ions are produced in the gas by the action of various agencies (i.e. ionization), and that these ions convey the current through the gas by their motion, under the action of an electrostatic field. These ions interact with neutral gas molecules and with solid surfaces with which they come into contact. The production, motion and interactions of these ions constitute the basic phenomena of gas discharge physics and are described in this first chapter.

1.2 Ionization Processes

Ionization processes can be broadly classified into two groups: gaseous processes and cathodic processes.

1.2.1 Gaseous Processes

a Electron Collisions with Gas Atoms and Molecules

Collisions between electrons and molecules can be

elastic or inelastic. If the colliding electron does not possess sufficient energy, eV_i, to ionize a molecule which is in its ground state (where V_i is the ionization potential of the gas atom or molecule), or sufficient energy eV_e to excite a molecule (V_e being the excitation potential of the gas atom or molecule), the collision will be elastic; the kinetic energy is conserved, while the internal energies remain the same. Assuming a Maxwellian distribution of energies for the molecules, Cravath (1) showed that an electron of mass m lost approximately $2 \cdot 66 \frac{m}{M}$ of its energy in an elastic collision with a molecule of mass M.

The probability of an electron exciting a molecule is a maximum when the electron energy is slightly above the excitation energy; and an excited molecule produced in a collision may, in a second collision with another low energy electron, be ionized. Thus there is a finite probability of ionization even when the electronic energy $\frac{1}{2} mu^2$ is less than eV_i. Such ionization by double impact of low energy electrons is more likely in gases which have metastable states, because metastables are more likely to survive in an excited state until the second collision - metastables having a mean life-time as high as 0.1 sec compared with about 10^{-8} sec for an ordinary excited state.

When the electron energy exceeds eV_i, an ionization can take place. The probability of ionization in such cases is a function of electron energy and is zero at an electron energy equal to the ionization energy, eV_i. The probability rises thereafter with electron energy up to

about 100 eV and then tends to fall off (2,3). This process, giving rise to a positive ion and two slow electrons, is by far the most important process in gas discharge physics.

b Ion Collisions with Gas Atoms and Molecules

While it was recognized from fairly early days that positive ions could ionize gases by collision, the mechanism of this is still not very clear. Thomson pointed out in 1912 (4) that the energy of the ions would have to be of the order of thousands of electron volts before they could ionize ordinary gas atoms. Although subsequent work, culminating in that of Varney (5) has established that this process can set in at very much lower voltages, it is still an improbable agency for the production of ionization in ordinary low pressure discharges since the mean energy of positive ions rarely exceeds a few electron volts.

When a positive ion captures an electron, the neutral molecule produced may have a high velocity and hence cause ionization as pointed out by Kallman and Rosen (6). The contribution of this process to the discharges discussed in this work is thought to be negligible.

c Photon Collisions with Gas Atoms and Molecules

When a photon is incident on a gas molecule, and $h\nu$, its energy, is greater than eV_i, either all of the energy could be absorbed resulting in the emission of a photoelectron, or the photon could be scattered knocking off a recoil electron from the molecule (7). Photoionization may be represented by the equation,

$$A + h\nu \longrightarrow A^{+} + e$$

It is apparent that this process involves only two end products as opposed to the three that are involved in an atom-electron collision resulting in ionization. Because of this, a photon has a maximum probability of ionization at a certain critical value of 0·1 to 1 eV above the minimum energy required for it. The actual probability will depend upon the wavelength of the radiation, and the nature and density of the gas concerned, and is usually expressed as a coefficient of absorption of the radiation in the gas.

If the photcn energy is less than eV_i, it may still produce ionization in the gas, but naturally this will have to be in stages and can be important only when the gas has metastable states, e.g. in mercury (~~8~~). If the photon energy is very much greater than eV_i, a different phenomenon occurs, since the larger part of the energy of the photon is given to liberate a firmly bound electron (from an inner shell) and the balance of energy is used up as the kinetic energy of the liberated electron.

d <u>Excited and Metastable Atom Collisions with Gas Atoms and Molecules</u>

While ionization by collision of neutral atoms is not an important process, collisions involving metastable atoms may be. The importance of such processes in gas mixtures where one gas has a metastable level lying above the ionization level of the other, is illustrated very well in the reaction which occurs in a mixture of helium and argon gases:

Fig 1.

Energy Diagram of Electrons in a Metal.

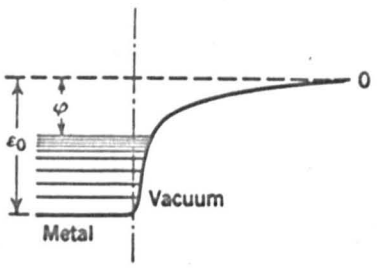

a. In vacuum.

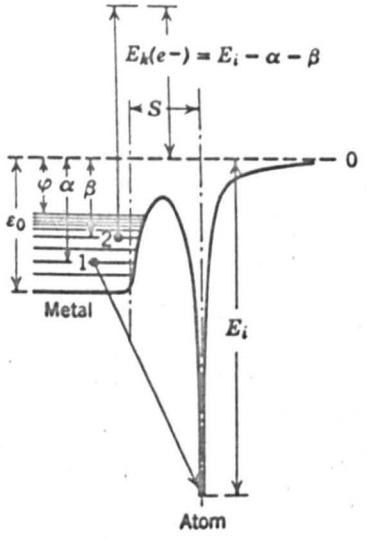

b. At the approach of a positive ion.

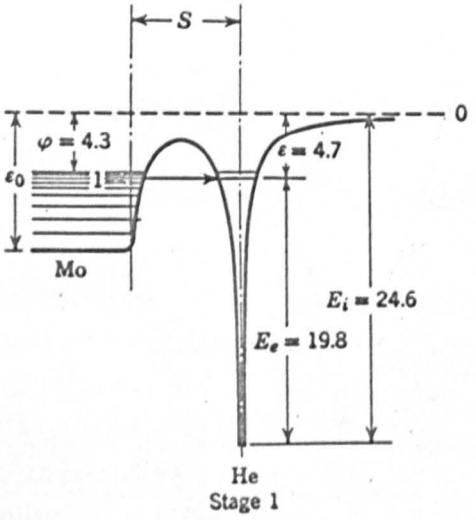

c. First stage of Auger process.

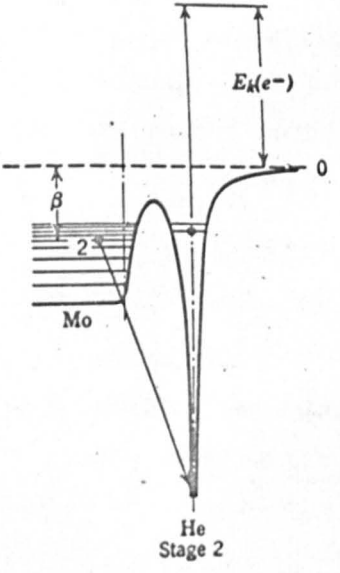

d. Second stage of Auger process.

$$He_m^* + A \longrightarrow He + A^+ + e$$

He_m^* being a helium atom in a metastable excited state. This process known as the Penning effect, explains why the highest gas purity should be aimed at in experiments to study the properties of inert gases. A similar sort of reaction can take place in pure gases also, especially if V_i is about $2V_e$. In helium the reaction would be:

$$He_m^* + He_m^* \longrightarrow He + He^+ + e$$

However, this process is detectable only when there is a high concentration of metastable states.

1.2.2 Electrode Processes

If a free electron in a metal has sufficient energy to overcome the potential barrier, it may escape into the space above the metal and can then take part in a gas discharge. But since the Fermi-Dirac distribution of energies for electron gases in metals predicts that very few electrons at room temperatures actually have energies above ϵ_m, the maximum at 0^oK, the number of electrons coming out of a metal under normal conditions would be almost zero, unless there is an external supply of energy. Several ways in which this extra energy may be acquired by the electrons are described in this section.

a Secondary Electron Emission

The electrons in a metal may be given sufficient energy to overcome the potential barrier shown in fig 1a and so escape from the surface, by simply bombarding the metal with charged particles of sufficient kinetic energy.

Consider a beam of primary electrons having an energy of several hundred electron volts, incident on a metal surface. Some of these primaries will be elastically reflected while some will penetrate into the solid and will lose energy by exciting lattice electrons into higher energy levels. The electrons whose energy has been increased, may then move towards the surface and could escape as secondary electrons. Also a primary electron could enter the metal, lose some of its energy and then escape from the metal. Thus it is necessary to distinguish between these three categories of secondary electrons.

Work is going on at Keele to enable the nature of secondary electron emission to be more fully understood. In the work which is described later in this thesis, secondary electron emission does not produce an appreciable number of electrons in the gas discharge.

b Emission due to the Incidence of Positive Ions

When positive ions impinge upon the surface of a solid, charged and uncharged particles may be emitted. The uncharged particles are often molecules of gas which were in contact with the solid surface, or they may be atoms actually sputtered from the surface.

The charged particles are mostly slow electrons and sometimes negative ions or reflected positive ions. The mechanism of energy transfer is not certain, but it does seem to depend upon the kinetic energy of the ion in some cases and on the potential energy in others. According to Hagstrum (9) ejection of electrons due to the potential

energy of the ion (kinetic energy assumed zero) from metals involves the electronic interaction between the incoming ion and the conduction electrons of the metal while the ion is at a distance of a few Angstroms from the surface.

Figure 1b shows the electron energy diagram for a metal which is modified by the approach of the ion at a few Angstroms distance. This ion is likely to be neutralized in a "direct Auger neutralization" in this condition by electron 1 tunnelling through the reduced potential barrier directly to the ground state of the ion and giving up its excess energy to another electron, 2, in the conduction band. If the minimum energy required by electrons 1 and 2 to escape from the metal is α and β, and E_i is the ionization energy of the incident atom, then the second electron would obviously be ejected with kinetic energy $(E_i - \alpha - \beta)$. It is apparent that the production of an external secondary electron is energetically impossible if E_i is less than 2φ, though neutralization takes place almost invariably if E_i is greater than φ, where φ is the minimum value of α and β (see also section 1.2.2c).

Neutralization can also take place in a two stage Auger process. This depends on the existence of an ionic metastable level which has the same energy as some level ε in the conduction band. Here electron 1 neutralises the ion but leaves it in an excited state, so that when the atom is de-excited, electron 2 tunnels to the ground state of the atom and gives its energy to the metastable electron which is ejected. The energy requirement in

this case is $E_i > \mathcal{E} + \varphi$.

It would appear from this discussion that the secondary electron yield would depend primarily on the excitation energy of the ion. However, emission due to ions with E_i less than 2φ can only be kinetic. As the kinetic energy increases, the electron emission increases until the emission due to kinetic energy predominates, becoming quite important when the energy is a few thousand electron volts. An explanation of emission under these conditions has been given by Kapitza (10), who suggests intense local heating of the surface at the incidence of the ion which gives rise to thermionic emission.

c Emission due to the Photoelectric Effect

In order to explain the liberation of electrons from metals by photons, it is convenient to refer again to fig 1a. Considering an electron of thermal energy ϵ_i within the metal, before it can escape it will have to be given a quantum of energy $h\nu$ such that its total energy $(\epsilon_i + h\nu)$ is greater than the work ϵ_o which must be done in overcoming the surface attractive forces. Any excess energy will appear as the kinetic energy of the liberated photoelectrons (11,12).

$$\frac{1}{2} mu^2 = h\nu + \epsilon_i - \epsilon_o$$

For a given radiation, the maximum value of this energy will be at $\epsilon_i = \epsilon_m$ and hence, the very minimum extra energy required by an electron to escape is $(\epsilon_o - \epsilon_m) = e\phi$, which is a characteristic of the metal, ϕ being known as the work function.

The probability of liberating electrons from the metal increases with photon energy, and sometimes electrons from the inner shells of the atoms may even be ejected, which having much larger velocities, are capable of producing further secondary electrons in their paths in the metal, and so increase the overall yield of secondary electrons per photon from the metal.

d Emission due to the Incidence of Excited Atoms

Emission from surfaces due to the incidence of atoms in the normal excited state does not contribute very much to any gas discharge, because their lifetime is too short. Atoms in metastable states are, however, capable of ejecting electrons from a surface, provided that their excitation energy is sufficiently high. The mechanism here does not necessarily involve Auger de-excitation. Under suitable conditions excited electrons may tunnel to an unfilled level in the conduction band in the metal surface with the formation of a ground state ion which can undergo Auger neutralization. Stebbing (13) and Hasted (14) have measured secondary yields for helium metastable atoms on different metal surfaces.

The ejection of secondaries from surfaces by metastable atoms can be important since they are uncharged and cannot be swept away from any region by electric fields. Thus they may diffuse to a surface which is inaccessible to ions and cause secondary emission. In oxygen discharges this is not a serious hazard but in discharges involving inert gases, mercury etc, metastables contribute a great deal towards the total secondary electron emission.

e Emission due to the Thermionic Effect

Even though it was known as early as 1885 that hot bodies emit negative charges, it was O.W. Richardson in 1912 (15) who first developed a theory relating the current density to the temperature and work function of the emitter. His equation for the current density I, derived on the basis of classical thermodynamics is

$$I = AT^2 e^{-e\phi/kT}$$

where A is a constant and kT is the equipartition energy at the absolute temperature T. Later it was found that a treatment of the problem on quantum mechanical principles also gave a similar relationship (16). The work function has the same significance and value here, as in the photoelectric phenomenon.

f Emission due to Electric Fields

The effect of a high electric field on the potential well is to reduce its thickness, so that electrons below the Fermi level can "tunnel" through the barrier. Fowler and Nordheim (17) have investigated this wave mechanical property and have obtained an expression which shows that the field required to give a current of the order of micro-amps from a metal surface is of the order of 10^7 V/cm. In fact, fields of the order of 10^6 V/cm are sufficient to remove electrons from electrodes in vacuum at room temperatures. Fields of this order are not ordinarily met in gas discharges, but field emission is important in the case of cathode surfaces with small projections which could give rise to localised intense fields and could become emission centres.

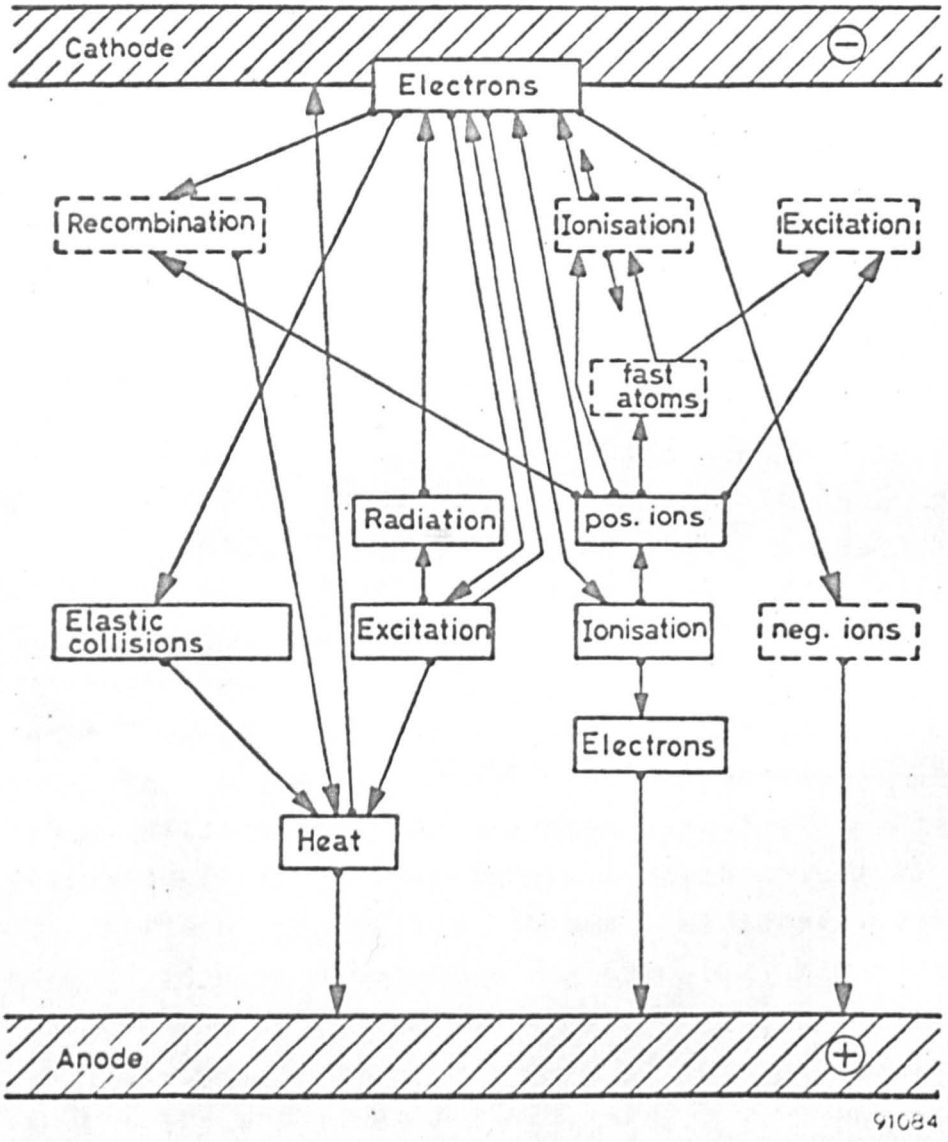

Collision Processes Possible in a Gas Discharge.

Fig 2.

Fig 2 gives a summary of the processes which are liable to occur between the two electrodes in a gas discharge.

1.3 Electron Loss Processes

a Recombination of Electrons and Positive Ions

In a system containing oppositely charged bodies, it is only natural that they should collide and neutralize each other by combining. The condition for this is that their total internal energy must decrease as a result of this reaction. This can be electron-ion recombination, which is more important in low pressure discharges, or ion-ion recombination. When an electron is captured thus, its excess energy can go to a third body as kinetic energy, or be emitted as radiation, but the probability for the latter is low. The third body can be the walls of the apparatus, or some other gas molecules in the case of high pressure discharges. If recombination is the only loss mechanism in a system with equal numbers of opposite charges, then:

$$\frac{dn}{dt} = -Rn^2$$

where R is the recombination coefficient. As this equation yields on integration:

$$\frac{1}{n} = \frac{1}{n_o} + Rt$$

it is obvious that the reciprocal of the number density is a linear function of time and therefore the coefficient R can be obtained from the loss rate of charges in the system. This is the principle which underlies most experiments to determine R, but diffusion losses, ion

molecule reactions, non-uniform spatial distribution of positive and negative charges etc make the experiments very much more complex.

b Attachment of Electrons and Atoms

It is quantum mechanically possible for electrons to attach themselves to atoms and molecules on collision thus forming negative ions. This process is important in the so-called 'electronegative gases' e.g. oxygen, the halogens etc. The following are the processes which can lead to formation of negative ions in gases:

(i) A free electron may be captured by a neutral atom with the emission of radiation.

$$A + e \longrightarrow A^- + h\nu$$

(ii) The capture of a free electron by an atom, with a third body taking up the excess energy, is a possible process which is important at high pressures.

$$A + B + e \longrightarrow A^- + B + K.E.$$

(iii) A molecule may capture an electron and go into a vibrationally excited level, becoming stabilised in a second collision, with another molecule.

$$AB + e \longrightarrow (AB)^{-*}$$
$$(AB)^{-*} + X \longrightarrow (AB)^- + X + K.E. + P.E.$$

(iv) An electron may be captured by a molecule which subsequently dissociates.

$$AB + e \longrightarrow (AB)^{-*} \longrightarrow A + B^-$$

This process is called dissociative attachment and is operative in the energy range of roughly 2 to 5 eV in

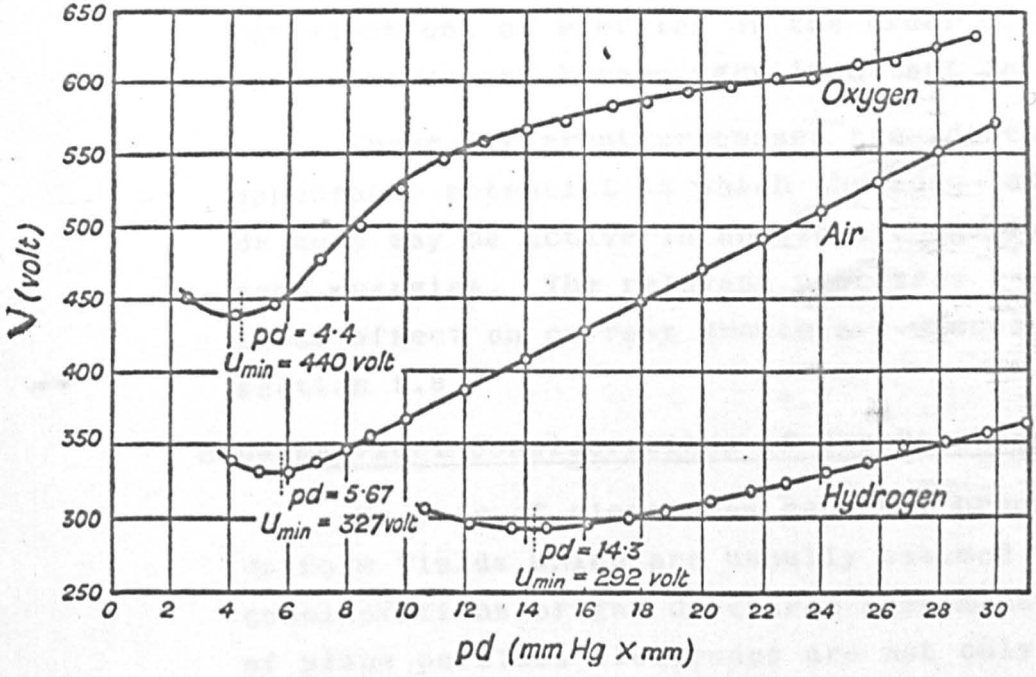

Breakdown Voltage Curves in Oxygen, Air and Hydrogen.

Fig 6

oxygen; this range is covered by the work described in chapter 5. Some molecules like carbon dioxide and hydrogen can also form negative ions through this process.

(v) An electron may leave a neutral excited molecule after a collision, and if the excitation energy in this case is greater than a critical value, the molecule can split up into a pair of ions.

$$AB + e \longrightarrow e + A^+ + B^-$$

For electrons of energies of the order of 20 eV or so, this process can become very important in oxygen.

These different processes are identified by the appearance potential at which the ions "appear" and one or more may be active in an electronegative gas at different energies. The relevant processes in oxygen and their effect on current growth are discussed further in section 1.9.

c Geometrical Considerations of Gas Discharges

No pair of electrodes can ever produce the perfectly uniform fields which are usually assumed for theoretical considerations of gas discharge phenomena. Ideally a pair of plane parallel electrodes are not only perfectly parallel, but also the electrode diameter is infinite, i.e. the ratio of the electrode diameter D to the gap distance d is considered to be infinite. In practice of course, D/d is finite and this must be considered when analyzing results.

The effect of finite electrodes on a discharge can be two kinds: one being due to field distortions and the other due to diffusion effects. The diffusion effects would be more significant for the uncharged

bodies in the discharge than the charged, as they cannot be constrained by the electric field. Thus, whether metastables and photons produced in the discharge will reach the cathode or not, is determined to a large extent by the geometry of the electrodes; and changing the ratio D/d has been shown in this laboratory to have an effect on sparking potential curves in both hydrogen and mercury vapour (38, 37). Field distortion is mostly an edge effect. For the charged particles in the discharge, this effectively means a longer drift path than 'd', but they may also be lost to the walls through diffusion. In the present investigation the walls were at the same potential as the cathode, so it is improbable that many electrons would have diffused to it, though the positive ions could have done so with greater ease. To correct for the edge effects, the ratio of D/d was kept as high as possible. It was never allowed to be smaller than 2 and was normally much greater; this, together with the use of guard rings ensured that any edge effects were kept to a minimum.

1.4 Growth of Current between Plane Parallel Electrodes

The current flow between two parallel electrodes in a gas shows a considerable variation when the voltage between them is altered continuously. Fig 3 shows the characteristics of such a uniform field gas discharge. The current growth measurements described later in this thesis were all taken in the "Townsend region" of the gas discharge spectrum, and the sparking potentials which were also measured, correspond to the voltage V_s on the diagram. It is interesting to observe that in the spectrum up to the point D, the current flow would cease

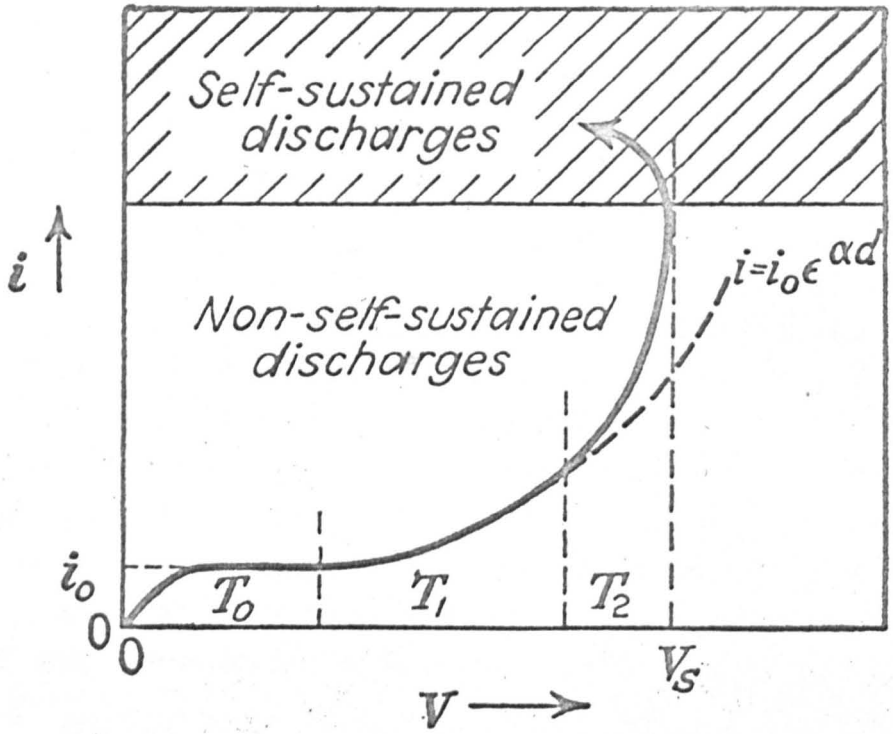

The Townsend Region of a Gas Discharge

Figure 4.

when the initial current I_o was withdrawn, whereas in the regions beyond the point D the discharge is said to be self-maintained, and the current flow would continue even if I_o was reduced to zero. In the following section, the Townsend region is considered in more detail.

1.5 The Townsend Discharge

Fig 4 shows in greater detail the initial part of the discharge characteristic of fig 3, the cathode being irradiated with ultraviolet light to give an initial photoelectric current. As the voltage between the electrodes is slowly increased from zero, the current to the anode increases slowly as the electrons move through the gas with an average velocity determined by the field. Further increases in the voltage results in saturation when all the electrons emitted by the cathode reach the anode (T_o). The current is then seen to increase again with increasing voltage since the electrons acquire energy from the field to ionize the gas atoms (T_1). After this, a region where the growth of current is very much more rapid can be seen, where evidently some other ionization processes must be active (T_2), until at a critical voltage (V_s in fig 3), the very rapid increase in current results in the establishment of a self-maintained current. The discharge is not self-maintained in T_1 and T_2 because there the current only flows as long as there is an external agency producing electrons, whether or not this agency is photons incident on the cathode.

1.6.1 Townsend's First Ionization Coefficient

J.S.Townsend was the first to carry out systematic experiments to study the ionization of gas atoms by

electron collisions, between plane parallel electrodes(18). At first he used X-rays as the agency to produce his original supply of electrons within the gap (19), but later he adopted the now conventional ultra-violet illumination of the cathode (20). The theory of his experiments may be summarized as follows.

A primary electron produced from the cathode acquires an equilibrium energy in the field after numerous collisions. Let the average number of ions produced by it per centimetre path length in the field direction be α. These newly produced ions move towards the appropriate electrode under the action of the electric field, the new electrons producing further ion pairs. If the number of free paths in the gap is large and spatially distributed, ionization will occur throughout the volume. Townsend showed that the current at a distance x from the cathode was given by:

$$I_x = I_o e^{\alpha x} \qquad \text{(Eq. 1.1)}$$

(In this thesis the symbol x is used to denote distances from the cathode in the direction of the field and 'd' to denote the actual separation between the electrodes.)

The constant α, Townsend's Primary Ionization Coefficient, can be experimentally determined using this last expression, since the semi-logarithmic plot of I and x has a slope of α.

In order to discuss the ionization efficiency of electrons, a coefficient η_i is often introduced. η_i is defined as the average number of ionizing collisions an electron makes in passing through a potential difference of 1V in the gas. Assuming that the voltage required for

the electrons to reach equilibrium with the field is negligible, the current becomes

$$I = I_o e^{\eta_i V}$$

after passing through a potential difference V, where I_o is the initial photoelectric current. Taking logarithms one can see that

$$\log \frac{I}{I_o} = \eta_i V$$

is a straight line, as can be seen from the region T_1 in fig 4. In region T_o, V is not large enough for the current to be saturated. The region T_2 is explained in section 1.6.3. Thus one can see that η_i is related to Townsend's primary ionization coefficient by the expression

$$\eta_i = \alpha/E$$

1.6.2 The Relation between the First Ionization Coefficient and Electron Energy

Assuming that the electron energy is derived entirely from the field, the energy should be proportional to the field strength and the mean free path of the electrons in the gas, λ; λ, however, is proportional to the gas pressure, and the probability of ionization at a collision depends upon the electron energy. Thus it can be seen that (20)

$$\frac{\alpha}{p} = F\left(\frac{E}{p}\right)$$

The classical semi-empirical formula gives this relation as

$$\frac{\alpha}{p} = A\, e^{-B/(E/p)} \qquad \text{(Eq. 1.2)}$$

where $A = 1/\lambda_o$ and $B = V_i/\lambda_o$ with λ_o as λ at unit pressure. Because of the nature of the simplifying assumptions made

in deriving this expression, and because the probability and distribution functions have been neglected in this derivation, the calculated values of A and B do not agree with the experimental values. But by a judicious choice of A and B, experimental values of α/p can be made to fit this expression in a limited range of E/p.

From the functional relationship between α/p and E/p it is clear that for a given E/p, α/p should be a constant and also, it is meaningless to talk about α at any pressure unless E/p is specified. Thus, when plotting the logI-x curve, it is necessary to keep E/p constant while x is varied.

The relationship between the mean energy of an electron swarm and η_i may be derived as follows. Let $N(\epsilon)d\epsilon$ be the number of electrons in unit volume with energies between ϵ and $\epsilon + d\epsilon$, and $P_i(\epsilon)$ be the probability of ionization by an electron of energy ϵ; then the number of ionizing collisions per second per electron of energy ϵ is given by,

$$\sqrt{2\epsilon/m}\ \frac{P_i(\epsilon)}{\lambda}\ ,$$

and the total number of ionizing collisions per unit volume in one second is,

$$\sqrt{2/m}\int_0^\infty N(\epsilon)\ \epsilon^{1/2}\ P_i(\epsilon)\ \lambda^{-1}\ d\epsilon$$

But, if the drift velocity of the electrons is v_e, the number of electrons crossing unit area perpendicular to the field per second would be

$$v_e\int_0^\infty N(\epsilon)\ d\epsilon$$

which makes the total number of ionizing collisions per unit volume per second equal to

$$\eta_i\ \frac{dV}{dx}\ v_e\int_0^\infty N(\epsilon)\ d\epsilon$$

Equating these two expressions, the ionisation efficiency comes out to be

$$\eta_i = \frac{\sqrt{2/m}}{v_e(E/p_o)} \frac{\int_o^\infty N(\epsilon)\, \epsilon^{1/2}\, P_i(\epsilon)\, \lambda_o^{-1}\, d\epsilon}{\int_o^\infty N(\epsilon)\, d\epsilon}$$

Further evaluation of η_i from this can be done only if some simplifying assumptions are made regarding the energy distribution. P_i and λ_o. For example, assuming the energy distribution to be Maxwellian, λ_o to be independent of ϵ and $P_i(\epsilon) = a(\epsilon_i - \epsilon)$, where a is a constant,

$$\eta_i = \frac{64}{\sqrt{2\pi m}} \frac{a}{\lambda_o v_e} \frac{\sqrt{-}}{(E/p_o)} \left(\epsilon_i + \frac{4}{3}\bar{\epsilon}\right) e^{-3\epsilon_i/2\bar{\epsilon}}$$

From energy balance considerations in the gas discharge another expression may be derived for η_i which comes out to be

$$\eta_i = \frac{1}{(1 + r + \bar{\epsilon}/\epsilon_i)} \frac{1}{V_i}$$

where r is the ratio of energy losses in exciting collisions to those in ionizing collisions. Assuming that

$$P_i(\epsilon) = a_i \frac{\epsilon - \epsilon_i}{\sqrt{\epsilon\epsilon_i}}$$

and that the excitation probability is

$$P_c(\epsilon) = a_e \frac{\epsilon - \epsilon_i}{\sqrt{\epsilon\epsilon_e}}$$

and that the energy distribution is

$$N(\epsilon) = C \exp\left(-\frac{\sqrt{3p}}{e\, E\, \lambda}\epsilon\right) \qquad \text{for } \epsilon > \epsilon_e$$

(Druyvesteyn's derivation)

$$\eta_i = \frac{a_i}{a_e} \frac{1}{\sqrt{V_i V_e}} \exp\left(-Bp_o/E\right)$$

at low E/p, which is of the same form as that obtained empirically for α (Eq.1.2).

1.6.3 Townsend's Secondary Ionization Coefficient

The region T_2 in fig 4 cannot be explained on the basis of primary ionization alone, because here the current growth is hyper-exponential, indicating the existence of an additional process or processes. This is hardly unexpected since the primary electron beam produces not only further electrons along its path, but also positive ions, excited atoms and photons. It has already been mentioned in section 1.2 that all these can, under suitable conditions, liberate electrons from the gas as well as from the cathode.

Historically, the first of these agencies to be investigated was positive ions. Townsend assumed that the positive ions were producing ion pairs in the volume of the gas and he introduced a coefficient β to represent the average number of ion pairs produced by a positive ion in moving unit distance in the field direction, obtaining the expression

$$I = I_o \frac{(\alpha-\beta)\exp(\alpha-\beta)x}{\alpha - \beta\exp(\alpha-\beta)x}$$

β/p depends on the nature of the gas and the E/p value.

Holst and Oosterhuis (21) later explained the curvature in terms of the emission of electrons from the cathode due to positive ion bombardment. If γ_i is the average number of electrons released from the cathode due to a single positive ion striking it, then for each electron leaving the cathode, $(e^{\alpha d}-1)$ ions are formed in the gap which on returning to the cathode release $\gamma_i(e^{\alpha d}-1)$ electrons from it. Let this number be f_i. This second generation of electrons results in $f_i e^{\alpha d}$ more electrons reaching the anode. But at the same time, $f_i(e^{\alpha d}-1)$ ions are also produced which give rise to a further generation

of electrons at the cathode, $\gamma_i(e^{\alpha d}-1)f_i = f_i^2$. Thus the total number of electrons arriving at the anode due to one primary electron is,

$$e^{\alpha d}(1 + f_i + f_i^2 + f_i^3 + \ldots) = \frac{e^{\alpha d}}{(1 - f_i)}$$

So, in the steady state,

$$\frac{I}{I_o} = \frac{e^{\alpha d}}{(1 - f_i)} = \frac{e^{\alpha d}}{1 - \gamma_i(e^{\alpha d}-1)}$$

which is of the same form as the expression obtained by Townsend, if $e^{\alpha d}$ is much greater than 1, as is usually the case. Thus it would appear that the current growth produced by assuming either of these processes is approximately the same.

The effects of secondary ionization in the gas volume and at the cathode, due to other processes, can be studied in a similar manner. Consider first the emission from the cathode produced by photons. Assume that θ photons, energetic enough to produce emission from the cathode, are produced by an electron moving 1 cm in the field direction. Then each initial electron produces $\theta e^{\alpha x}$ dx photons in the thickness dx at x, considering primary electron multiplication. Photons being neutral, are not constrained to move in any particular direction by the field and therefore only a fraction g (approximately 1/2) of these will reach the cathode. If the absorption coefficient is μ in the gas, the number of photons reaching the cathode will be $\theta e^{(\alpha-\mu)x}$ dx, from dx, in the special case where g=1; proceeding along the same lines as for positive ions, the steady state equation is obtained as,

$$\frac{I}{I_o} = \frac{e^{\alpha d}}{1 - \frac{\theta\gamma' g}{\alpha-\mu}(e^{(\alpha-\mu)d}-1)}$$

The expression for the effect of metastables on the cathode is very similar to this; however, here g will be a function of x as the metastables would tend to diffuse to the cathode where their concentration is zero. Variation of the secondary coefficient with x could, then, be indicative of the presence of metastables in the discharge. Oxygen, the subject of this investigation, however, does not have any known important metastable states.

An exact analysis of secondary ionization in the gas due to photons has been given by Dutton et al (22). A simplified derivation given by Little (23) is as follows. If θ be the number of photons created by an electron in moving 1 cm in the field direction, the total number of photons created by one electron crossing the gap is $\frac{\theta}{\alpha}(e^{\alpha d}-1)$. Assuming that they are created at the anode, as most of them are, and that a fraction g of them move parallel to the field to reach the cathode, the number of photoionizations in dx can be seen to be

$$\frac{\theta g \mu_i}{\alpha} \left(e^{(\alpha-\mu)(d-x)}\right) dx$$

where μ is the total absorption coefficient and μ_i that corresponding to absorption leading to ionization. These photoelectrons in turn multiply, and on integration, the current due to second and later generations of electrons is seen to be

$$\gamma'' \, e^{\alpha d} \, (e^{(\alpha-\mu)d}-1).$$

The steady state current equation in this case would be

$$\frac{I}{I_o} = \frac{e^{\alpha d}}{1 - \gamma''(e^{(\alpha-\mu)d}-1)}$$

where $\gamma'' = \theta g \mu_i / \alpha(\alpha-\mu)$. This is of the same form as the others if α is greater than μ, but if it is not, then this

equation would not explain the upcurving of the logI-x curves. The other possible gaseous secondary processes are not very important in practice and are not discussed here.

It is obvious that the different secondary processes cannot be distinguished in a study of I/I_o versus x curves alone. Also, since the expressions come out to be of a very similar form, it is possible to introduce a generalized secondary coefficient w/α, which is the linear sum of the individual coefficients.

The modified equation for the current in the steady state, taking into account secondary processes may be written as

$$\frac{I}{I_o} = \frac{e^{\alpha d}}{1 - (\frac{w}{\alpha})(e^{\alpha d} - 1)} \qquad \text{(Eq. 1.3)}$$

Since $\alpha = E\eta_i$ by definition, equation 1.3 can be rewritten as

$$\frac{I}{I_o} = \frac{e^{\eta_i V}}{1 - \frac{w}{\alpha}(e^{\eta_i V} - 1)}$$

which would directly explain the hyper-exponential growth of current with V in the region of T_2 in fig 4.

1.7 The Breakdown

Fig 4 shows that for a constant pressure and gap distance, the current increases to very high values at a certain voltage. This behaviour is indicated in equation 1.3 also, where the current should tend to infinity for a certain value of the gap distance, d, at a given pressure and E/p; it can be seen that when this happens,

$$\frac{w}{\alpha}(e^{\alpha d} - 1) = 1 \qquad \text{(Eq. 1.4)}$$

and also that if the external source of primary electrons is removed at this point, i.e. if I_o is reduced to zero,

the current will continue to flow unaffected. This means that at this voltage, (or gap distance, as the case may be) the discharge in the tube undergoes a transition and becomes self-maintained. Equation 1.4 in other words, is the breakdown criterion. This is valid for uniform fields, moderate pressures and constant w/α (which effectively means constant surface conditions). If the pressure is too low, there will not be many primary ionizations occurring in the gas and hence the use of α in equation 1.3 is not justifiable. If the pressure is too high, there will be too many gas excitations for any cathode secondary process to be really effective.

1.8 Paschen's Law

To get the value of the breakdown voltage, or sparking potential from the breakdown criterion, αd is written as $\frac{\alpha}{p}.pd$ and then $\frac{\alpha}{p}$ is replaced by the expression given in equation 1.2. Thus one obtains

$$V_s = \frac{Bpd}{\log \frac{Apd}{\log(1+\frac{1}{\gamma})}} \qquad \text{(Eq. 1.5)}$$

Paschen's law (24) states that the sparking potential is a function of the product of the pressure and gap distance as can be seen from equation 1.5 and has been verified by experiments in different gases. Accurate measurements, however, have revealed deviations from Paschen's law, i.e. variations in V_s independent of pd. The deviations can be explained on the basis of the finite nature of the parallel plate electrodes used, as this would lead to loss of electrons, positive ions and photons (agents producing secondary ionization) from the gap.

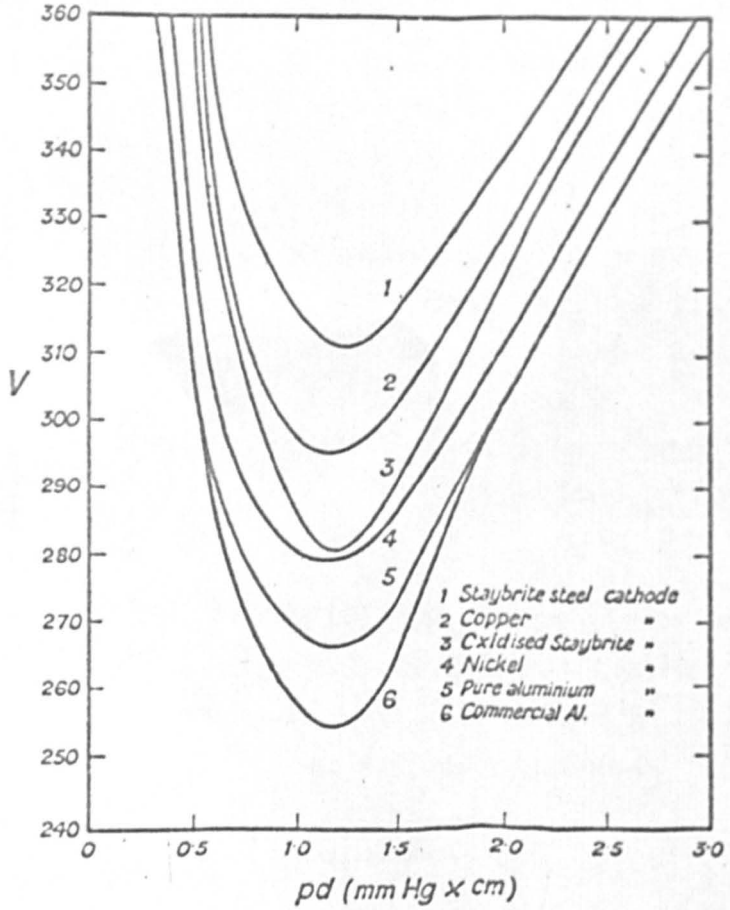

Breakdown voltage curves in hydrogen for different cathode materials.

Fig 5

Further, it has been assumed in the derivation of the law that w/α is a function of E/p only, and so if w/α does depend upon p or d, which it often does to some extent, then deviations from the law are only to be expected.

A minimum for V_s can be predicted from equation 1.5 since V_s should be increasing at high as well as at low values of pd. At low pd the logarithmic variation of the denominator is greater than the linear variation of the numerator and therefore V_s should increase with decreasing pd; on the other hand, the logarithmic term varies very slowly at high pd and therefore the sparking potential should increase almost linearly with pd at high pd. Thus analytically, a minimum for the V_s versus pd curve is to be expected. This is easily explained on the basis of physical principles also. Considering the collisions in the gas, at very low pressures, the probability of collisions is very small and so the number of ionizations will be fewer, while at high pressures the mean free path of the electrons is too small for it to acquire sufficient energy to ionize by collisions. So at both high and low pd, V_s would have to be high.

It is obvious that the sparking potential will depend very critically on w/α i.e. the gas and the nature of the cathode surface. Figure 5 shows breakdown voltage curves obtained for different cathodes in hydrogen studied by Llewellyn Jones and Henderson (25) and figure 6 shows breakdown curves for oxygen and hydrogen obtained by Fricke and for air obtained by Meyer (26,27). The minimum sparking potential measurements of Llewellyn Jones and Davies (28) show how sensitive they are to the history of the cathode surface, i.e. to the thickness of films, baking, outgassing,

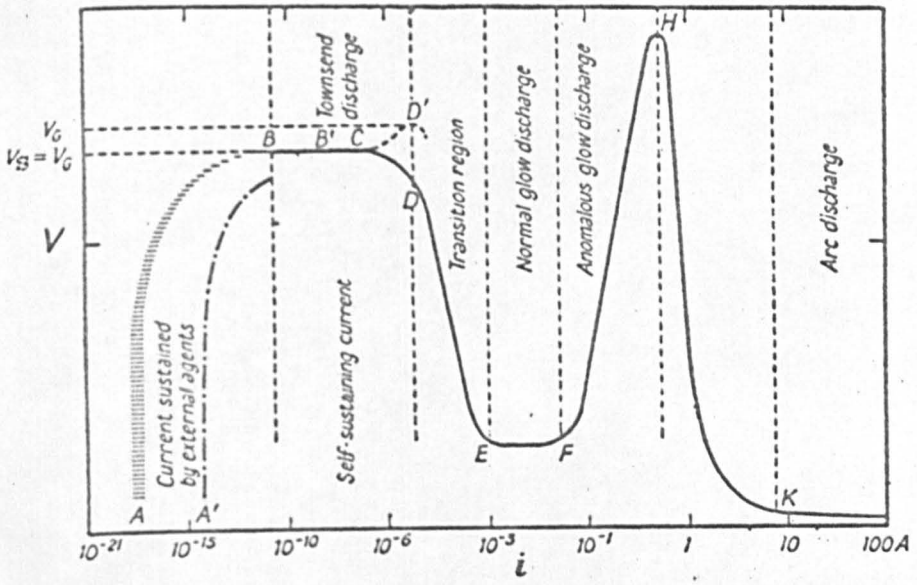

Schematic characteristic of a gas discharge between flat parallel plates. Scale for the current: logarithmic between 100 and 0·1 amp, still more contracted for lower values of i. — · — · — current with photo-emission from the cathode; - - - - - - (CD') positive characteristic of the Townsend discharge; the breakdown potential V_S is lower than the starting potential of the glow discharge V_G; ——— (CD) negative characteristic of the Townsend discharge; $V_S = V_G$.

Fig 3

oxidation, flushing with gas, etc. Davies and Fitch (29) have observed a lowering of the work function of a copper cathode due to the passage of a spark which caused the minimum sparking potential to drop by up to 30 volts. This was attributed to positive charge build up on the cathode which would obviously reduce the potential barrier for conduction electrons in the metal and would therefore reduce the work function of the surface. Gozna (30) has further shown by formative time lag studies that the original surface conditions of a copper cathode reappear only after a time interval of about ten seconds after a discharge in hydrogen.

1.9 Current Growth in the Presence of Electron Attachment

It is obvious that the loss of electrons in producing negative ions, influences the current growth in oxygen and that consequently the current growth equation has to be modified. To do this Harrison and Geballe (31) consider the following three types of reactions leading to negative ion formation in oxygen:

1 $AB + e \longrightarrow AB^-$

2 $AB + e \longrightarrow A + B^-$ (Dissociative process)

3 $AB + e \longrightarrow A^+ + B^- + e$ (Ion pair production)

The first two types of reaction are described by a parameter η, which is defined in analogy with α as the number of attachments per centimetre path of the electron in the field direction. At a constant E/p, (for the number of attaching collisions is bound to depend on the mean electron energy), assuming that secondary processes are not important, the continuity equations can be written as,

$$\frac{\partial n_e}{\partial t} + v_e \frac{\partial n_e}{\partial x} = \alpha v_e n_e - \eta v_e n_e$$

$$\frac{\partial n_+}{\partial t} + v_+ \frac{\partial n_+}{\partial x} = \alpha v_e n_e$$

$$\frac{\partial n_-}{\partial t} + v_- \frac{\partial n_-}{\partial x} = \eta v_e n_e$$

with subscripts e,+ and - referring to electrons, positive ions and negative ions respectively and n and v referring to numerical density and drift speed in the gas. Solving these for steady state conditions gives for the I-x characteristic,

$$\frac{I}{I_o} = \frac{\alpha\, e^{(\alpha-\eta)x}}{\alpha - \eta} - \frac{\eta}{\alpha - \eta} \qquad \text{(Eq. 1.6)}$$

When reaction 3 is predominant, the appropriate continuity equations yield the equation

$$\frac{I}{I_o} = \frac{(\alpha+\lambda)\, e^{\alpha x}}{\alpha} - \frac{\lambda}{\alpha} ,$$

where λ is the parameter describing the third process, being the number of pairs of ions produced by an electron moving one cm in the direction of the field.

When all three processes are active,

$$\frac{I}{I_o} = \frac{(\alpha + \lambda)}{(\alpha - \eta)} e^{(\alpha-\eta)x} - \frac{(\eta + \lambda)}{(\alpha - \eta)}$$

These equations have been obtained on the assumption that secondary processes are not important. When secondary processes and dissociative attachment take place at the same time, the equation has to be modified to

$$\frac{I}{I_o} = \frac{1}{\alpha - \eta} \cdot \frac{\alpha\, e^{(\alpha-\eta)x} - \eta}{1 - \frac{w}{\alpha-\eta}(e^{(\alpha-\eta)x} - 1)} \qquad \text{(Eq. 1.7)}$$

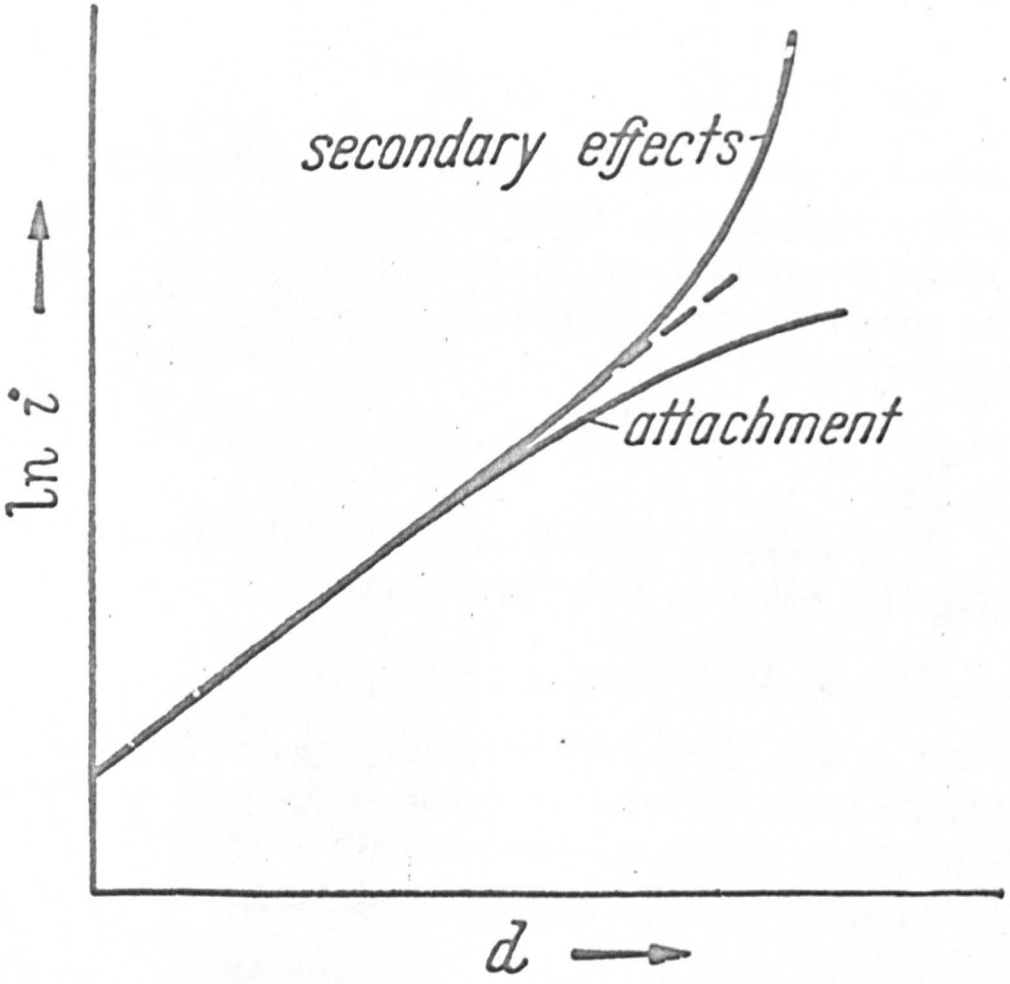

Current Growth Curves - Modified due to Secondary Effects and Electron Attachment.

Fig 7.

Figure 7 shows the nature of the logI-x curve when in addition to the primary process, attachment takes place and secondary processes are present.

b Probability of Negative Ion Formation

The probability of an electron attaching itself to a molecule or atom depends very strongly on the nature of the gas and the energy of the electron. The attachment probability, h, is defined as the probability that an electron will attach itself to a molecule or atom in a single collision. h relates the attachment or capture cross section to the total collision cross section by the equation

$$\bar{q}_a = h\,\bar{q}_{tot}$$

It is easy to see that the number of electrons lost in a distance dx due to attachment is

$$dn = \frac{h\bar{u}}{\lambda v_e} n\,dx$$

where $\bar{u}$ is the mean agitation velocity. Assuming that $n = n_o$ at $x = 0$,

$$n = n_o e^{(-h\bar{u}/\lambda v_e)\,x} = n_o e^{-\eta x}$$

Thus η comes out to be equal to $\frac{h\bar{u}}{\lambda v_e}$. Using the expression

$$v_e = k_e E = a \frac{eE}{m} \frac{\lambda}{\bar{u}}$$

where k_e is the mobility of the electrons and a is a constant for a given electron energy distribution, this can be rewritten as

$$\eta = -\frac{a h e}{m k_e^2 E} \qquad \text{(Eq 1.8)}$$

This is a useful expression enabling one to correlate η and capture cross sections, and has been used to compare the results of experiments using different techniques.

1.10 Breakdown in the Presence of Electron Attachment

Geballe and Reeves (32) discuss the effect of attachment on the breakdown of gases starting with the current growth equation (1.6) which takes into account both secondary processes and electron attachment. As in the case of non-attaching gases the threshold for a self-maintained current is obtained when the denominator of the equation is zero, i.e. when

$$\frac{w}{\alpha - \eta}\left(e^{(\alpha-\eta)x} - 1\right) = 1 \qquad \text{(Eq 1.9)}$$

It is obvious here that breakdown is possible if α is greater than η, irrespective of the values of α, η and w, for sufficiently large pd. But if α is less than η or equal to it, breakdown is impossible regardless of the value of pd, since under these circumstances, electrons are removed from the gas by attachment as fast as they can be produced by collision ionization. Since α/p and η/p are both functions of E/p, and α/p increases with E/p, there must be a limiting value of E/p below which breakdown cannot take place. From eq 1.9, the exact E/p at which this happens should be defined by the condition

$$\frac{\alpha}{p} = \frac{\eta/p}{1 + \gamma} \qquad \left(\text{where } \gamma = \frac{w}{\alpha}\right)$$

According to this expression, as pd increases, V_s/pd i.e. E/p at the sparking potential should approach the limiting value asymptotically. Geballe and Reeves

consider a number of gases where this condition is found to hold. They also point out that it is valid to assume that γ is very small for gases at the experimentally observed limiting E/p, so that the condition may be written as

$$\frac{\alpha}{p} = \frac{\eta}{p}$$

for all practical purposes.

Crowe and Devins (33) verify the sparking condition for SF_6 and CF_2Cl_2. They have also found that Paschen's law is obeyed by a large number of electro-negative gases. However, their suggestion of an empirical relationship between the molecular structure and the sparking potential is probably open to question since it is based on the assumption that γ does not vary with E/p, which is not always true.

1.11 Temporal Growth of Current

The time that elapses between the instant of application of the voltage and the occurrence of a spark, is known as the time lag and is the sum of two parts. First, the statistical time lag which is the time that elapses after the voltage is applied before an initiatory electron appears in the gap, and second, the formative time lag which is the time taken for the discharge to become self maintained after an initiatory electron has appeared within the gap.

The statistical time lag is a random quantity which depends on the possibility of ionization in the gas, for example on the presence of ultraviolet radiation, radioactive material etc, and may of course be reduced to zero

if there is a sufficient amount of suitable radiation in the gap. Experiments on statistical time lags indicate that the lower the amount of radiation in the gap, the higher the peak value of voltage pulses have to be to produce breakdown in the same time.

An approximate theory of the temporal growth of a discharge and an expression for the formative time lag has been given by Druyvesteyn and Penning (34). The formative time lag is found to be approximately proportional to $1/(V - V_s)$, where V is the applied voltage and $(V - V_s)$ is the "overvoltage". When $V = V_s$, the formative time lag approaches very high values. Experimental results are normally plotted in the form formative time lags versus percentage overvoltage $(V-V_s).100/V_s$, and figure 6 shows some typical curves.

Formative time lag studies are important in gas discharges because they are valuable tools in determining the relative importance of the various secondary processes active in the gas under the relevant conditions. The actual analyses of Bartholomeyczk, Davidson etc are too involved to give here (35,36), but have been applied in this laboratory to low pressure hydrogen and mercury discharges to evaluate the relative importance of the secondary processes active in the discharge(37,38).

1.12 Conclusion

An outline has been given of the basic phenomena which occur in gas discharges. The work described in this thesis deals with the ionization and attachment processes and their effects on breakdown and pre-breakdown currents

in uniform fields in oxygen. The next chapter gives an account of the theoretical and experimental background of the study.

CHAPTER II

REVIEW OF PREVIOUS WORK

2.1 Introduction

In this chapter it is intended to give a summary of the work that has already been done on negative ion formation and ionization processes in oxygen. In many experiments these processes have been studied simultaneously. Most of these experiments can be broadly classified into two groups, depending on whether they make use of a swarm, or a beam of electrons, and in each of these methods several different experimental techniques have been adopted.

2.2 Experimental Methods

2.2.1 Experiments Using Electron Swarms

a Diffusion Method

Healey and Reed (39) describe the method used by Bailey (40) and his colleagues to study the attachment coefficient in oxygen. Bailey's experiment consisted of measuring currents received by a series of electrodes of which all but the last contained a slit through which the ions and the electrons passed. The same method has been refined and used for the measurement of η and the Townsend energy factor k_1 by Huxley, Crompton and Bagot (41) in 1960, where k_1 is the ratio of the mean agitation energy of the electrons to the molecular energy. They allowed a stream of thermionically produced electrons, already in a steady state of motion in an electric field E, to enter a diffusion chamber through a small hole in the cathode, and to move under the same field to the anode which consisted of a central disc and two

annuli. The ratio of the current received by the inner annulus to that received by both annuli together is expressed in terms of the dimensions of the apparatus, the relation $v_e/D = 40.29\ E/k_1$, and the attachment coefficient. Assuming the ionization to be small, the expression was analyzed and values of η and k_1 obtained, for gas pressures of a few torr.

b Electron Filter Method

The electron filter, devised by Loeb (42), is a grid, between alternate wires of which a high frequency alternating field may be applied, so that from a beam of electrons and ions, the electrons are swept away by it, while the ions which have a greater inertia can pass through. Bradbury (43) used this idea in his measurement of η. He had two filters G_1 and G_2 which could be inserted one at a time in between a photocathode and an anode, at known distances. The electrons diffused under a field maintained uniform by guard rings, and the current at the anode was measured with G_1 in position, with and without a high frequency voltage on it; the procedure was repeated for G_2 after retracting G_1. The radio frequency voltage was adjusted so as to produce a minimum disturbance of the uniformity of the field and maximum efficiency of electron capture. The electron current in the beam at the filter is given by the difference in the values of anode currents with and without the alternating voltage on. From the current values thus obtained, the field and gas pressure values and the dimensions of the tube, the attachment probability could be determined, provided that the electron drift velocity is known. Bradbury used gas pressures of 3 to 90 torr and his pyrex apparatus was baked out at 200°C which reduced his background pressure to 10^{-6} torr. His results in oxygen are given at the end of this

chapter.

Kuffel (44) employed the same type of apparatus in 1959 to study η in dry and humid air gaps and also in oxygen. He used a larger chamber which permitted the use of higher field gradients before the onset of corona, and thus enabled him to extend the range of electron energies.

Chatterton and Craggs (45) used the filter method again in 1961 to investigate attachment coefficients. They also obtained a vacuum of about 10^{-6} torr and the gas employed in their investigation was spectroscopically pure oxygen. Photoelectrons were produced by focussing ultraviolet light on to a platinum coated disc set in the centre of the cathode. The pressure was set to be higher than the minimum required for negligible electron diffusion corresponding to the E/p value investigated, ranging from 24 torr at E/p=0.2 V/cm.torr to 5 torr at E/p=30 V/cm.torr. In Bradbury's and Kuffel's experiments there must have been some electron diffusion, but the error introduced by the loss of negative ions at the filter due to too large a voltage on the grid would have tended to cancel out the error due to diffusion; the fraction of ions collected at the filter was considerable in Bradbury's experiments. In this experiment, a criterion for filter voltage was set for the collection of only upto 2% of the negative ions; for any lower voltages the resolution had to be sacrificed to an unacceptable extent. The filter voltage was also kept low enough to prevent the detachment of electrons from the negative ions which would have produced a systematic lowering of the measured η values. The E/p range covered extended from 3 to 30 V/cm.torr. In addition to the real or apparent attachment coefficient, η or $\alpha-\eta$, the three-body coefficient (section 1.3.biii) also has been investigated here.

c Time of Flight Method

These experiments involve the measurement of the time dependence of the currents of electrons and negative ions as they drift across a tube. The three most important experiments in this group were done in 1952 by Herreng (46) and Doehring (47) and in 1959 by Chanin, Phelps and Biondi (48).

Herreng used a pyrex tube with plane parallel electrodes as his ionization chamber with initial ionization produced by a beam of x-rays parallel to the electrodes. The x-ray tube was pulsed 50 times a second at 1 μs duration and one of three windows was used to let the x-rays in, the windows being at different distances from the anode. The uniform field maintained between the electrodes drove all the ions produced on to the anode in one impulse before the next impulse came along. The current at the anode was amplified and displayed on an oscilloscope. In oxygen (or any attaching gas) the current can be expressed in the form

$$I = I_o \exp(-kt)$$

where k can be determined from the oscillogram. But k is related to the attachment probability h in a simple manner,

$$h = kmE/0.75ev_c ,$$

and hence he was able to determine the attachment coefficient. In the same experiment, Herreng also measured the drift velocity of electrons. He covered a range of E/p from 0.1 to 20 V/cm.torr, with 'very carefully purified' gas at pressures of a few torr, on its own and mixed with Argon.

Doehring measured the ion current reaching the anode after the electron current had virtually died out. He derived the relation,

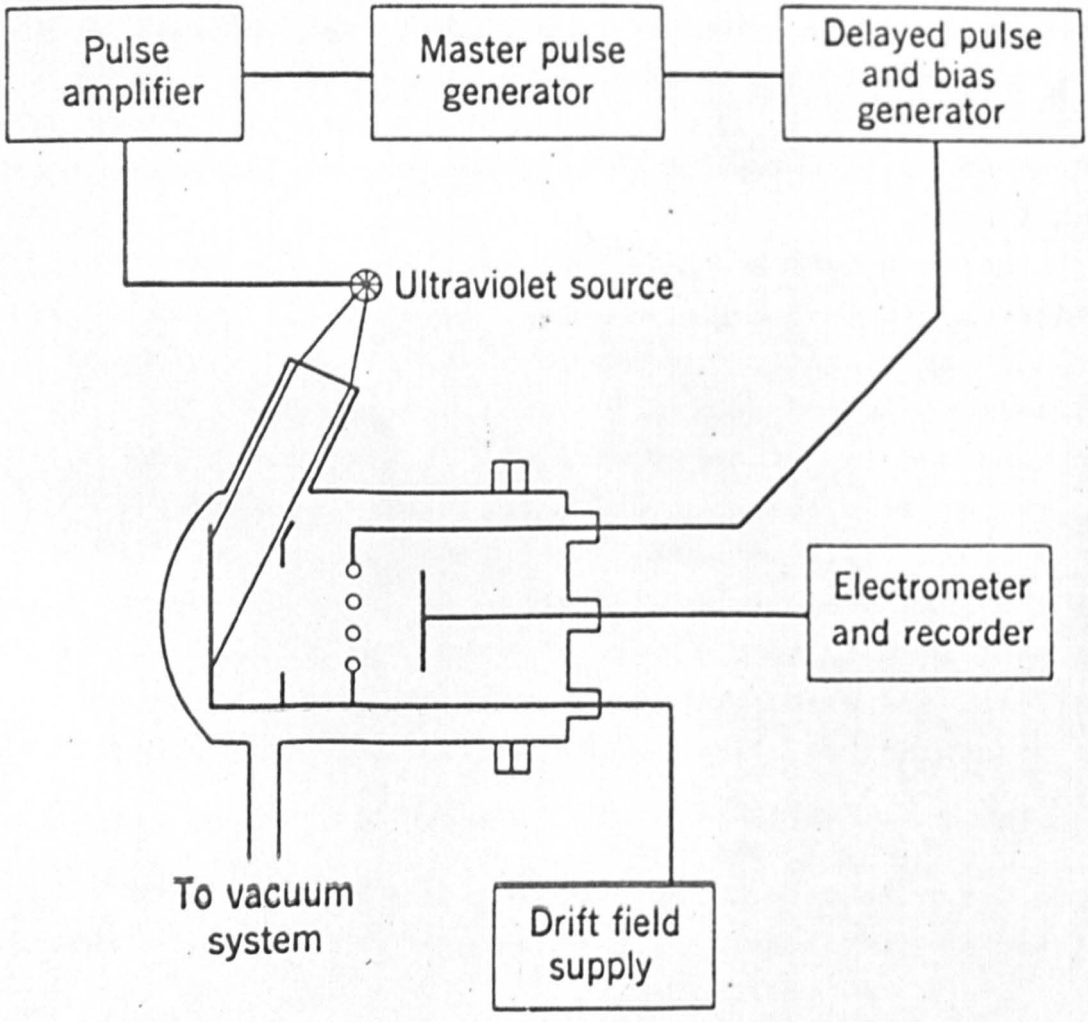

Apparatus Used by Chanin, Phelps and Biondi.

Figure 8.

$$I_i = \text{const. } e^{\eta v_i t} \quad \text{for } 0 < t < \frac{L}{v_i}$$

and $$I_i = 0 \quad \text{for } t > \frac{L}{v_i}$$

L_i being the flight length. He used thermionic electrons to initiate the ionization. The ions had a grid in their path which acted as an inlet gate and in front of the anode there was an exit gate. Both the 'gates' were similar in construction and were operated by rectangular voltage pulses. Using these grids, pulse generators and and a quartz oscillator, the required time sampling could be achieved. Doehring used the same discharge tube to determine the drift velocity of electrons after modifying the circuitry. Here positive and negative peaks of an oscillatory voltage were applied to open the inlet and exit gates respectively, so that only electrons with their flight times an integral multiple of the half cycle got through both gates to the anode. The frequency of the oscillating voltage was variable in this case. Doehring's apparatus was made of Jena 20 glass and bakable at 500°C. He used electrodes made of a steel alloy and two samples of gases, one produced electrolytically, and the other obtained from industrial cylinders, after further fractional distillation.

Chanin, Phelps and Biondi (48) used a method similar to that of Doehring's. They had photoelectrons liberated in pulses and only one shutter grid to control the arrival of ions at the collector (fig 8). The time of opening of the shutter was controlled in relation to the electron pulse to study the time dependence of the current. Here again the electron drift velocity could be determined. The measurement of η as a function of

E/p was carried out in the range of 0.01 to 10 V/cm torr for pure oxygen, and with oxygen-helium mixtures, the lower energy limit was extended even further.

Schlumbohm's experiments deserve special mention here (49), since his results are the first to cover the E/p range greater than 70 V/cm torr, after Karl Marsch's (50). Schlumbohm looked at electron avalanches between plane parallel electrodes of 21 cm diameter with gap distances upto 4.7 cm, enclosed in a glass vessel, at gas pressures of 0.01 to 5 torr. His electrons were produced photoelectrically by a pulsed light source (about 15 ns duration) and diffused across to the anode where the current was subjected to wide-band amplification and displayed on an oscilloscope. From the positive ion current at time t

$$I_+(t) = \frac{en_o}{T_+} (\exp \alpha d - \exp \alpha v_+ t)$$

where $T_+ = d/v_+$, the ion transit time which can be measured, α and v_+ were determined. Diffusion was neglected here, as the drift energy was very large compared to the diffusion energy.

d Microwave Cavity Methods

At extremely low E/p's the electron loss rate in the afterglow of a pulsed microwave discharge can be used to study diffusion coefficients, recombination coefficients and, under special conditions, also the attachment coefficients. The method originally suggested by Biondi (51) has been employed by Mulcahy et al (52) and Chantry (53) in oxygen.

e Townsend Method

The equation for current growth between parallel plates has been derived in the last chapter, and for an electronegative gas, neglecting secondary effects, it is

$$\frac{I}{I_o} = \frac{\alpha}{\alpha-\eta} e^{(\alpha-\eta)d} - \frac{\eta}{\alpha-\eta}$$

As has been mentioned already, from a measurement of the steady state currents at different d's it is possible to compute the values of α and η. On the other hand, the continuity equations may be solved for the temporal or non-steady state, and the resulting current growth equation can be used in the determination of the attachment coefficient. This is referred to as the avalanche method.

Using the Townsend method, Masch obtained a curve of α/p as a function of E/p in oxygen as early as 1932. His experimental tube for low pressures (less than 1/2 an atm.) was of glass and he used zinc electrodes at separations of a few mm. Oxygen obtained in steel cylinders was used after drying with P_2O_5 and the pressures were measured on a mercury manometer. He used the Townsend relationship to calculate α without taking attachment into consideration in an E/p range of 30 to 500 V/cm torr. For E/p less than 70 V/cm torr his results would be in considerable error, of course, as the attachment coefficient is still significant in the range $30 < E/p < 70$ V/cm torr. (For this reason, his results are presented only for $E/p > 50$ V/cm torr in the results section.) Masch conducted his experiments in air and nitrogen also, and with nitrogen, he tried two samples: one from steel cylinders and the other, an 'absolutely

pure' sample produced by heating a nitride of sodium. From these he concluded that the purity of the sample has no effect on the ionization coefficient and therefore, one gathers, did not attempt to purify his other gases any further. None of his gases could have been very pure in fact, as they were all mercury contaminated.

The most important experiments in the steady state in oxygen have been those of Harrison and Geballe (31) and Prasad and Craggs (54). Both sets of experiments covered roughly the same E/p range - a few tens of V/cm torr - though the pressures at which the experiments were carried out were different.

Harrison and Geballe used polished copper electrodes of 9 cm diameter with contoured edges. The anode was perforated with a large number of holes in the middle. The cathode was mounted on a nut and screw which allowed d to be varied between 0 and 4 cm, by means of an iron armature and external magnet. Photoelectrons were liberated from the cathode by the normal incidence of ultraviolet light. A coating of 'dag' on the walls provided an equipotential surface which could be kept at any potential desired, so that diffusion to the walls could be kept to a minimum. The pyrex vessel holding the assembly was a five litre flask which could be baked at 400°C and the background pressure was found to be 10^{-5} torr after baking. Oxygen was produced by the decomposition of three compounds, HgO, $KMnO_4$, and MnO_2, and purified with liquid nitrogen traps. The gas was never permitted to break down. Current measurements were made at different gap distances for the same E/p. The E/p range was roughly 25 to 65 V/cm torr at 11 to 40 torr pressure.

Prasad and Craggs used a pair of dural electrodes as well as platinum ones in their experimental tubes. Photoelectrons were produced from the cathode by vertical illumination through a perforated anode. The tube was of 80 litres capacity, giving background pressures of 10^{-5} torr. Prasad (55) has described the apparatus in detail in connection with similar experiments done in air. The intensity of the ultraviolet lamp was monitored by a photocell incorporated in the assembly. The gas pressure was measured on an oil manometer at lower pressures and on a manometer with metal bellows at higher pressures. A rigidly supported micrometer measured the gap distance to ± 0.005 mm while the ionization currents were measured by an electrometer bridge and were reproducible to 5%. An E/p range of 30 to 50 V/cm torr was covered at pressures of 60 and 150 torr with the dural cathode, and 100, 150, 200, 300 and 600 torr with the platinum electrodes. Breakdown voltages were also measured in this experiment using both cathodes at pressures of 150, 300, and 700 torr. The secondary coefficient was calculated from prebreakdown currents at E/p greater than 45 V/cm torr for the dural cathode while it was obtained in both cases from the breakdown criterion (eq. 1.9).

The results of Prasad and Craggs are in fair agreement with those of Harrison and Geballe as can be seen from fig 11 in section 2.4.

2.3.2 Experiments Using Electron Beams

The formation of ions has been studied by several workers using well-collimated beams of electrons of known energy in gases at low pressures. The most important of these experiments are outlined in this section.

a Lozier Tube

Lozier devised this method to study positive and negative ion formation in several gases (56). His apparatus (57) consisted of a field-free collision chamber in which the gas under consideration was maintained at a pressure of the order of 10^{-5} torr and through which a narrow beam of electrons - confined by slits outside, and an axial magnetic field inside the collision chamber - was passed. At the other end the electrons escaped from the chamber and were collected on a plate kept slightly positive with respect to earth, while the ions produced in the chamber were drawn out by a set of vanes which were concentric with the axis of the tube, and collected on a cylindrical electrode.

Absolute cross sections for the production of negative ions are measured in this method by a comparison of the yield with that of a known positive ion. The electron affinity may be determined from energy considerations, provided that the dissociation energy of the molecule, the total kinetic energy of the products of dissociation, the appearance potential of the ion considered and any changes in internal energy involved are known.

Craggs, Thorburn and Tozer (58) have used this arrangement with slight modifications to study attachment in several gases. Fig 9 shows the schematic diagram of their apparatus. A tungsten filament produced electrons which were accelerated up to about 40 eV and limited by slits before their entry into the collision chamber. The magnetic field used was about 200 gauss. The inner set(I) of concentric vanes was maintained at earth potential, while the outer set (O) had a drawout potential applied

Figure 9.

Lozier Type Apparatus of Craggs, Thorburn and Tozer

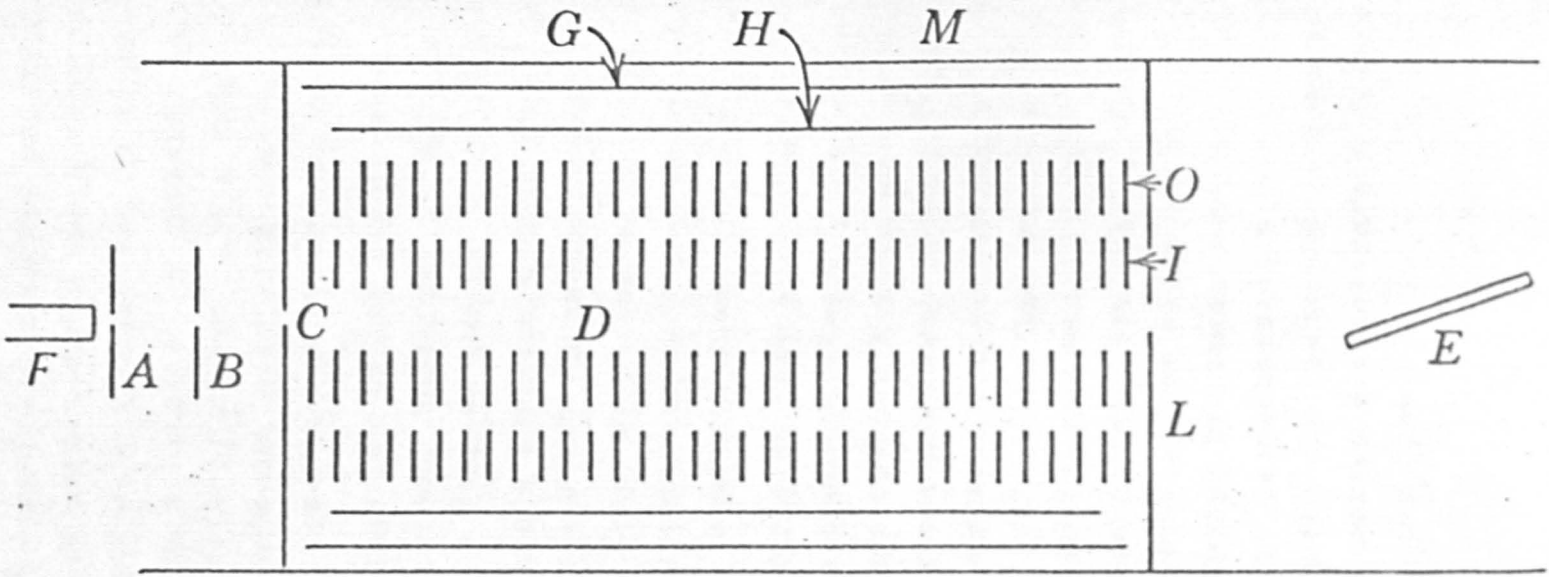

on it. The cylindrical electrode (H) collected the ions while G acted as a guard. If the kinetic energy of the ions is to be measured, a retarding potential is applied to the cylindrical electrode, while for cross section measurements the potentials of O and H are kept the same. The electron beam energy was varied to determine the minimum energy required for the production of a specific ion as well as the relative efficiencies of producing ions of a specific kinetic energy. By reversing the polarity of the draw-out potentials, positive or negative ions could be studied, obviously. The ions collected in this method were only those which have directions of motion within about 12^{o} of the perpendicular to the axis, because of the geometry of the vanes. This has the inherent disadvantage that angular anisotropies which accompany dissociative attachment will introduce large errors in the results.

Asundi, Craggs and Kurepa (59) used a Lozier type tube again in 1963, in what was virtually a repetition of the experiment of Tozer et al (58). One of the improvements was, however, regarding the collector voltage, Realizing that the efficiency of the collector depended on the kinetic energy of the ions collected, Tozer et al had used appropriate potentials on the collector in the inverse ratio of the kinetic energy of the ion. This, however, meant a correction for the collection efficiency for high energy ions owing to the small potentials applied in the presence of the magnetic field. Asundi et al used a collecting potential sufficient to overcome the magnetic field in all cases and the collection efficiencies were normalized using a correction factor which had been

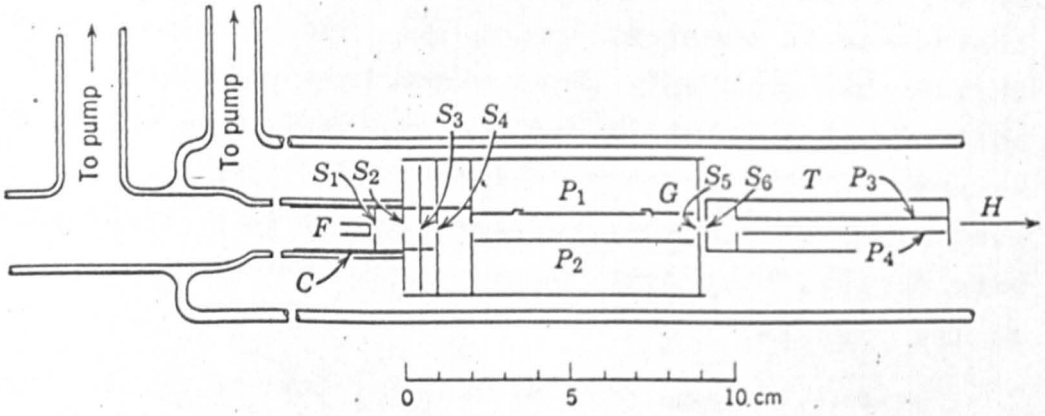

Apparatus of Tate and Smith

Figure 10

evaluated. In addition to the Lozier tube, a Tate and Smith type of apparatus (described in the next section) was also used by these authors.

Buchel Nikova (60) made measurements on oxygen, water vapour and other gases in an experimental set-up very similar to that of Lozier's; however, she did not use vanes perpendicular to the electron beam direction, so her results would be free from angular discrimination effects which are inherent in Lozier's measurements.

b Tate and Smith Apparatus

Tate and Smith (61) used a tube with two compartments, each of which was pumped separately (see fig 10). The filament F produced the electrons which pass through S1 and S2 to the accelerating field between S3 and S4. A constant potential difference is applied between F and S1 and between S2 and S3 so that the total electron current is independent of the accelerating voltage. A solenoid around the tube produced a field of a few hundred gauss to prevent scattering of the electrons. The ions produced were collected by the plate P1 with a guard ring G. The collector voltage was as low as 4 V for electrons of energy up to 4500 eV. (The validity of this was questioned recently (62)). Ionization and attachment cross sections are calculated using the formula,

$$Q = \frac{i_+}{i_e} \frac{T}{273} \; L \; p \; 3{\cdot}56 \; . \; 10^{16}$$

where L is the length of the collector and the other symbols have their usual meaning. Massey and Burhop have suggested that the effect of the axial magnetic field on the path length of the electrons would introduce a fairly

large error in the results (63), but Asundi shows ~~that~~ that the increase in path length in this experiment would in fact be negligible (64).

Schulz's (65) apparatus, based on similar principles, employed a retarding potential difference electron current and was designed to collect all the ions formed, irrespective of their kinetic energy and angular distribution. The system was bakable, giving background pressures of 10^{-9} torr. A magnetic field was used to align the electron beam in the collision chamber which also housed the cylindrical electron and ion collectors. Differential pumping was employed to keep the purity of the gas high in spite of the hot filament. The positive ion cross sections were assumed and therefore, only the ratio of the positive and negative ion currents had to be measured to calculate the negative ion cross sections.

In addition to the Lozier apparatus, Asundi et al (59) also used a Tate and Smith apparatus. The experimental pressure was about 10^{-4} torr with a suitably accelerated electron beam passing through it, collected by a collector plate. The ion collector plate collects all the ions that are formed, and not just a fraction as in the Lozier tube. The pressure was measured on a McLeod gauge and the absolute cross sections calculated from the formula quoted on the previous page. Asundi et al determined not only attachment cross sections but also ionization cross sections in his experiments.

Beam experiments have the advantage of using monoenergetic electrons, but a hot filament has to be used and the experimental pressures have to be quite low, so that very low background pressures are quite essential

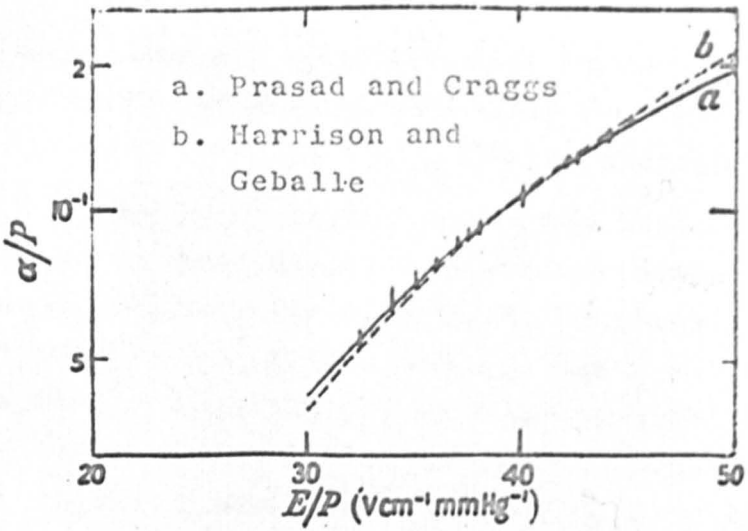

α/p vs E/p for low E/p in oxygen

Figure 11

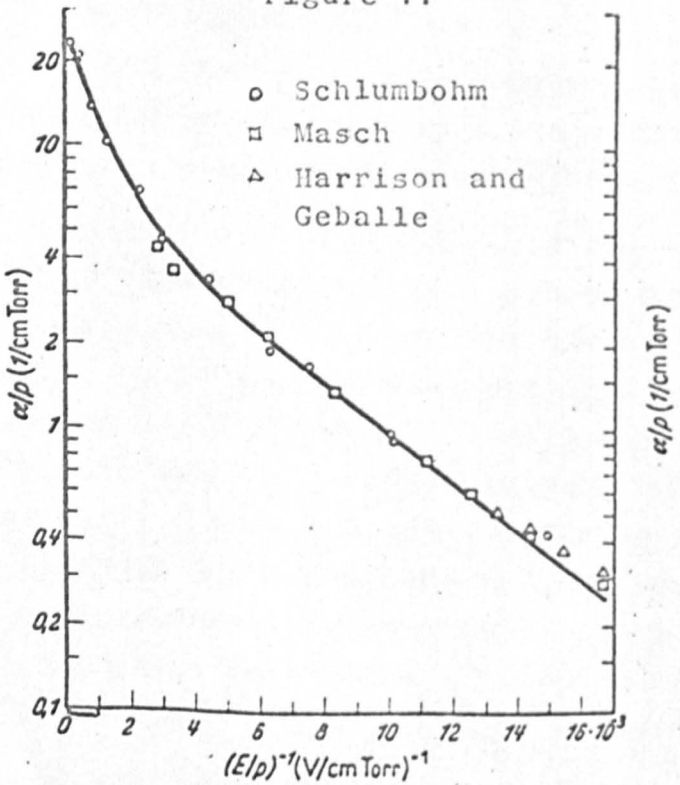

α/p vs E/p for high E/p in oxygen

Figure 12

for high gas purity and differential pumping is often necessary. The experimental data obtained from these experiments are discussed in the next three sections along with those obtained from the other experiments described in this section.

2.4 Experimental Data on Primary Ionization Coefficient

Experimental data on α's in oxygen appear to be mainly in the region $30 < E/p < 50$ V/cm torr. At low E/p the ionization processes are far less predominant, of course, than electron attachment processes and this explains the accumulation of data on η with hardly any on α, in the region $0 < E/p < 30$ V/cm torr. For example, Kuffel (44) uses the expression

$$\frac{I_2}{I_1} = e^{-\eta(x_2-x_1)}$$

which 'does not allow for the formation of new electrons by ionization', to determine η, while α is considered to be merely a correction term, even when the 'correction' turns out to be more than 100%.

Masch (50) obtained a wide range of the ionization coefficients in oxygen using a Townsend type apparatus. This was the first set of results to be published in this region since those of Townsend himself (20). Harrison and Geballe (31) used the Townsend method again in 1952, but they measured α and η simultaneously using a curve-fitting technique employing equation 1.6. In 1961 Prasad and Craggs (54) published their results which agree reasonably well with those of Harrison and Geballe (figure 11), but the agreement with the results of Masch is not very good, possibly because Masch's values have not been corrected for attachment. This is apparent from the fact that in the

higher E/p region where attachment is almost negligible, the agreement is quite good.

Schlumbohm (49) has determined α's for oxygen (as well as many other gases) in the range $60 < E/p < 2000$ V/cm torr from analyses of oscillograms of electron avalanches. Considering the different techniques used, and the time interval of 32 years between the two investigations, the agreement between the results of Schlumbohm and Masch is remarkable. (Figure 12).

The ionization cross sections have recently been measured by Asundi, Craggs and Kurepa (59) using electron beams in the energy range of 13 to 90 eV. This was done with both a Lozier type apparatus and a Tate and Smith type apparatus.

2.5 Experimental Data on the Attachment Coefficient

There is a great quantity of data available on η in the lower E/p region, but unfortunately they do not all agree very well with each other. This is hardly surprising, however, when one takes into account the widely different techniques used.

In the region $0 < E/p < 50$ V/cm torr, a two body attachment process

$$e + O_2 \longrightarrow O_2^{-*} \longrightarrow O + O^- + \text{k.e.}$$

was assumed to take place right up until 1959, when the experiments of Chanin, Phelps and Biondi (48) established that in this region η/p is a pressure dependent process up to an E/p of 3 V/cm torr. They also established that in this region η/p^2 is a pressure independent function indicating a three body attachment process of the type

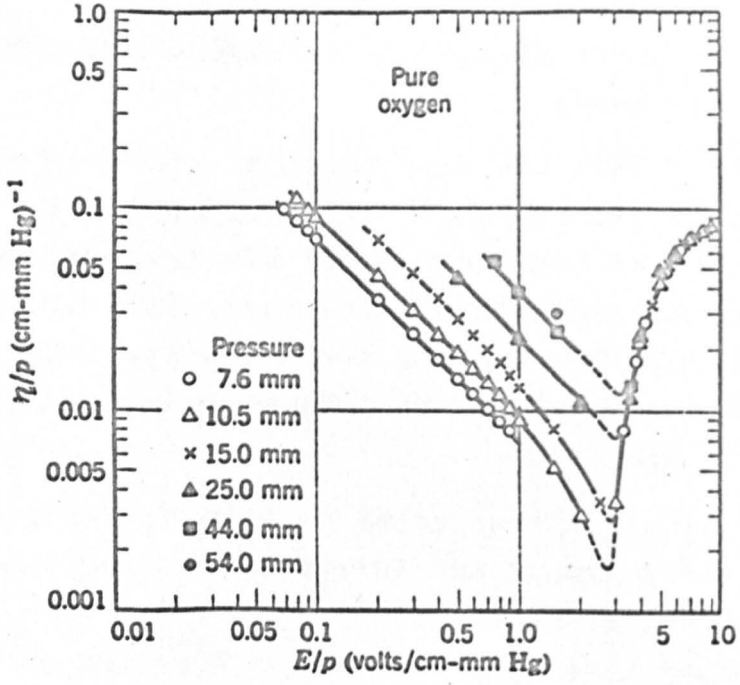

η/p vs E/p in oxygen for very low E/p.

Figure 13 a

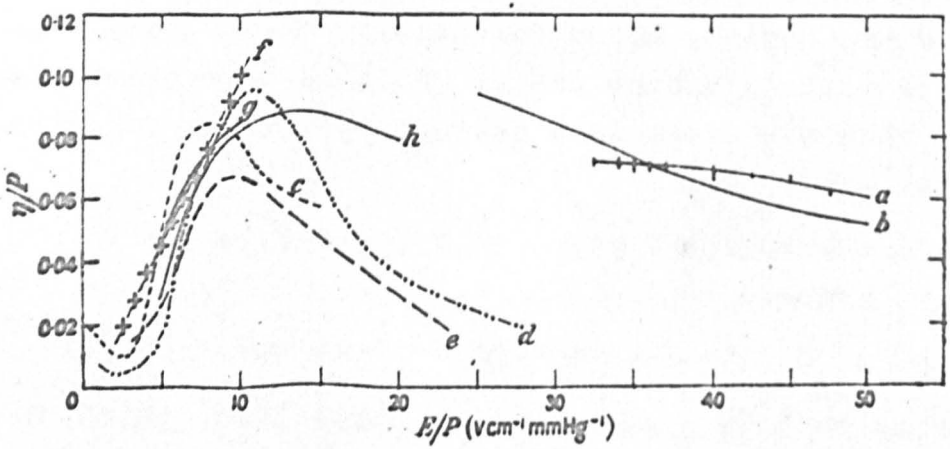

η/p vs E/p in oxygen for moderate E/p.

a. Prasad and Craggs, b. Harrison and Geballe, c. Bradbur

d. Kuffel, e. Herreng, f. Doehring, g. Chanin et al

h. Huxley et al

Figure 13 b

$$e + O_2 + X \longrightarrow O_2^- + X + k.e.$$

This pressure dependence of η/p below E/p = 3 V/cm torr was not known to or investigated by earlier experimenters and therefore, below this E/p their results of η/p are not significant. Chanin et al also measured the effectiveness of other gases like nitrogen and helium in playing the part of the third body required in the above process. They found a maximum for the three body attachment at an average electron energy of about 0·01 eV. Figure 13a is a summary of their results. The pressure dependence of η/p has been verified since by Chatterton and Craggs (45).

The variation of η/p with E/p has been investigated by a fair number of workers (see fig 13b). De Bitteto and Fisher (66) confined their experiments to the region where $\alpha = \eta$ and they found that the critical E/p for this was 35.6 V/cm torr. Harrison and Geballe (31) covered the region $20 < E/p < 70$ V/cm torr and the results of Prasad and Craggs agree with these reasonably well in the region where they overlap, viz $30 < E/p < 60$ V/cm torr. Llewellyn Jones, Dutton and Morgan (67) publish results in the region $34 < E/p < 39$ V/cm torr, which are less than half the magnitude of the others. However, no explanation for the lower values has been given.

The normalized cross section for formation of O^- ions by the dissociative attachment process has been obtained by Schulz (65), Craggs, Thorburn and Tozer (58), Buchel'Nikova (60) and Asundi, Craggs and Kurepa (59) in recent years. These are all results from beam experiments (described in previous sections). The agreement among these authors is very good indeed as regards the appearance potential

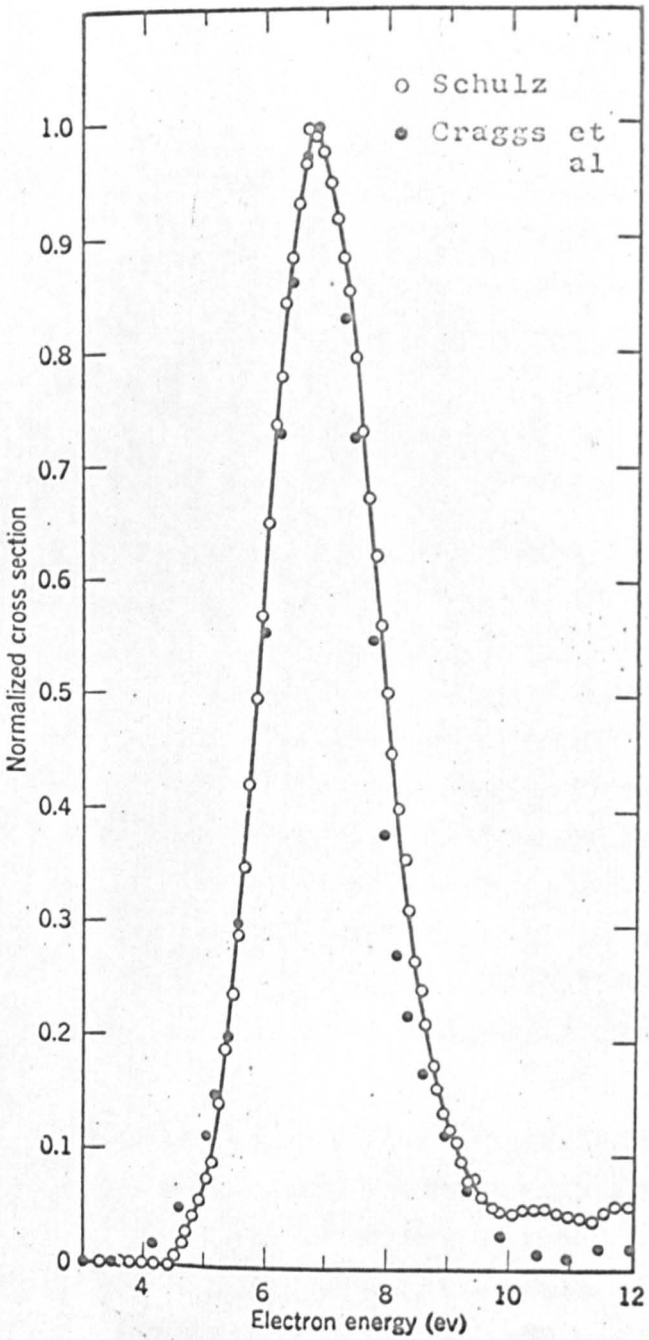

Cross Sections for O^- Production vs Electron Energy

Figure 13 c

corresponding to an energy of 4.6 eV and the energy for maximum cross section at 6.7 eV. The maximum cross section itself comes out to be 1.3×10^{-18} cm^2 in all the experiments except that of Craggs et al ($2{\cdot}25 \times 10^{-8}$ cm^2). Fig 13c shows the results of Schulz and Craggs et al.

Ion pair formation is possible in oxygen at electron energies above 17 eV:

$$e + O_2 \longrightarrow O^- + O^+ + e$$

The dissociation energy of O_2 is 5·1 eV while 13·6 eV is required to ionize an oxygen atom. But the electron affinity of the atom, 1·5 eV is released in capturing the electron, and thus the threshold for this reaction comes out to be 17·2 eV. This has been experimentally verified by Lozier with the retarding potential method in 1934 (68) and Hagstrum and Tate (69) using a mass spectrograph method.

2.6 Breakdown Voltages

Fricke's curves (26) appear to be the earliest published for the relationship between sparking potentials and pd in oxygen. He used iron electrodes and covered the pd range of 0·2 to 12 cm torr at pressures of a few torr. His results are given in fig 6. This gas could not have been very pure, because of the poor vacuum techniques used, but this is further discussed in Chapter 5.

De Bitteto and Fisher (66) chose the value of E/p where $\alpha = \eta$, for their investigation of the breakdown phenomenon in oxygen. At this value, the breakdown condition becomes $\gamma.pd.\alpha = 1$. The value of γ at an E/p of 35;4 V/cm torr has been reported by them as 0·045 for a nickel cathode at gas pressures of the order of 300 torr. The not too high

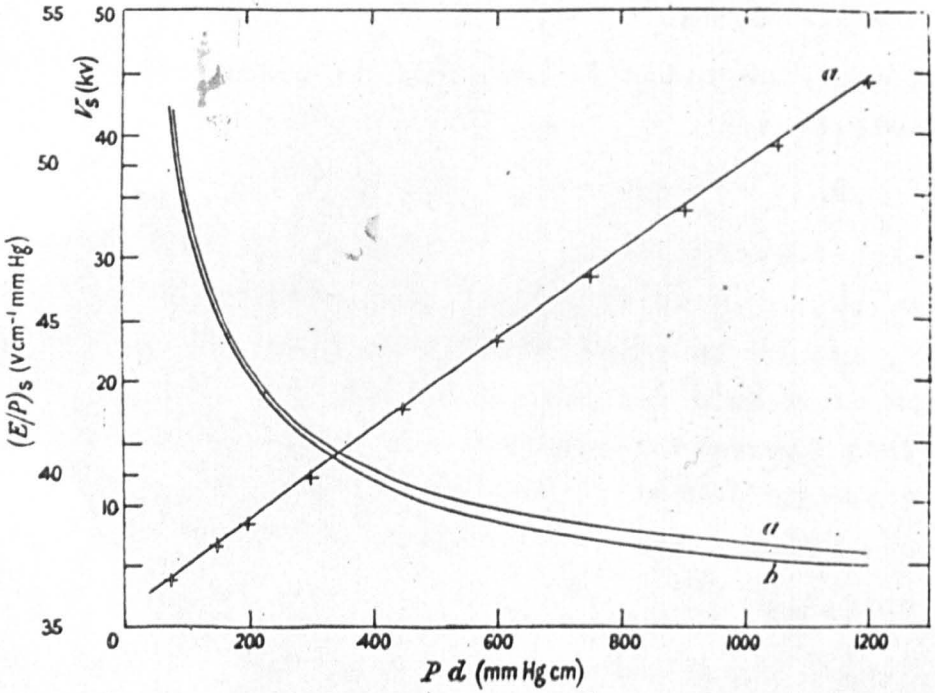

Sparking Potential Measurements

of Prasad and Craggs

(a - dural cathode; b - platinum cathode)

Figure 14.

values of V_s in oxygen in spite of the loss of electrons from the avalanche due to attachment are here attributed to the large secondary coefficient which seems to compensate for this.

Prasad and Craggs (54) have investigated the variation of V_s over a pd range of 50 to 1200 cm torr in oxygen with platinum and dural cathodes. Their results are given in figure 14. They were able to deduce the values of the secondary coefficient in two ways: by estimating the effects of γ on the upcurving part of the log I vs d curve and by making use of the breakdown criterion and sparking potential measurements, the values obtained in both these methods seeming to agree quite well.

2.7 Conclusions

While there is a considerable amount of data available for some regions of electron energies for both the ionization and attachment coefficients, it is obvious that there is a great deal of discrepancy among the results and also there are several regions where more work still needs to be done, particularly in the region $E/p > 50$ V/cm torr. It was with these facts in mind that the work described in this thesis was undertaken.

CHAPTER III

DESCRIPTION OF APPARATUS

3.1 Introduction

Townsend's method was adopted to investigate the discharge phenomena in oxygen referred to in section 1.10, i.e. pre-breakdown currents and sparking potentials were measured. For convenience the apparatus used in this investigation has been divided into four sections, the vacuum system including the manifold, the gas supply, the experimental tube and the electrical equipment.

3.2 The Vacuum System

The vacuum system was made of pyrex glass. A conventional rotary oil pump was used as a backing pump while a boat containing phosphorous pentoxide prevented water vapour getting to the rotary pump. The high vacuum was produced with a Jencon three-stage mercury diffusion pump. Grease taps were used only on the higher pressure side of the diffusion pump while liquid nitrogen traps were used immediately above the diffusion pump to prevent mercury vapour contaminating the high vacuum side. The manifold was mounted above the cold traps.

In the earlier part of the work, a Penning gauge positioned under the manifold was incorporated in the system, between the traps and the manifold. The Penning gauge was made in the laboratory and it consisted of a double cathode made of nickel sheet cut into circles of 1 cm diameter and kept apart at a distance of about a cm with a nickel ring shaped anode between them. A magnetic field of 600 Gauss was applied normal to the plates by a

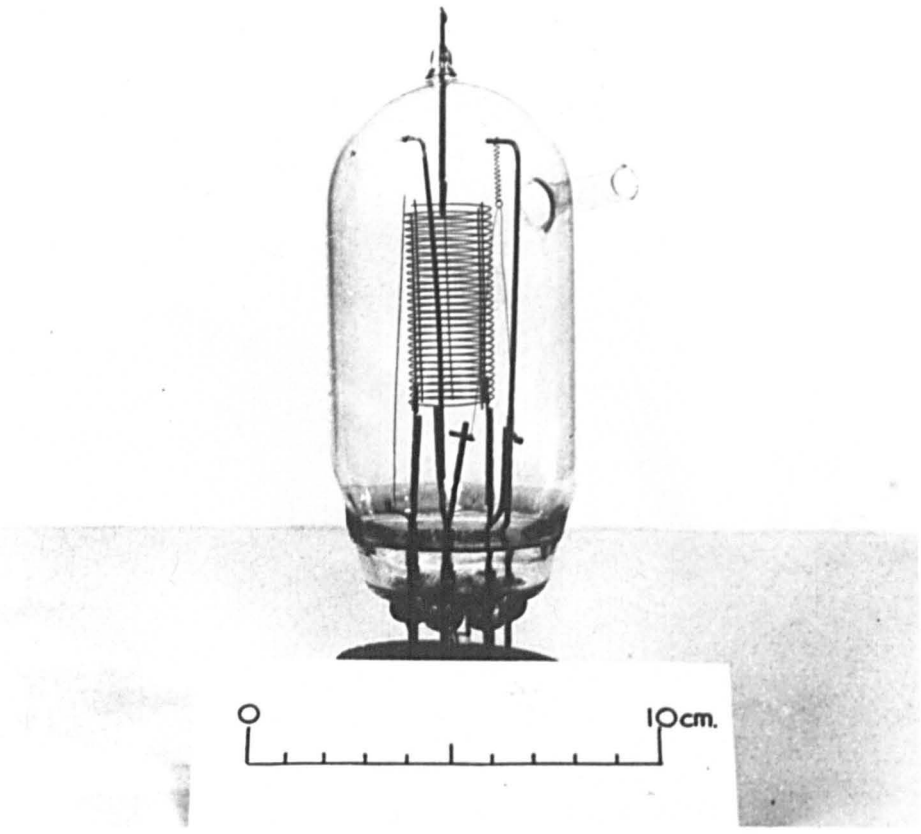

A Bayard-Alpert Ionization Gauge

Figure 16.

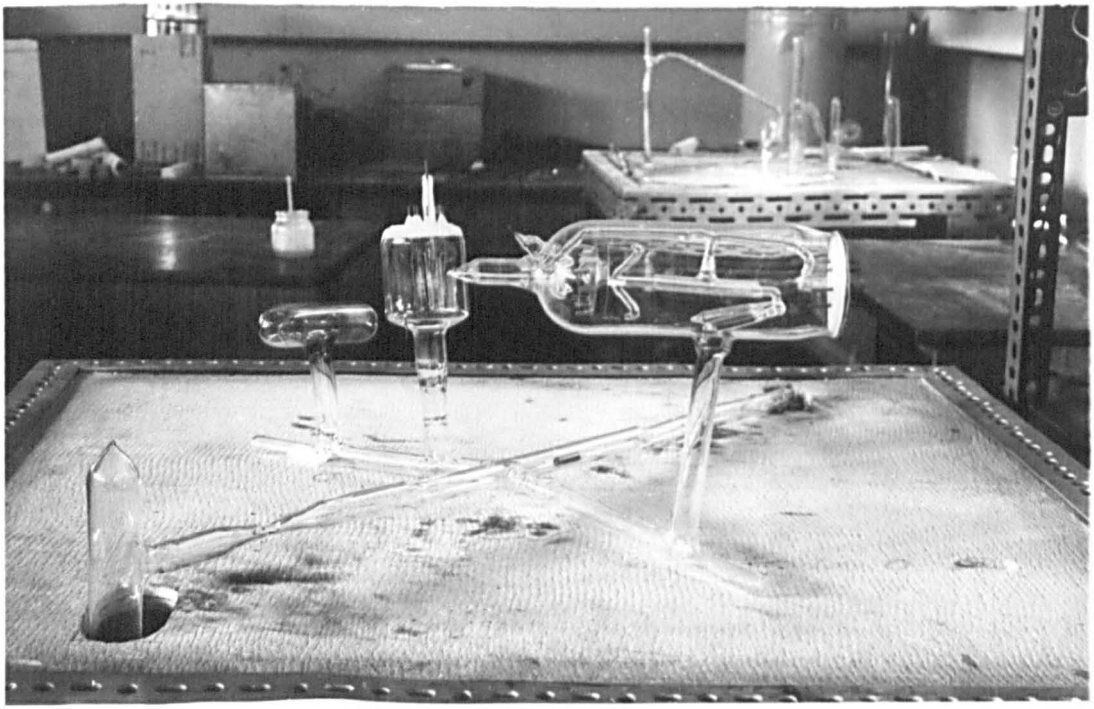

A Typical Manifold

(Photograph taken with tube 5 mounted)

Figure 15.

small permanent magnet, while the potential difference between the anode and a cathode was 2 kV. This arrangement should read pressures of 10^{-3} to 10^{-6} torr, but owing to the weakening of the magnetic field the pressure readings were found to be inaccurate on comparison with the results of the Alpert gauge and therefore, the Penning gauge was not included in later vacuum circuits.

The backing pump produced pressures of the order of 10^{-3} torr while the mercury diffusion pump could produce pressures as low as 10^{-7} torr.

3.3 The Manifold

The manifold was connected to the pumps through a constriction which could be sealed off to isolate the manifold. Fig 15 shows a typical manifold. The constituents of the manifold were the experimental tube, an Alpert gauge and a getter tube, the whole assembly being bakable at 440°C.

The Bayard-Alpert gauge (70) was used as a pressure measuring instrument (in high vacua) and also as a pump. The gauges used in the earlier circuits were constructed in the laboratory (see fig 16). A commercial seven pin pinch was used to mount the cathode and the grid, two directly heated cathodes being provided, in case one burnt out, though only one was used at a time. These were made of fine tungsten wire mounted on nickel supports. The grid was again fine tungsten wire, wound round a copper former at roughly six turns per centimetre and spot welded on to three nickel rods. These acted as supports for the grid for mounting it on the pinch in between the two cathodes. The anode was a very fine tungsten wire, often etched to get it finer, placed along the axis of the grid structure and was suspended by a tungsten seal from the glass envelope. The pinch was then drop-sealed on to the envelope. The pumping action is described by

Schwartz (71) who points out that the major part of the pumping is done by the walls of the tube. The gauge when used as a pump is able to reduce the pressure in a sealed off manifold to below 10^{-8} torr.

In later experiments, commercially constructed Alpert gauges (Mullard 10G-12) were used. With the grid kept at -24 V and the anode at 144 V with respect to the cathode, the pressure in the system was given by

$$p = \frac{1}{12} \frac{I_g}{I_a}$$

where I_g and I_a are the anode and grid currents respectively. The filament current was supplied by a regavolt and the voltages on grid and anode supplied by dry batteries with suitable tappings.

The getter tube was just a glass tube sealed at both ends with a pumping arm and containing barium getters. These were spot-welded on to a nickel rod which was provided with "legs" such that the getters did not touch the walls of the tube: otherwise they could have cracked the tube when they became red hot. Provided the getters had been out-gassed very thoroughly beforehand, they were capable of bringing the pressure down by almost an order of magnitude after the system had been sealed off at 10^{-7} torr.

The manifold was provided with a side arm containing a "pig's-tail" breaker, in case it had to be pumped again after sealing off. The breaker was made by closing one end of a glass tube after drawing it very thin and narrow and also butt-joining the tube on to another tube. An iron slug (enclosed in glass tubing to prevent the metal

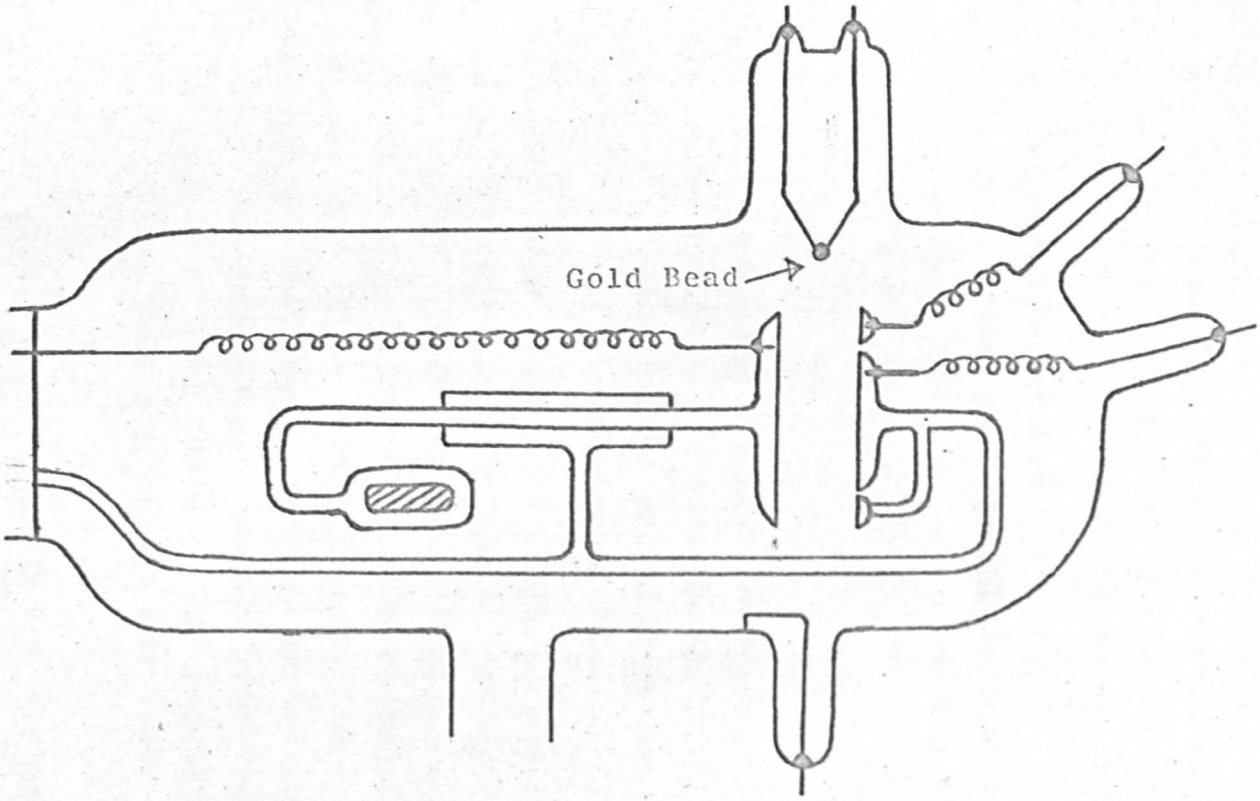

An Experimental Tube with Gold Film Electrodes

Figure 17.

outgassing) was moved magnetically to break the pig's-tail when necessary.

The connection between the manifold and the gas supply was also through a pig's-tail breaker which could be opened at will.

3.4 The Experimental Tube

The experimental tube consists mainly of the electrode assembly, a side tube to hold a gold bead in the case of tubes using evaporated gold film electrodes, and a quartz window (fig 17).

3.4.1 Electrode Assembly

The first four experimental tubes used evaporated film electrodes while the final one had a pair of solid platinum electrodes. The glass substrates for the gold film electrodes were prepared by melting hard glass rods on to carbon moulds and pressing them flat. When the required shape had been formed in the mould, a very hot but tiny flame was applied to one spot on the disc and a tungsten rod was pushed in until it just got through the whole thickness. A length of glass rod was also joined on at this stage to facilitate the final mounting of the electrode system and the whole electrode was annealed. This procedure was adequate to make the anode, cathode and the guard ring.

The surface of the electrodes was far from smooth on their removal from the carbon block. It was ground successively with different grades of carborundum powder and finally with Jewellers' Rouge to get it as smooth as

possible. The edges could still be rather jagged and sometimes had to be filed down. The oxide layer is removed from the tungsten rod also in the process, and so as to keep it conducting, a drop of aquadag was placed on it. Except for tube 3 the cathodes were all of 2.5cm diameter with a guard ring of width 0.5 cm around them, and the anodes were 3.6 cm in diameter. The electrodes of tube 3 had an overall diameter of 4.5 cm.

The cathode was then placed within the guard ring and the two joined together by means of the projecting glass rods. This joint was softened and the structure forced against a plane surface so that the two surfaces lay in the same plane and the cathode was arranged symmetrical within the guard ring. By moving the anode perpendicularly with respect to the cathode the gap distance was varied. Thus it was necessary to get the anode parallel to the cathode assembly. This was achieved by passing the glass rod (fixed normally to the anode) through a glass tube and bending the other end twice at right angles to form a 'U'. An iron slug enclosed in glass tubing was fixed on at the end of this, so that it could be operated magnetically from the outside. (The iron slug being heavy also ensured that the rod rested in the tube for all values of the gap distances so that the plane of the anode remained the same in all positions. In the case of tube 5 where platinum electrodes were used, the weight of the anode tended to tilt the iron slug upwards for small gap distances, but equilibrium could be restored by applying a small magnetic field to increase the downward force on the iron slug.) A connection from the glass tube which acted as

"rails", to the pinch ensured that the system was firmly fixed. Except in the case of tube 3, where the diameters of the electrodes were too large, the cathode assembly was also supported from the pinch. The cathode support for tube 3 had to be supplied from the envelope. This support was softened in all cases to get the cathode parallel to the anode in its equilibrium plane.

The electrical connections to the anode were made through the pinch. The cathode and guard ring had connections made to them directly through the envelope, because had they also been connected to the pinch, there could have been sparking over between the wires at high voltages. All electrical connections through the envelope were achieved by means of tungsten seals with spot welded nickel ribbons connecting them to the electrodes.

3.4.2 The Quartz Window

The quartz window was positioned so that ultraviolet light would fall at grazing incidence on the cathode from a suitably positioned mercury lamp. To join it on to the hard glass envelope, a quartz to pyrex graded seal was used.

3.4.3 The Gold Bead

The preparation and mounting of the gold bead was a lengthy and tedious process. A few inches of fine gold wire was wound on a notch made of tungsten wire spot welded on to strong nickel supports. This was mounted in a glass envelope through which a steady stream of hydrogen was passed (and burnt at the outlet). A

current was passed through the tungsten frame and gradually increased, until the gold wire melted and formed a bead. The bead was further heated and kept mobile for about a minute for further reduction of any impurities by the atmosphere of hydrogen. The cooled bead was mounted in a side tube of the experimental tube by two more tungsten seals. The mounting had to be arranged so that it was symmetrically between the electrodes at their maximum separation, and low enough to get a good coating of gold on the electrodes, while on the other hand, it had to be not so low as to produce field distortion by its presence.

The deposition of the gold film on to the glass substrate was carried out in ultra high vacuum by Joule heating at a current of about 10 A. A movable iron slug, prepared in the usual manner, was used to provide an optical window on the side of the tube, so as to facilitate the measurement of gap width. During the evaporation of the film, this was held in the position of the window by a small permanent magnet outside the tube.

The film deposited on the walls of the tube was used as an electrical screen and was earthed by means of a tungsten seal. A shield formed of a small piece of nickel sheet and suitably spot welded on to the bead assembly prevented the film from being deposited on the pinch, thereby short circuiting the high voltage supply (to the anode) and earth.

3.4.4 Tube 5

Tube 5 had platinum electrodes. This meant that the construction of the tube was a great deal easier, there

being no gold bead to prepare, position and evaporate, though the platinum electrodes did have to be outgassed. The electrodes themselves were of 3.6 cm diameter (including the guard-ring) and were machined to order by Johnson, Matthey and Company. They all had "tags" on them which were bent back to be normal to the plates and which were used for providing the mechanical support for the electrodes and for spot welding the electrical connections to them. The mechanical support was provided in the following way: tungsten rods with a bead of glass at one end, were spot welded on to two diametrically opposite tags and a short glass rod was fused on to the beads so that it formed a bar across the electrode; another glass rod was then joined on to the middle of this bar normally to the electrode. The assembly thereafter was exactly the same as for the other tubes, except for the fact that two iron slugs were needed instead of one, to balance the weight of the electrodes in this case. The envelope was also similar to the previous ones, only the side-arm carrying the gold bead was no longer necessary.

3.5 The Gas Supply

Several vacuum systems had to be constructed and tried before a satisfactory one was obtained. Originally, oxygen produced in the laboratory by electrolysis of barium hydroxide solution in distilled water was used, but later on spectroscopically pure oxygen supplied by the British Oxygen Company replaced this. A silver diffusion tube for the purification of the oxygen was thought desirable but found impractical. The details of

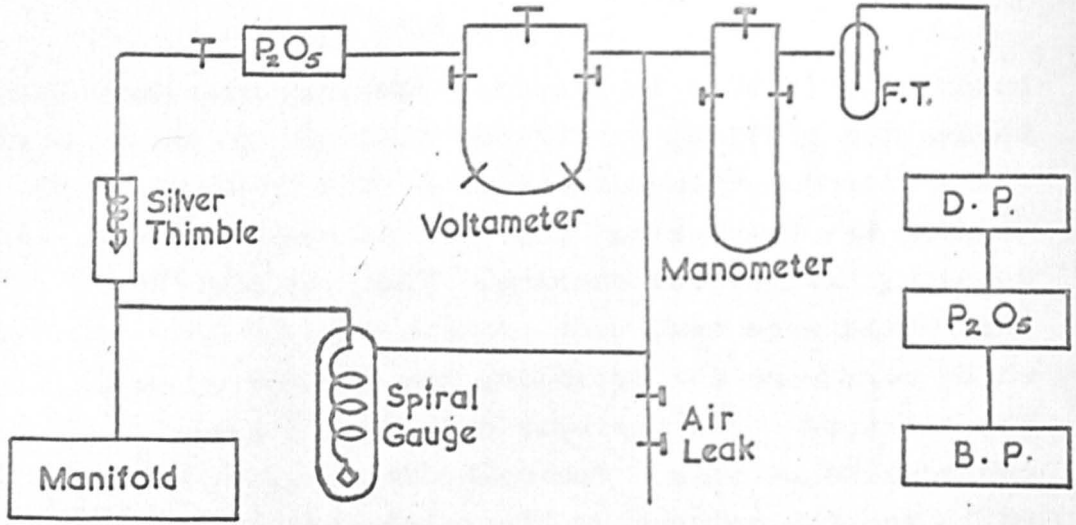

The First Vacuum System

Fig: 18.a

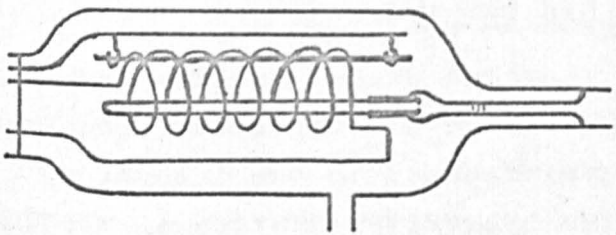

A Silver Diffusion Tube

Fig: 18.b

this part of the vacuum system are described in this section.

3.5.a Pumping

The same rotary oil pump that was mentioned in section 3.2 was used to pump the gas side also, to backing pressures. This was a perfectly adequate arrangement, while being economical and compact. The phosphorøus pentoxide trap was also shared, though a separate three-stage Jencons mercury diffusion pump was used to reach high vacua. Unfortunately grease taps could not be avcided altogether on this side of the vacuum system, but Apiezon N grease which has a vapour pressure of only 10^{-8} torr at room temperature was used on the taps. Freezing traps were used on the gas side also, to stop mercury vapour contaminating the rest of the system.

3.5.b Gas Supply System 1

The first vacuum system designed and constructed is shown in fig 18a. The oil manometer contained silicone fluid oil, with one arm connected directly to the pumps and the other one to an air leak and the voltameter through grease taps. The oxygen from the voltameter was passed through phosphorøus pentoxide traps to dry it before it could get to the silver thimble. The other side of the silver thimble was connected to the manifold. To measure the pressure of the gas in the manifold, a spiral gauge was used, the spiral being connected to the manifold and the outer tube to the air leak.

(i) Silver Diffusion Tube

These were supplied by Johnson, Matthey and Company

and were made of silver tubing of about 1 mm bore; the length was about 90 mm with one end closed and the open end joined to a piece of platinum tubing of the same bore, 15 mm long. The platinum was sealed on to a piece of lead glass tubing which was joined via a graded seal to a pyrex tube. The coils for electrical heating were spot welded on to two pins of a commercial pinch and the pinch drop-sealed on to an envelope with a pumping arm and another arm to take the silver tube. The joint between the hard glass tube leading to the silver tube and the side arm of the envelope was achieved by means of an internal seal, and is shown in fig 18b. The tube was arranged so that it lay along the axis of the heating coils. At first a length of about 9" of platinum wire was used as the heater coil but as the tube refused to diffuse any appreciable amount of oxygen even when the current was sufficient to deposit black platinum all over the tube and eventually to burn out the wire, another tube had to be constructed. This was done on similar lines as those of Whetten and Young (72). The main difference between this and the previous tube was that here the heating element was a 20 mil nichrome wire with six turns per inch. The coil was supported by letting it rest on a ceramic rod suspended by two hooks on a thick nickel rod. The diffusion rate is quoted as only 0.5 c.c./hr/cm^2/mm thickness at a temperature of 700^{o}C and a pressure difference of 1 atmosphere (73) and is very much lower for lower temperatures. In the pyrex system used, it did not seem very safe to go very much beyond 500^{o}C, with air cooling provided for the glass envelope by means of a compressor. As the life of the coil turned out to be

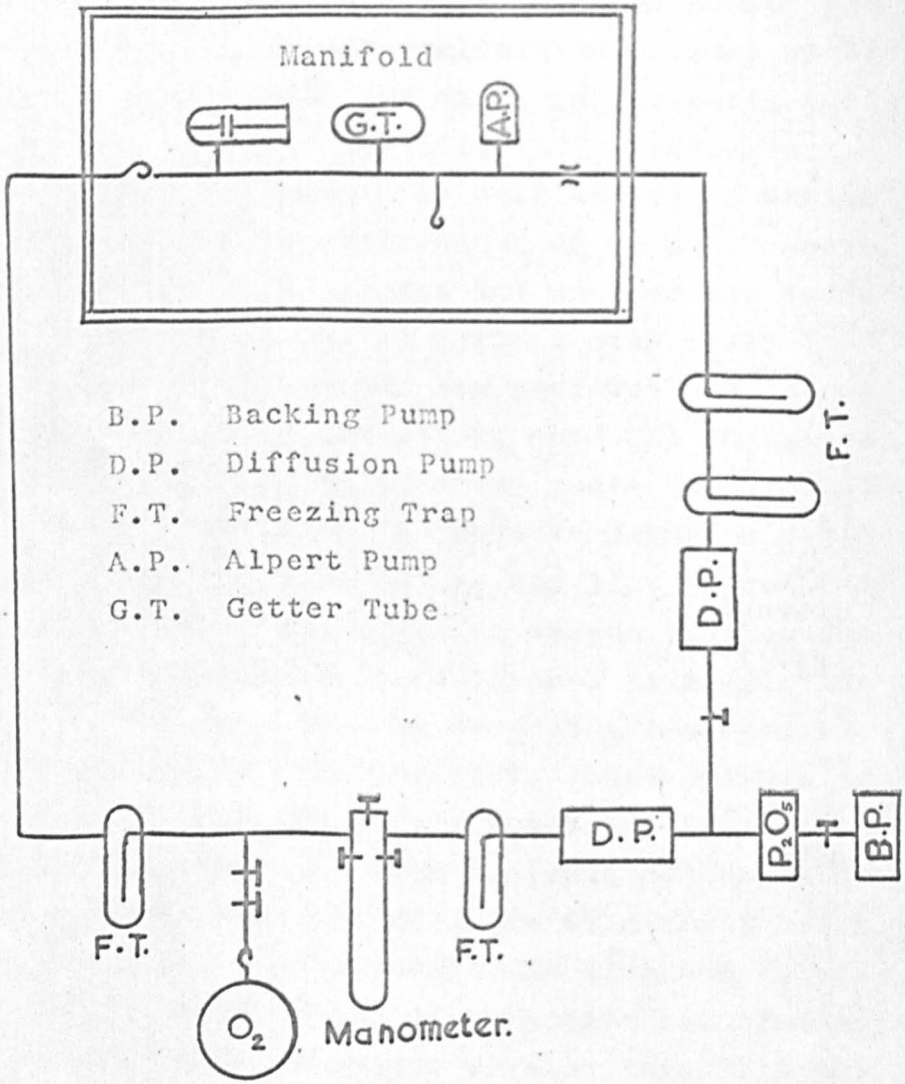

The Final Vacuum System

Fig: 19

much shorter than the time it took for any appreciable build up of pressure in the manifold, this arrangement had to be discarded finally. The heater current for both tubes was supplied from a "regavolt".

(ii) Spiral Gauge

The spiral gauge is a useful instrument for the measurement of pressures where grease taps, manometer oil etc have to be avoided. It works on the principle that the twist of a coil of thin glass tubing changes when the pressure inside the spiral is different from that outside it. The spiral was connected to the manifold, in this case, and the outer tube to the manometer. The suspension of the spiral carries a small mirror on it, so any deflection can be magnified several times by a suitable lamp and scale arrangement in conjunction with the mirror. With any pressure in the manifold, the air-leak arrangement could be used to let air into one arm of the previously evacuated manometer, till there was null deflection recorded on the scale. Now the pressure inside and outside the spiral should be equal and could be read off the manometer directly.

3.5.c Gas Supply System 2

The system described in the last section had to be modified after the abandoning of the silver diffusion tube. The voltameter was replaced by a litre flask of oxygen supplied by the British Oxygen Company and a further freezing trap was introduced just before the manifold to freeze out impurities such as water vapour, vapour from the grease taps, and vapour from the oil manometer. The air leak was no longer necessary and

Voltage Source and Measuring Apparatus

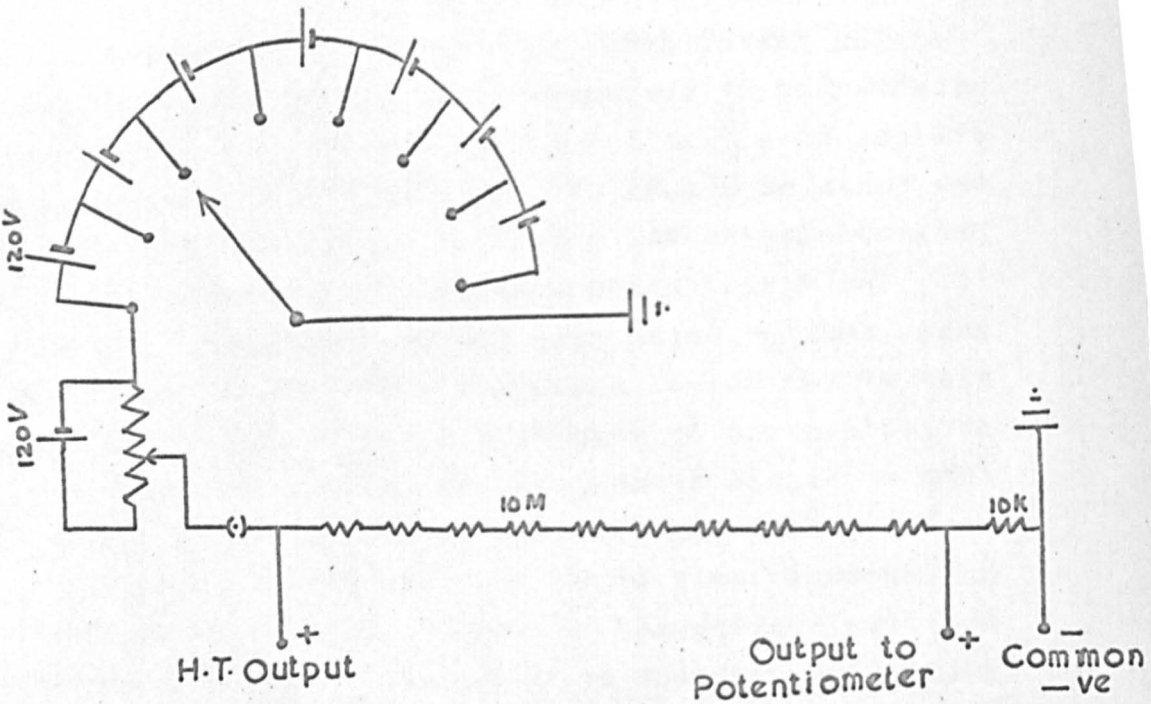

Fig: 20

therefore was eliminated. The whole system can thus be schematically represented as in fig19.

The oxygen flask was supplied with a long neck and a pig's tail breaker. A side arm was therefore put on it to take an iron slug and two taps were attached in series to the neck, so that after pumping, the breaker could be shattered by the slug and by operating the two taps oxygen could be let into the system in small quantities. The inclusion of the grease taps was inevitable, but the freezing trap just before the manifold should have removed the bulk of impurities before the gas entered the manifold.

3.6 Electrical Equipment

3.6.a Voltage Source and Voltage Measuring Apparatus

For both parts of the experiment (i.e. sparking potential measurements and pre-breakdown current measurements), the voltage was supplied by a bank of about eight 120 V dry batteries connected in series. The negative of this was earthed and the positive connected to the anode. The guard ring was also earthed through a high resistor of about 3 Mohms while the cathode was earthed through the electrometer for the pre-breakdown current measurements and through a Cambridge spot galvanometer and a 3 Mohm resistor for the sparking potential measurements. A potential divider arrangement was made by connecting a 100 Kohm resistor across one of the batteries and the circuit shown in fig 20 was constructed so that any voltage (0 - 960) could be obtained easily at the output terminals. The bank of batteries was chosen for the voltage supply because of their high stability.

To measure the voltage accurately, a resistance chain was made. Ten 1 Mohm resistors were each calibrated against a standard 1 Mohm, and then connected in series with a calibrated 10 Kohm. The total voltage output was connected across this chain and the voltage across the 10 Kohm measured on a conventional potentiometer (Cropico P3). With this arrangement, changes in voltage as small as o.1 V could be produced and measured.

3.6.b Current Measurements

The ionization currents were measured by means of a Vibron 33B electrometer in the earlier tubes and by a Keithly 600A electrometer in the last two tubes.

The currents measured were of the order of 10^{-11} A. The Vibron had scales corresponding to 1 V to 10 mV and the resistors included were 10^{6}, 10^{9} and 10^{10} ohms, so that it was possible to measure currents down to 10^{-13}A. The accuracy claimed by the manufacturers is 2% of the full scale reading. In spite of using screened co-axial cables throughout, keeping the length of this to a minimum and screening the tube by means of the earthed gold film internally and by a sheet of metal foil wrapped round it externally, the reading of the instrument was found to be very very unstable under laboratory conditions, and therefore nowhere near the accuracy claimed could be achieved in practice.

The Keithly 600A was basically a d.c. vacuum tube voltmeter with electrometer tube inputs. It could measure 3 to 10^{-13}A full scale on overlapping scales and the manufacturers quote an accuracy of 4% on the 3.10^{-11} to 10^{-13}A scales. The input resistance was of the order of

10^{14} ohms. In spite of the slightly lower accuracy, this instrument was found very much more preferable to the Vibron because of its stability and ease of cutting out external noise.

3.7 Conclusion

In this chapter, some of the essential features of the apparatus used in this investigation have been described, while in the following chapter some of the experimental techniques used will be discussed.

CHAPTER IV

EXPERIMENTAL TECHNIQUES

4.1 Introduction

This chapter describes the techniques used in this work, mainly consisting of two parts: vacuum techniques involving the processing of the experimental tubes and techniques for analysing the data obtained from the experimental tubes.

4.2 Vacuum Techniques

The apparatus has been described in the last chapter. The first step towards processing the experimental tubes, after construction was, of course, pumping the whole manifold system. The backing pump was switched on first, and the system examined for leaks; at backing pressure the "tes-vac" was found to be extremely useful for detecting pinholes, small pinholes being enlarged and made visible by the instrument. When the system was free of pinholes, the diffusion pump was switched on and the freezing traps filled with liquid nitrogen. The pressure could then go down to 10^{-5} torr. If the manifold pressure stayed very much above this, a leak was again suspected and searched for by a process of elimination. If there were no leaks, however, one could then proceed to bake the manifold, with both pumps still running. As soon as the oven was switched on, the pressure would obviously increase, because of the outgassing of the glass and metal parts of the system. In a leak-free system, however, this would be pumped away eventually and after

about 24 hours, the oven could be switched off. While the glass was still warm, the oven was taken off and all the metallic parts outgassed at a higher temperature, since 440°C, which is about the highest possible outgassing temperature for pyrex, is far too low for metals. The filament of the Alpert pump was outgassed for about 2 hours by passing a current through it from the "regavolt" (which was able to deliver a current of 10 A at a p.d. of 20 V) until it was hotter than it would ever get during the pumping. The grid of the Alpert pump, the barium getters and the bulk-metallic parts of the experimental tube (e.g. nickel shields) were outgassed by heating them to red heat by a radio-frequency heater. The gold bead also was outgassed by getting it mobile and evaporating it slightly with a regavolt. The constriction between the pumps and the manifold needed special treatment, of course, as it would get much hotter than 440°C during seal-off. For this reason, a gas flame was allowed to play on it for about 10 minutes, until the glass was on the verge of collapsing. The typical pressure at the end of this procedure was about 10^{-7} torr. If at this stage the pressure was much higher, then a leak was suspected but it was very difficult to detect it, and a process of elimination had to be adopted.

Another period of baking at 440°C followed, lasting for about 48 hours, at the end of which the outgassing of the metal parts was repeated. The pressure registered on the Alpert pump at this stage was below 10^{-7} torr, when the constriction was sealed off using a small but hot flame so that the outgassing was kept to a minimum. A getter was also fired at this point to pump any gas away.

As a further test for leaks, the Alpert pump was switched off then, and the system left for a day. If the pressure stayed constant during this period, it was assumed that the system was leak-free and the Alpert pump was switched on so that it could reduce the pressure further. The pressure after a day of Alpert pumping was less than 10^{-8} torr, when the spot galvanometer ceased to register the ion current, and at this stage pumping was usually stopped.

4.3 Evaporation of the Gold Bead

The evaporation of the film on to the glass substrates was carried out with the electrodes at their maximum separation, so that the electrode surfaces would subtend the largest solid angle at the bead. Before evaporation, the loose iron slug in the tube was held against the walls of the tube using a small magnet to act as a shield, so that when evaporation was completed and magnet withdrawn, the iron slug rolled off leaving a transparent "window". The window was so positioned that the gap separation was clearly visible from outside the tube. The evaporation itself was done with the regavolt which was earlier used for the outgassing. Care had to be taken during evaporation not to jerk the tube at all as this could have caused the liquefied bead to fall off, and further, not to overheat the bead as this could have caused the tungsten seals to get red hot and crack the glass. The maximum current was switched on and off gradually at the beginning and the end of the operation, as any sudden change in temperature would have cracked the seals.

4.4 Sparking Potential Measurements

For the measurement of sparking potentials, the electrical circuits were only slightly different from the circuit used for ionization current measurements. The electrometer was obviously not necessary in this case and was replaced by a Cambridge spot galvanometer with a 3 Mohm resistor in series with it. The anode voltage was varied very slowly by means of the potentiometer arrangement on the voltage supply system and the current growth observed on the galvanometer. Under most circumstances, the sudden rapid increase in current on breakdown could very easily be seen on the meter, but in some cases the rise was more gradual. To allow for the latter case, the breakdown voltage was taken to be that voltage for which the current in the circuit was 0·5 μA. The current was seen to be self-maintained for this condition. To repeat the experiment the same procedure was adopted, but knowing the approximate value of the sparking potential, one could be even more careful in changing the voltage gradually; care was taken not to repeat the measurements with less than 2 minutes interval between sparks, as the electrodes could have got charged up in the first spark and thus affected the work function of the cathode. With this procedure the sparking potentials could be determined to $\pm$ 2 V using gold film electrodes and $\pm$ 0.2 V using the platinum electrodes. The method of varying $p_o d$ was to keep the pressure p_o a constant and to use the whole range of gap distances possible for any one curve, and then to change p_o to another value.

4.5 Current Measurements

4.5.a Initial Photoelectric Current

It is of primary importance that the initial photoelectric current I_o stays a constant throughout any one run of the ionization current measurement, as can be seen from equation 1.6. The test for constancy was carried out in two parts. The first part was to check the output of the low pressure mercury lamp. Fletcher (74) has already analysed the intensities of the spectral lines of such a lamp and shown it to be monochromatic in the electron emitting region (λ less then 2747 Å), 99·92% of the total intensity being due to the 2536 Å line. The experimental tube was used to observe the constancy of the output of the lamp, by measuring the photoelectric saturation current in the tube over a period of time. This was done with the tube at a pressure of 10^{-8} torr, after the lamp had been allowed to "stabilize" for a couple of hours, the measurements being taken every 5 minutes for about 2 hours, roughly the time taken for a single run, and at intervals of about an hour for about 8 hours. The current stayed constant to within 3% in both cases.

The second part consisted of checking that the initial current stayed constant in the presence of oxygen for any given pressure, which effectively means checking that the work function of the cathode stayed constant. To check this indirectly, gas was allowed in at some pressure (a few torr), and the ionization current was measured every 15 minutes for a few hours. The voltage applied being the same in each case, the current I should

be a constant (see equation 1.6) provided that the photoelectric current I_o was. On checking I_o thus, a 5% random fluctuation was observed in the current. Since no gradual or systematic changes could be observed, the fluctuation was attributed to changes in room temperature rather than to any systematic changes in the work function of the cathode surface. The liquid nitrogen trap could easily have affected the temperature of the gas in the tube (depending on whether it was completely filled up or not) in addition to random fluctuations in room temperature.

Prasad discusses (54) the effect of oxygen pressure on I_o; using a platinum cathode, he observed an exponential decrease in I_o with gas pressure, the current dropping by a factor of four on reducing the gas pressure from 500 torr to 10 torr. As the pressure range covered by the present work was 1 torr to 10 torr, the drop in current due to this effect would be by a factor of only 1·05 over the whole range; moreover, as I_o was computed for each value of the pressure and each curve, this effect should not have any significance in this investigation.

4.5.b Variation of I_o with gap distance

It has already been mentioned that in this investigation, ultraviolet light was shone at grazing incidence on to the cathode. There was thus a risk that at small gap distances, the light could have been partially cut out by the anode, resulting in a reduction in I_o. The exact amount cut out would of course, depend upon the positioning of the lamp and the quartz window. Thus it

was necessary either to ensure that I_o stayed a constant at all measured gap distances or to estimate the percentage reduction in I_o for the gap distances affected and apply a correction to the measured value of current. With tube 1 a correction had to be applied for all gap distances up to 0.4 cm, but with tubes 4 and 5 the largest gap distance where any reduction in I_o took place was 0.15 cm and 0.10 cm respectively, which were less than the smallest gap distances used. This measurement was carried out before the gas was admitted into the tube in each case. Along with this, the saturation voltage was also determined and no measurement was taken involving smaller voltages.

4.5.c Procedure for Measuring I

The preceding sections have described the procedure adopted in getting the experimental tubes ready for taking readings. The actual procedure for taking readings was quite simple. The gas was let in at the required pressure, the pressure read off the oil manometer and converted to pressure in torr at 0^oC. Three or four values of E/p_o at intervals of 10 V/cm torr were chosen such that for the lowest values of gap distance and E/p_o the voltage to be applied was still above the saturation voltage, and for the largest gap distances and E/p_o the voltage was still well below the sparking potential. The voltage corresponding to each gap distance was calculated and applied to the electrodes and the corresponding ionization currents measured on the electrometer. Variation of gap distances was achieved by using an external magnet as mentioned earlier; gap distances were chosen at random

to begin with at intervals of 0·06 to 0·15 cm measured with a travelling microscope, but later on increments of 0·1 cm were used even though this was slightly more difficult to do as the cross wires of the travelling microscope had to be fixed at the required point and then the anode had to be moved to coincide with that. The maximum gap distance employed was 1·0 to 1·2 cm. For each E/p_o, about ten pairs of current and gap distance values (i.e. I, d values) were obtained, to enable a meaningful curve to be drawn.

4.6 Analysis of Readings to Determine α and η

It has been mentioned in chapter 2 that some earlier workers had used a curve-fitting method to determine α and η simultaneously. Moruzzi (75) pointed out that unless I_o was known, I_o would have to be taken as a third unknown in equation 1.6 , and then these techniques could only yield mean values of α and η with a spread of $\pm$100% and therefore that this method would hardly be of any use. However, if I_o could be estimated to any degree of accuracy, then the α and η values would be the only unknowns and they could be determined with a corresponding degree of accuracy and thus it can be seen that for this technique it is very important to obtain accurate values of I_o. Moruzzi lists three methods of determining I_o.

(i) Extrapolating a family of log I vs d curves to the single point where d = 0, I_o can be determined. Where α is greater than η, I_o can be found to $\pm$ 10%.

(ii) With a fixed electrode separation, current measurements are made as a function of applied voltage (arranged to produce no ionization) and the saturation current I_o

is determined. The accuracy is $\pm$ 5% for favourable conditions, but can be up to $\pm$ 30% for other conditions.

(iii) When $\frac{\alpha}{p} = \frac{\eta}{p}$, then

$$I = I_o(1 + \alpha d)$$ (de Bitteto and Fisher, 66)

So, the plot of I against d should yield a very accurate value of I_o. If the appropriate E/p is known, I_o can be determined to an accuracy of $\pm$ 2%. But this method can be of use only for a limited range of E/p's.

Sukhum (76) mentions another method for calculating $\frac{\alpha}{\eta}$. He considers two currents I_1 and I_2 and gap distances d and 2d and obtains an expression

$$\frac{\alpha}{\eta} = \frac{(I_1 - I_o)^2}{I_1^2 - I_o I_2}$$

This value can be substituted in the original equation to get α and η individually. He claims an accuracy of 3% for a given E/p. But I_o has to be estimated here also using one of the methods quoted above and should α be much bigger than η, a graphical method has to be used when the accuracy is reduced considerably.

Thus it would appear that calculating α, η and I_o from the readings obtained is a rather tedious process and therefore a simpler and more direct way of analysing the results was devised.

4.6.a Theory

To begin with, the effect of the secondary coefficient on the growth of current was assumed to be negligible and so the relevant current growth equation was equation 1.6 , which reads

$$I = I_o \frac{\alpha}{\alpha - \eta} \exp(\alpha - \eta)x - \frac{\eta I_o}{\alpha - \eta}$$

x being the gap distance.

It is obvious from this that a semilogarithmic plot of I against d would not have any simple form and therefore this was not attempted. However,

$$\frac{dI}{dx} = I_o \alpha . \exp(\alpha - \eta)x$$

and $$\log \frac{dI}{dx} = (\alpha - \eta)x + \log I_o \alpha$$

Therefore, $\log \frac{dI}{dx}$ plotted against x will be a straight line of slope $(\alpha - \eta)$ and y-intercept, $\log I_o \alpha$. Thus substituting for α and η and αI_o in the original equation, and using a pair of values (I,x) enabled ηI_o to be evaluated. Then knowing αI_o, ηI_o and $(\alpha - \eta)$, all three unknowns α, η and I_o can be calculated.

It may be pointed out that subsequent to the procedure outlined in the last paragraph being decided upon, a very similar method was suggested by Govinda Raju (77). He argued that

$$I + \delta I = \frac{\alpha I_o}{\alpha - \eta} e^{(\alpha - \eta)(x + \delta x)} - \frac{\eta I_o}{\alpha - \eta}$$

where δI is the increase in current corresponding to an increase in gap width δx, and as

$$I = \frac{\alpha I_o}{\alpha - \eta} e^{(\alpha - \eta)x} - \frac{\eta I_o}{\alpha - \eta}$$

$$I + \delta I = I\, e^{(\alpha - \eta)\delta x} + \frac{\eta I_o}{\alpha - \eta} (e^{(\alpha - \eta)\delta x} - 1)$$

It is evident from this that a plot of $(I + \delta I)$ against I for a constant δx would be a straight line of

slope $\exp(\alpha - \eta)\delta x$. Therefore, $(\alpha - \eta)$ could be found and then by a substitution in the original equation, α, η and I_o could all be determined.

4.6.b Modification of Davies-Milne Analysis

The Davies-Milne analysis was formulated for non-attaching gases to correct for the effect of the secondary coefficient on the linear part of the log I vs d curve and therefore α, the slope of this region. In the analysis described in the last section, it was mentioned that the effect of the secondary processes has been neglected. An analysis was formulated so that the method of successive approximation could be applied to the case where there are two variables. This is outlined in the next paragraph.

The full current growth equation reads as follows:

$$\frac{I}{I_o} = \frac{\alpha\, e^{(\alpha - \eta)x} - \eta}{(\alpha - \eta)\left[1 - \frac{W}{\alpha - \eta}(e^{(\alpha - \eta)x} - 1)\right]}.$$

With I_1, I_2, I_3 and I_4 referring to the ionization currents at gap distances of x_1, x_2, x_3 and x_4, it is possible to define two functions f_I and f_{II} where:

$$f_I(\alpha,\eta) = 0$$

$$= (I_1-I_2)I_3(e^{(\alpha-\eta)x_1} - e^{(\alpha-\eta)x_3})(e^{(\alpha-\eta)x_2} - \frac{\eta}{\alpha})$$

$$-(I_1-I_3)I_2(e^{(\alpha-\eta)x_1} - e^{(\alpha-\eta)x_2})(e^{(\alpha-\eta)x_3} - \frac{\eta}{\alpha})$$

$$f_{II}(\alpha,\eta) = 0$$

$$= (I_1-I_2)I_4(e^{(\alpha-\eta)x_1} - e^{(\alpha-\eta)x_4})(e^{(\alpha-\eta)x_2} - \frac{\eta}{\alpha})$$

$$- (I_1-I_4)I_2(e^{(\alpha-\eta)x_1} - e^{(\alpha-\eta)x_2})(e^{(\alpha-\eta)x_4} - \frac{\eta}{\alpha})$$

Taylors theorem can be applied to these functions since $f_I = 0$ and $f_{II} = 0$. If α' and η' be the approximate values of α and η, then leaving out all but first order terms, one can write

$$(\alpha-\alpha')\left(\frac{f_I}{\alpha}\right)_{(\alpha',\eta')} + (\eta-\eta')\left(\frac{f_I}{\eta}\right)_{(\alpha',\eta')} = -f_I(\alpha',\eta')$$

$$(\alpha-\alpha')\left(\frac{f_{II}}{\alpha}\right)_{(\alpha',\eta')} + (\eta-\eta')\left(\frac{f_{II}}{\eta}\right)_{(\alpha',\eta')} = -f_{II}(\alpha',\eta')$$

Solving these two simultaneous equations, one can obtain values of α and η which in turn can be substituted in the equation as α' and η' to get a new and more accurate set of values of α and η. This process can, in theory, be carried out until $(\alpha - \alpha')$ and $(\eta - \eta')$ are within any small limit that has been specified.

In practice, however, this was an extremely difficult procedure and could not be successfully applied to many readings for several reasons: the accuracy of the current measurements did not warrant the use of the functions f_I and f_{II} and their derivatives to any degree of accuracy, the convergence of $(\alpha - \alpha')$ and $(\eta - \eta')$ was very small and the process took an almost unjustifiably long time to work out. Therefore, while this was recognised as a possible method to correct α and η for secondary effects, it was not pursued much further in this investigation.

4.6.c Details of Analysis

The practical application of the theory outlined in section 4.6.a involves finding out the rate of change of variation of current with gap distance. With the

preliminary results a graphical procedure was adopted for this purpose. For each E/p, a linear plot of I against x was made, the best curve drawn through them and the gradient of the curve at different points determined by drawing the tangents at these points. These gradients were then plotted against the appropriate gap distances on semi-logarithmic graph paper. This procedure established that log $\frac{dI}{dx}$ vs x was in fact a straight line, provided one did not exceed d beyond 0·8 cm or so, but the scatter in the calculated values was so high as to make another method of finding $\frac{dI}{dx}$ very desirable. (This method was applied actually, to the results from tube 1 only; the history of the tube, described in Chapter 5, is probably partly responsible for the results being what they are.)

The final analysis was, in fact, done using an IBM 1620 computer. Numerical analysis was employed to find the derivatives at the different points. As the gap distances had been changed in unequal steps, an interpolation formula had to be used before the derivative could be determined. Lagrange's polynomial for unequal intervals was used to effect the interpolation; given (n+1) pairs of values (I_o,x_o), (I_1,x_1), $\ldots\ldots(I_n,x_n)$, the n'th degree polynomial can be derived as (78),

$$I = P(x)$$

$$= \sum_{o}^{n} I_s \frac{(x-x_o)\,(x-x_1)\ldots(x-x_{s-1})(x-x_{s+1})\ldots(x-x_n)}{(x_s-x_o)(x_s-x_1)\ldots(x_s-x_{s-1})(x_s-x_{s+1})\ldots(x_s-x_n)}$$

which would go through all the (n+1) points.

The computer was programmed (see appendix 1 for the actual programme) so that given the currents for say, five

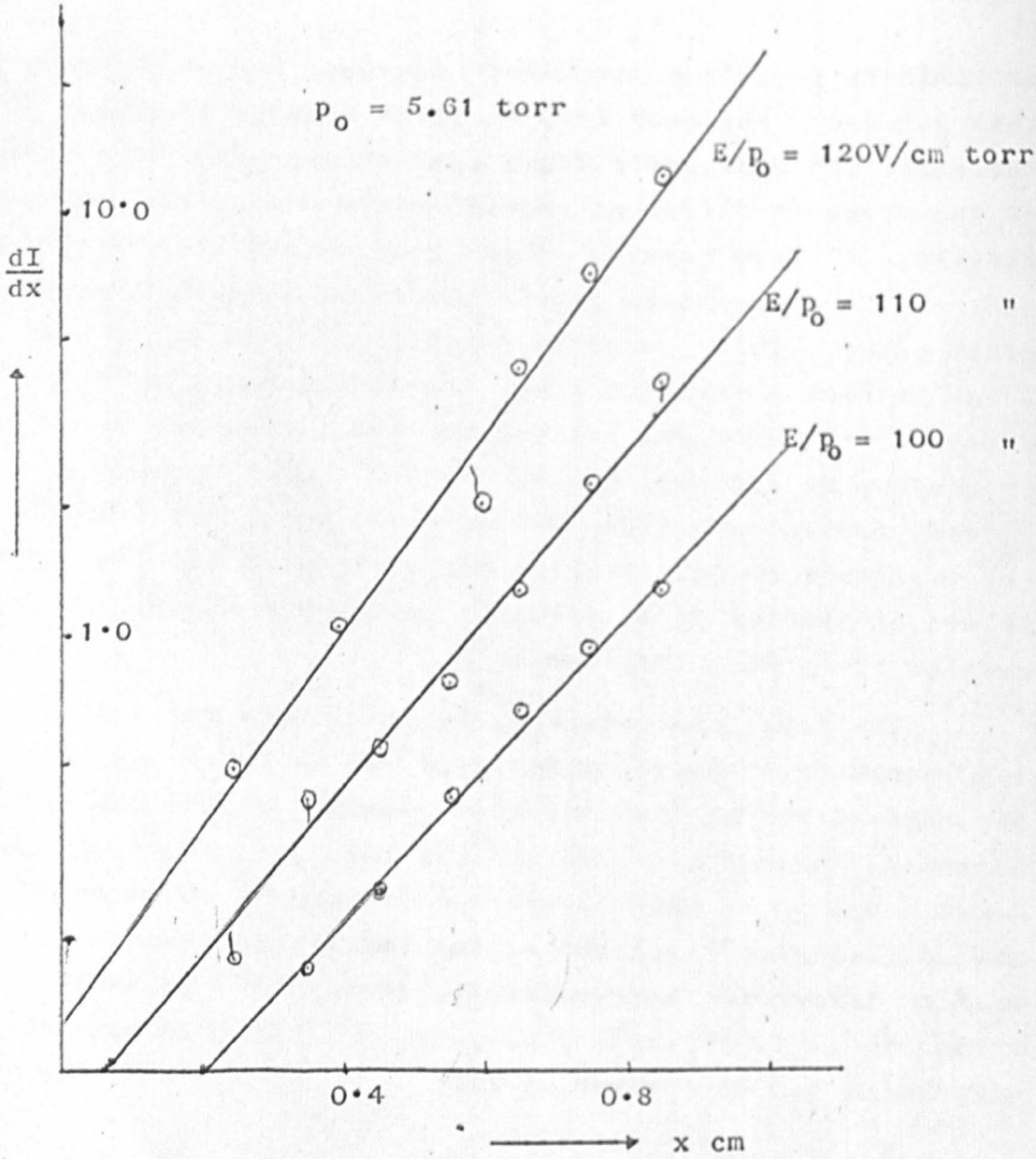

A Typical Plot of log $\frac{dI}{dx}$ vs x.

Figure 21.

gap distances ranging between 0·15 and 0·8 cm, it would produce values of currents for regular intervals of 0·02 cm, e.g. at 0·16, 0·18, 0·20 ... up to 0·80 cm. Once this had been achieved, it was of course an easy matter to calculate $\frac{(I + \delta I) - I}{(x + \delta x) - x}$ for any value of gap distance.

Fig21 shows a log $\frac{dI}{dx}$ vs x graph drawn at this stage from a set of computed values. This is only given as an illustrative example, as the procedure of drawing a graph was not followed as a rule. Instead, the method of least squares was applied to each set of values to obtain the slope and the y-intercept of the best straight line through these points. The programme given in appendix 2 was used for this purpose. This programme also went on to substitute the values of slope and y-intercept for $(\alpha-\eta)$ and log αI_o in the original equation (eq. 1.6). Thus one could obtain values of ηI_o and therefore α, η, and I_o separately. The programme was written in such a way that α/p, η/p and I_o were printed out as output of the computer.

4.7 Conclusion

Some of the experimental techniques used in the investigation have been mentioned in this chapter. Ultra-high vacuum techniques used with the hard glass system were conventional. The data analysis mentioned in this chapter, however, does have the advantage that a knowledge of the initial current is not needed; the importance of this fact is apparent from the references (75, 76, 79). It may be mentioned here that I_o obtained from the individual members of a family of curves was a constant within experimental error.

CHAPTER 5

RESULTS AND DISCUSSION

5.1 Introduction

In this final chapter, the results obtained from the experimental tubes are set out and attempts are made to interpret them in terms of the gas discharge phenomena discussed in chapter 1. Five experimental tubes were made, and at this stage it is useful to consider briefly the history of each and then in subsequent sections the results obtained from them are discussed in some detail.

5.2 History of the Five Tubes

The first tube was constructed for use with the silver thimble using the platinum wire heater. A residual pressure of about 10^{-8} torr had been obtained and the gold film laid down before it was realized that the thimble did not function properly, with the filament burning out, and so the tube had to be let down to air and processed again. This meant that the gold film electrodes were no longer very clean and so the sparking potential and prebreakdown current measurements which were taken with tube 1 had to be checked with another tube under cleaner conditions.

The second silver thimble had a nichrome heater which was found to work before the gold film was laid down, but unfortunately burnt out again during the actual run before any appreciable pressure had built up in the tube. So once again the thimble had to be discarded and the tube let down to air. However, after reprocessing the tube, it was

thought desirable to put a fresh layer of gold on the electrodes, so that the actual surface would be as clean as possible. The results found with this tube were found to be rather unusual and are discussed in section 5.3.

The third tube had the largest pair of electrodes used in this investigation, but soon after beginning to take readings, it was found that no reproducible or consistent readings could be obtained. The spread in sparking potentials was so great that no Paschen curve could be drawn through them. It was thus decided to discard the third tube at this point because the sparking potential measurements definitely indicated very inconsistent surface conditions. This was unexpected but was perhaps due to an insufficient coating of gold on the surface. The anode diameter was about 5 cm and probably the gold bead was not sufficient to lay down an even film on the whole area. Insulating patches on cathode surfaces have been known in this laboratory to influence measurements greatly, due to charge build-up and consequent field distortions. In fact Myatt (80) has found that primary ionization coefficients were changed by up to 50% when he used an annular glass surface to separate the guard ring and cathode in his experiments on hydrogen. The results from tube 3 are not discussed any further in this thesis.

Tube 4 was the best one with gold film electrodes, and both Paschen curves and ionization coefficients were obtained from it. Unfortunately, at one point a power failure resulted in the pumps being cut off which caused air to leak into the tube through the gas side of the system, thus preventing all the wanted readings from being obtained from this tube. Tube 5 with solid platinum

electrodes had already been constructed at this stage and so this was put on the manifold and the final set of readings obtained.

Tubes 1, 4 and 5 were similar and readings were obtained from all three of them. Tube 3 obviously does not merit any further discussion, but the results from tube 2, though not contributing anything significant to the study of ionization processes in oxygen, did have some interesting features and these are described briefly in section 5.3.

5.3 The 'Sandwich' Effect in Tube 2

After obtaining some preliminary results from tube 1 it was not quite clear if gold film electrodes were, in fact, the most suitable for work in oxygen. They had been successfully used in this laboratory for work in hydrogen and inert gases, but oxygen is a chemically active gas and an O_2 ion is about 10^7 times larger than an H_2 ion and so the behaviour of the electrodes when used in oxygen could be quite different, especially as the adherence between the film and the glass substrate is not very strong (81). This was the reason for investigating the behaviour of the second tube.

The history of this tube has been described in the last section. The special feature about it was that two layers of gold had been laid down on the electrodes, in between which the tube had been exposed to air. The usual practice with all the tubes was to check that there was no significant variation of I_o with d, then to determine the saturation voltage and finally to adjust the position of the ultraviolet lamp for maximum I_o before any gas was let in. This procedure was in fact followed after laying down

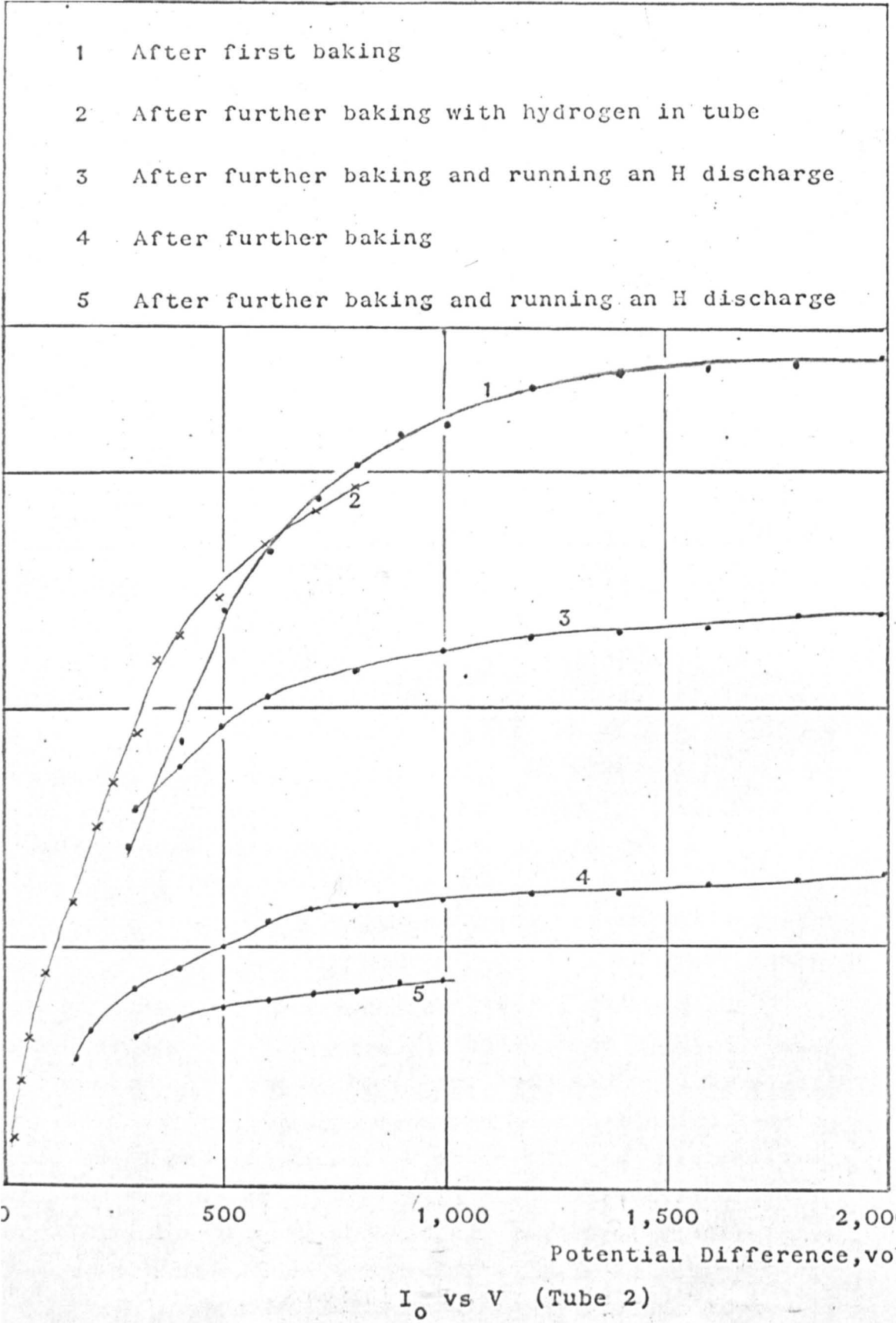
1 After first baking
2 After further baking with hydrogen in tube
3 After further baking and running an H discharge
4 After further baking
5 After further baking and running an H discharge
1
2
3
4
5
0
500
1,000
1,500
2,000
Potential Difference, volts

I_o vs V (Tube 2)

the first layer, but taken for granted after the second layer. When, later on, the saturation voltage was checked, it was found that on raising the potential difference between anode and cathode to 200 volts, I_o was still increasing. The saturation voltage was usually only about 25 V, so the actual saturation voltage was examined using a high voltage power pack instead of the bank of batteries. Finding this to be of the order of kilovolts, the saturation voltage was now measured after subjecting the tube to various treatments such as baking the tube with hydrogen in, and running a hydrogen discharge in the tube followed by subsequent diffusion pumping. The photoelectric current is plotted against the applied voltage in figure 22. The curves are numbered in chronological order and it is apparent that the saturation voltage decreased after baking and flushing with hydrogen. (The relative intensities of the maximum I_o are not significant here as the position of the ultraviolet lamp had to be changed each time the tube was baked.) The higher saturation voltage would seem to indicate a higher surface work function. As none of the other tubes showed this effect, it is perhaps justifiable to assume that the surface in this case was composed of a layer of gold, an adsorbed layer of gas and then another layer of gold. This seems a plausible explanation since the work function in this case could be expected to be composed of the work function of the surface and the energy required to ionize the sandwiched layer of gas. The ionized gas layer probably enhances the emission from the gold. This seems to take place only in the sandwich layer because no such effect was noticed when the cathode of tube 4 was exposed to oxygen and tested for increased saturation voltage. (The

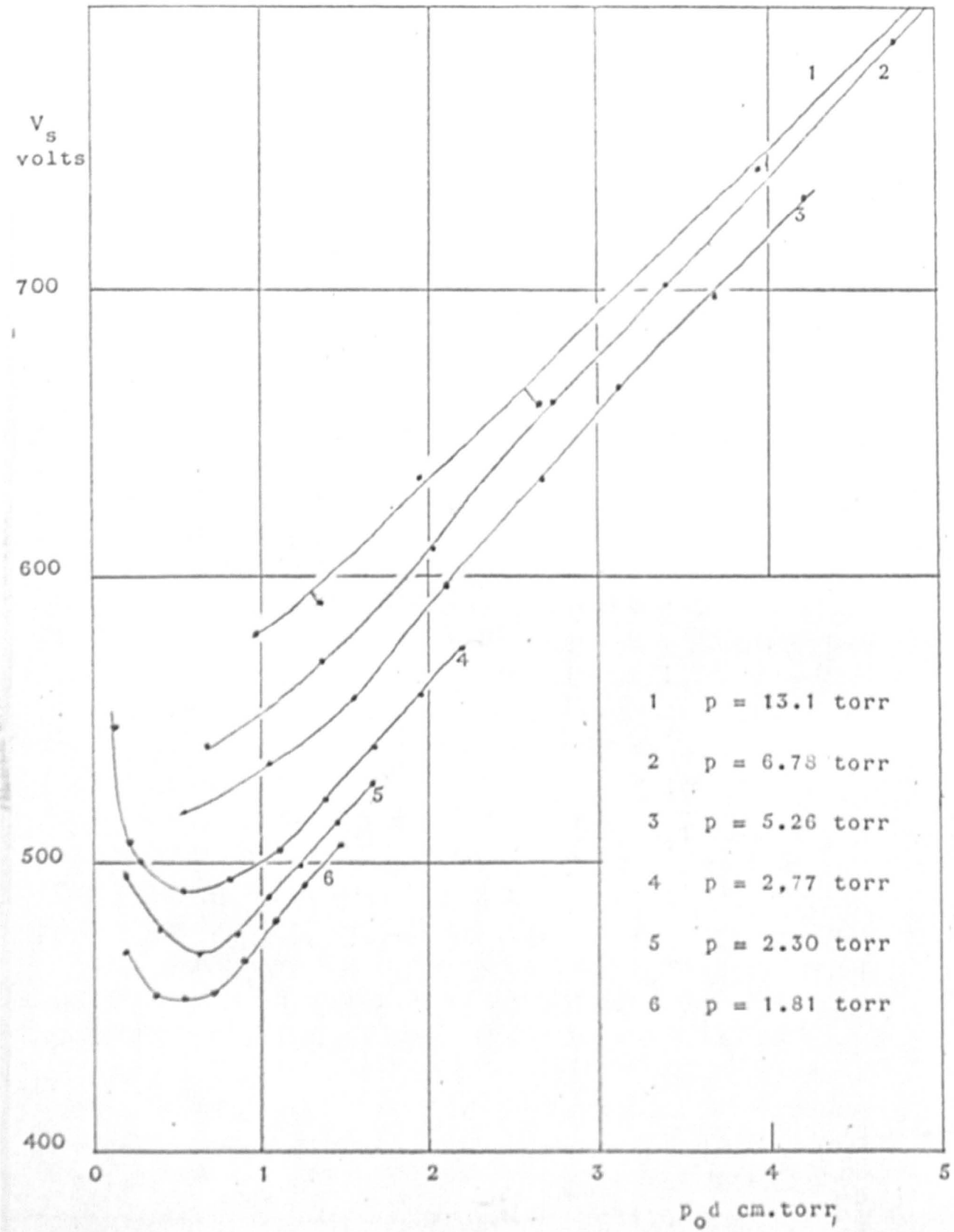

SPARKING POTENTIALS vs $p_o d$ (Tube 1)

Figure 23

saturation voltage did, in fact, increase to about 45 V in this case, but this is still very much less than 1600 V.) The sandwich layer was most probably mainly oxygen as flushing with hydrogen and running a hydrogen discharge tended to reduce the effect. It was not possible to do any quantitative study here because the tube was not equipped for work function measurements and the conditions were not reproducible as the thickness of gold layers was not known.

At this stage it could not be decided whether this was a gold-oxygen effect or not. When the next tube was put on the manifold, however, the saturation current was observed carefully and it was found that after the introduction of oxygen there was no spectacular change in I_o, which indicated that the behaviour of tube 2 was due to the sandwich layer.

5.4 Paschen Curves

The usual procedure with all the tubes, after letting in the oxygen, was to take sparking potential measurements at different gap distances for different gas pressures. This had the effect of "stabilizing" the electrodes and also enabled one to prevent the anode voltage from exceeding the sparking potential during ionization current measurements. The procedure for measuring sparking potentials has been described in chapter 4. The readings are plotted in the form of Paschen curves, V_s (sparking potential) being plotted against $p_o d$.

5.4.a Tube 1

Figure 23 shows the Paschen curves obtained from tube 1 using electrolytically produced oxygen. The different curves correspond to different gas pressures. With

this tube, the measured minimum sparking potentials seem to vary from 452 V to 490 V at a $p_o d$ of 0·55 (±0·15) torr cm. The lowest sparking potential, however, seems to correspond to the lowest pressure which is not what one would expect considering primary ionization processes alone; for at the lower pressures, the primary ionization processes would become less effective. Thus to explain this phenomenon one has to consider some other process, but it is difficult to specify which. These points were also replotted so that each curve corresponded to a particular d/D ratio, where D is the diameter of the cathode. No strong trends became observable, although the curves for the smaller d's lay slightly above those for the larger d's in general, but almost within experimental error. The fact that the Paschen curves do not exhibit any marked dependence on d/D would seem to indicate that the photon secondary process was not the predominant secondary process. If a photon secondary process was active, however, then some other effect, like absorption in the gas, must also be active masking the d/D effect. There is also the possibility that the measured sparking potentials for the lowest d's was exaggerated somewhat, because a reduction in I_o was observed with this tube for d values less than 0·6 cm and sparking potentials have been reported to have a strong dependence on the intensity of illumination (66). It must be remembered, however, that the cathode surface of this first tube was not very clean as it had been exposed to air, and thus too much importance should not perhaps be placed on these sparking potential measurements.

5.4.b Paschen Curves From Tube 4

Tube 4 also had gold film electrodes, but the film

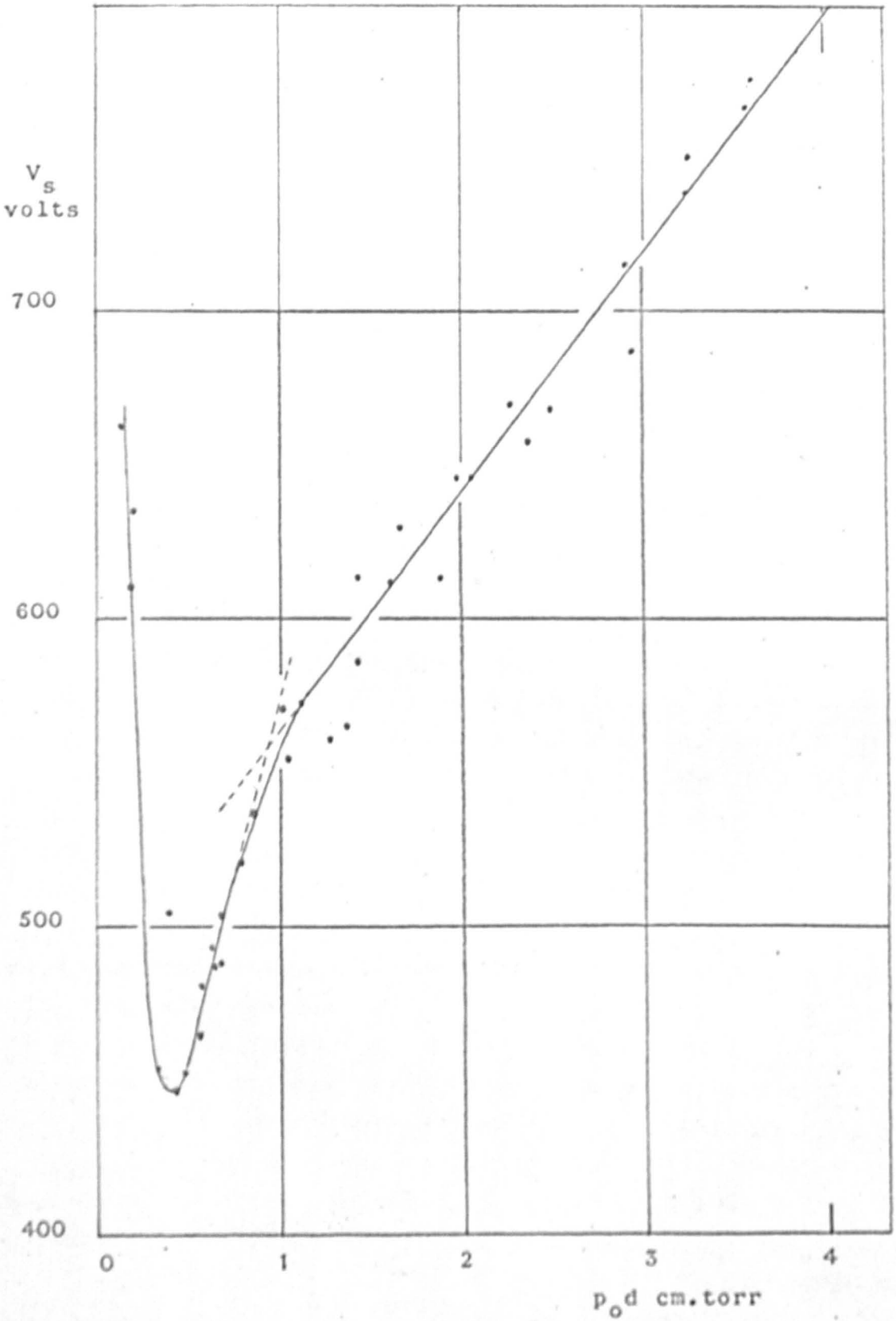

SPARKING POTENTIALS vs $p_o d$ (Tube 4)

Figure 24

was in a relatively clean state, not having been exposed to grease taps, mercury vapour, etc after deposition. The Paschen curves obtained from this tube are given in figure 24. In spite of taking the readings as carefully as possible, the points can be seen to have a lot of scatter. However, the curve does have some distinctive features.

The minimum sparking potential comes out to be 446 ±2 V at a $p_o d$ of 0·43 ± 0·02 cm torr, corresponding to an E/p of 1,037 V/cm torr. (The lowest observed sparking potential in the case of tube 1 was 452 V, 6 V higher than this.) The left hand side of the curve has a very high slope, V_s increasing rapidly as $p_o d$ decreases. As $(p_o d)_{min}$, the $p_o d$ corresponding to $(V_s)_{min}$, is so small (0·43 compared with 1·5 cm torr in hydrogen), it was not easy to take many points on the left hand side of the minimum with any degree of accuracy. On the right hand side of the minimum, there appeared to be two distinct parts to the Paschen curve; the part of the curve where $p_o d$ lies between $(p_o d)_{min}$ and 0·7 cm torr consists of one straight line, while the part for which $p_o d$ is greater than 1·3 cm torr is a second straight line, of a different slope from the first. The portion $0{\cdot}7 < p_o d < 1{\cdot}3$ cm torr is in fact curved, bridging over the two straight lines of different slopes. The transition occurs at 558 V and a $p_o d$ of 0·93 cm torr, i.e. at an E/p of about 600 V/cm torr.

On replotting the points, no change was observable due to changing d/D ratios or variations in pressure.

5.4.c Paschen Curves From Tube 5

This was the only solid metal (platinum) electrode tube used, and the gas was spectroscopically pure oxygen.

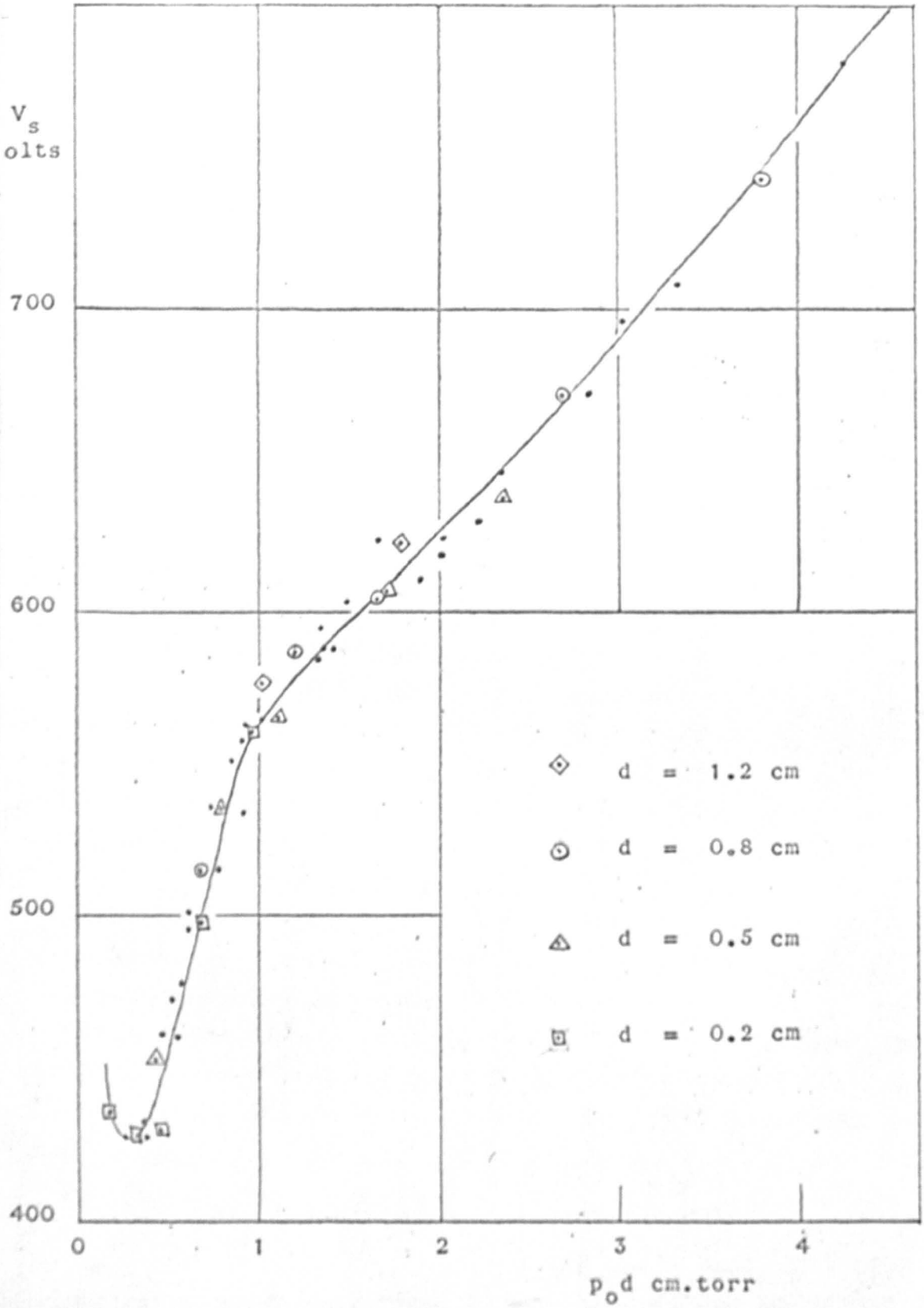

SPARKING POTENTIALS vs $p_o d$ (Tube 5)

Figure 25

The Paschen curves obtained from this tube are shown in figure 25. The minimum sparking potential for platinum comes out to be 426 ± 1 V, at a $p_o d$ of 0·33 ± 0·03 cm torr, corresponding to an E/p of the order of 1300 V/cm torr. This value of $p_o d$ is even lower than those observed earlier and it was not possible here to obtain the part of the Paschen curve for which $p_o d$ is less than $(p_o d)_{min}$. The two almost linear portions are clearly visible here also; the transition from one region to the other is much sharper here than that observed earlier, but this is perhaps because of the very much reduced scatter of the points. The transition point is almost exactly the same as in the previous case, V_s = 559 V, $p_o d$ = 0·93 cm torr, corresponding to an E/p of 601 V/cm torr. This would appear to be significant and is considered further in the next section. Comparing the curves themselves, it is easily seen that the sections of the curves between the minimum and the transition point are identical which would again appear to be significant. Beyond this point, however, the curve for platinum electrodes lies lower than that for gold, i.e. the rate of change of V_s with $p_o d$ is smaller in the case of platinum.

Here also the deviation from Paschen's law was very small indeed. In figure 25, the points corresponding to the same gap distances have been marked similarly; clearly, no specific conclusions can be drawn from this, except perhaps to say that the points corresponding to the largest gap distances tend to lie above the mean curve. But this is hardly outside experimental error.

5.4.d General Discussion of Paschen Curves

There is quite good agreement between the results

obtained here and the measurements of Fricke (26). Fricke's electrodes were of iron and he obtained a minimum sparking potential of 440 volts at a pd of 0·44 cm torr, while 446 V at 0·43 cm torr and 428 V for 0·33 cm torr were observed in this investigation for minima with gold film and solid platinum electrodes.

Fricke also observed a 'curvature' in the Paschen curves for $0{\cdot}7 < pd < 1{\cdot}5$ cm torr, about which he comments that 'in this higher field strength region the ionization due to positive ions (β/p) becomes effective and produces the sharp decline in the sparking potentials'. The transition point from his curves would come out to be at about an E/p of 560 V/cm torr even though he does not consider it to be a transition point, but only ~~as~~ a curvature. As pointed out in sections 5.4.b and 5.4.c, in the present work, the transition point comes out to be at an E/p of 600 V/cm torr which would correspond to a mean electron energy of about 11 eV. (Schlumbohm (49) gives a correlation between E/p and mean electron energy in oxygen.) The work of Schulz (65) and Craggs, Thorburn and Tozer (58) on the cross section for production of O^- ions shows that the normalized cross section falls to about 0·05 at about 10 eV from its maximum value of 1 at 6·7 eV. As one moves from left to right on a Paschen curve, one is usually reducing the E/p value and therefore, as one moves from the transition point towards the right, one is reducing the mean electron energy, or increasing the cross section for the production of O^- ions, thus incurring the virtual loss of electrons from the gap. This appears to be satisfactory in explaining why the sparking potential falls slowly to the right of the transition point, and faster to the left.

The fact that this happens at virtually the same point for different cathode metals further confirms the fact that this is primarily a gas effect.

The results from tube 1 show that for the same p_od, V_s increases with increasing gas pressure. Fricke also notices this effect, though only for p greater than 3 torr, for p less than 3 torr, V_s increasing again as the gas pressure decreases. One factor that the measurements from tube 1 had in common with Fricke's was that they were both done in electrolytically produced oxygen contaminated with phosphorus pentoxide. Even though Fricke claims his gas to be 'extremely pure and dry', his experimental tube itself contained a crucible of phosphorus pentoxide while the oxygen in tube 1 was dried over phosphorus pentoxide for several hours, though subsequently passed through liquid nitrogen traps. This could hardly be a coincidence and especially as the effect was not noticed with tube 4, again using gold film electrodes, it is probably safe to assume that it is a gas impurity effect.

Prasad and Craggs (54) and De Bitteto and Fisher (66) have investigated breakdown in oxygen, but as they worked at pressures of the order of 0·5 to 1 atmosphere, and consequently at low E/p and high pd, no real comparison of results can be made here. However, it is interesting to note that De Bitteto and Fisher have observed a fluctuation in V_s with intensity of ultraviolet illumination. As suggested earlier, this could explain the variation of sparking potential with gap distance for the same pd, as observed with tube 1 which was the only one used where the tube design produced a variation of I_o with gap distance.

The breakdown mechanism itself is discussed further in section 5.6 along with the secondary ionization coefficient.

5.5 Townsend's Primary Ionization Coefficient (α) and Attachment Coefficient (η)

The method used for obtaining α and η values from the I and d measurements, using equation 1.6 has been outlined in chapter 4. This involves determining $\frac{dI}{dx}$ values at different values of x and obtaining the slope of the log $\frac{dI}{dx}$ vs x curve which should be a straight line. The slope should give $(\alpha-\eta)$ and the y-intercept log αI_o, which on substitution in the original equation would give ηI_o, whence α, η and I_o can be determined.

With tube 1, $\frac{dI}{dx}$ was found out by drawing tangents at different points to the hand-drawn curves. Following this procedure, no reasonable conclusions could be drawn from the results, the margin of error being far too large to draw any unique straight line through the (log $\frac{dI}{dx}$, x) points plotted. Therefore it was decided to try to get more dependable values from a new tube under purer conditions (see section 5.2). Tube 4 was the next successful tube and this is described first in this section.

5.5.a Tube 4

The E/p range covered by this tube was 50 to 200 V/cm torr in steps of 10, several of the E/p values being covered at different pressures. First of all log I vs x curves were plotted and the apparent α values obtained from the initial part of the curve (where secondary processes were apparently not active). This seemed to be a valid procedure

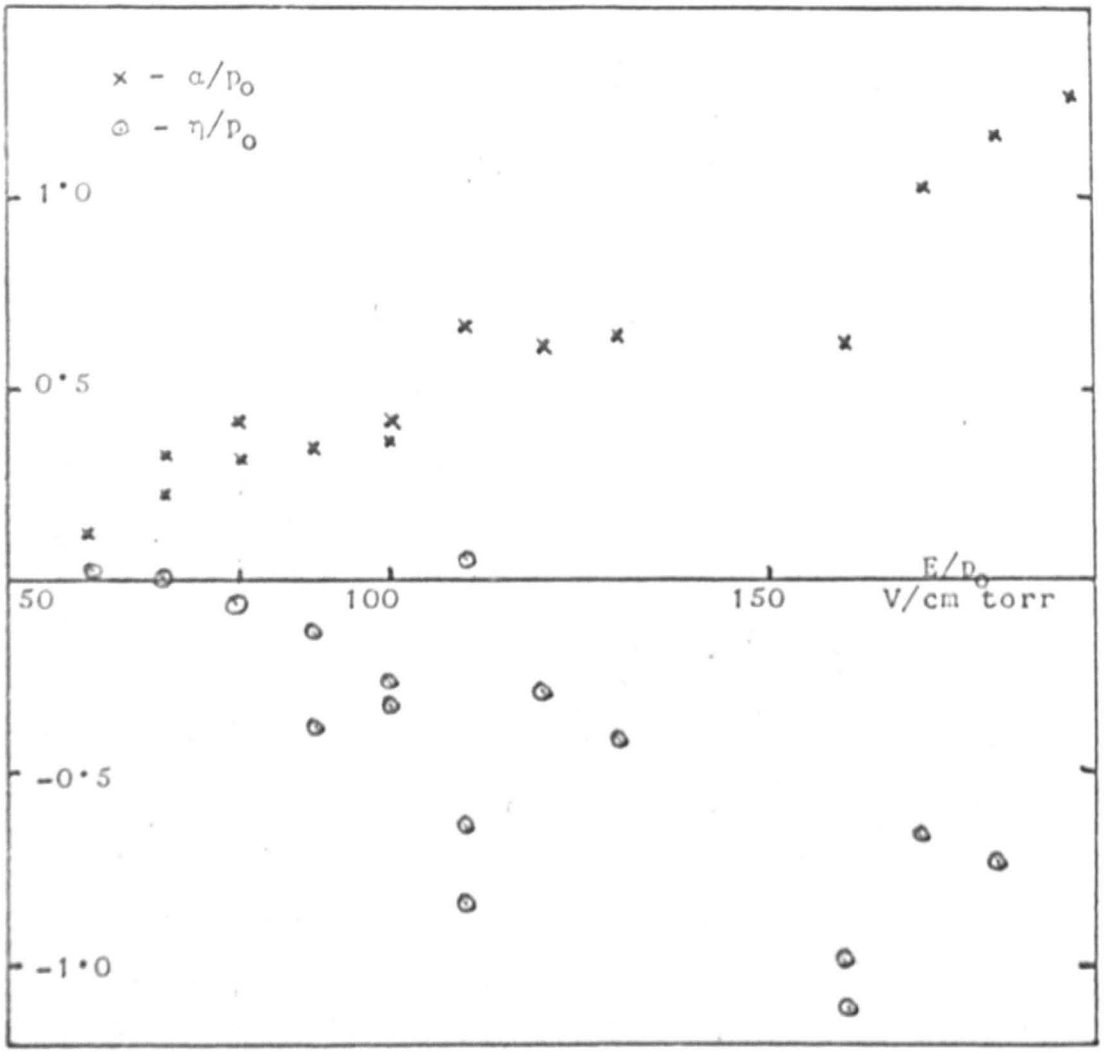

Computed Values of α/p_0 and η/p_0 as Functions of E/p_0 for Tube 4.

Figure 27.

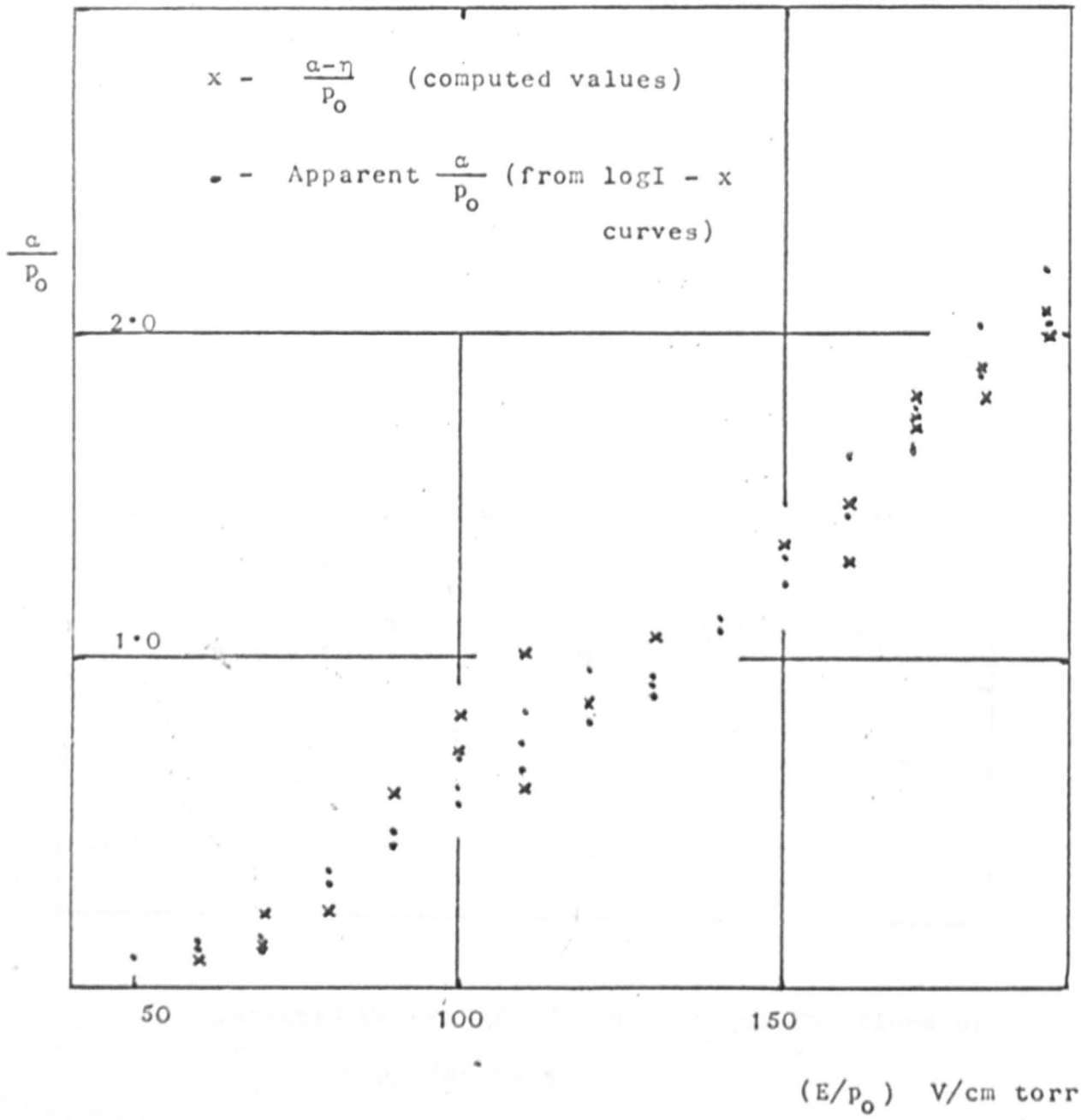

Apparent α/p_o vs E/p_o for tube 4

Figure 26.

as previous work in the field indicates that for E/p greater than 50 V/cm torr, attachment is very small compared to ionization and therefore can be considered to be a correction term in this region. The curve of $(\frac{\alpha - \eta}{p_o})$ vs E/p is shown in figure 26. While there is some scatter in the points, undoubtedly a curve can be drawn through them and this encourages one to analyse them further.

The analysis mentioned earlier was now applied to these points. As most of the d values were taken at random, first of all the Lagrangian interpolation was used to find $\frac{dI}{dx}$ with the aid of the computer and then these values were fed in again with appropriate I and x values, when the α, η and I_o values were computed corresponding to the best straight line through the $(\log \frac{dI}{dx}, x)$ points put in; these values were printed out in the output. The result is shown in fig. 27. It is easily seen that α/p is an increasing function of E/p, the scatter of the points being comparatively small. The so-called η/p function, however, is positive only in the region $50 < E/p < 80$ V/cm torr roughly, and there is a great deal of scatter in the points, even though they show a trend of increasing in the negative direction with E/p.

The negative attachment coefficient cannot, however, have any significance as such. If one assumes that η reduces to zero at an E/p of about 75 V/cm torr, (Frommhold (82) found no stable O^- ions for E/p greater than 70 V/cm torr), the negative η/p probably signifies secondary processes i.e. electrons being added to the gap rather than being removed from the gap; obviously it does not represent the secondary coefficient, since making η negative in eq. 1.6 does not lead one to the current growth equation

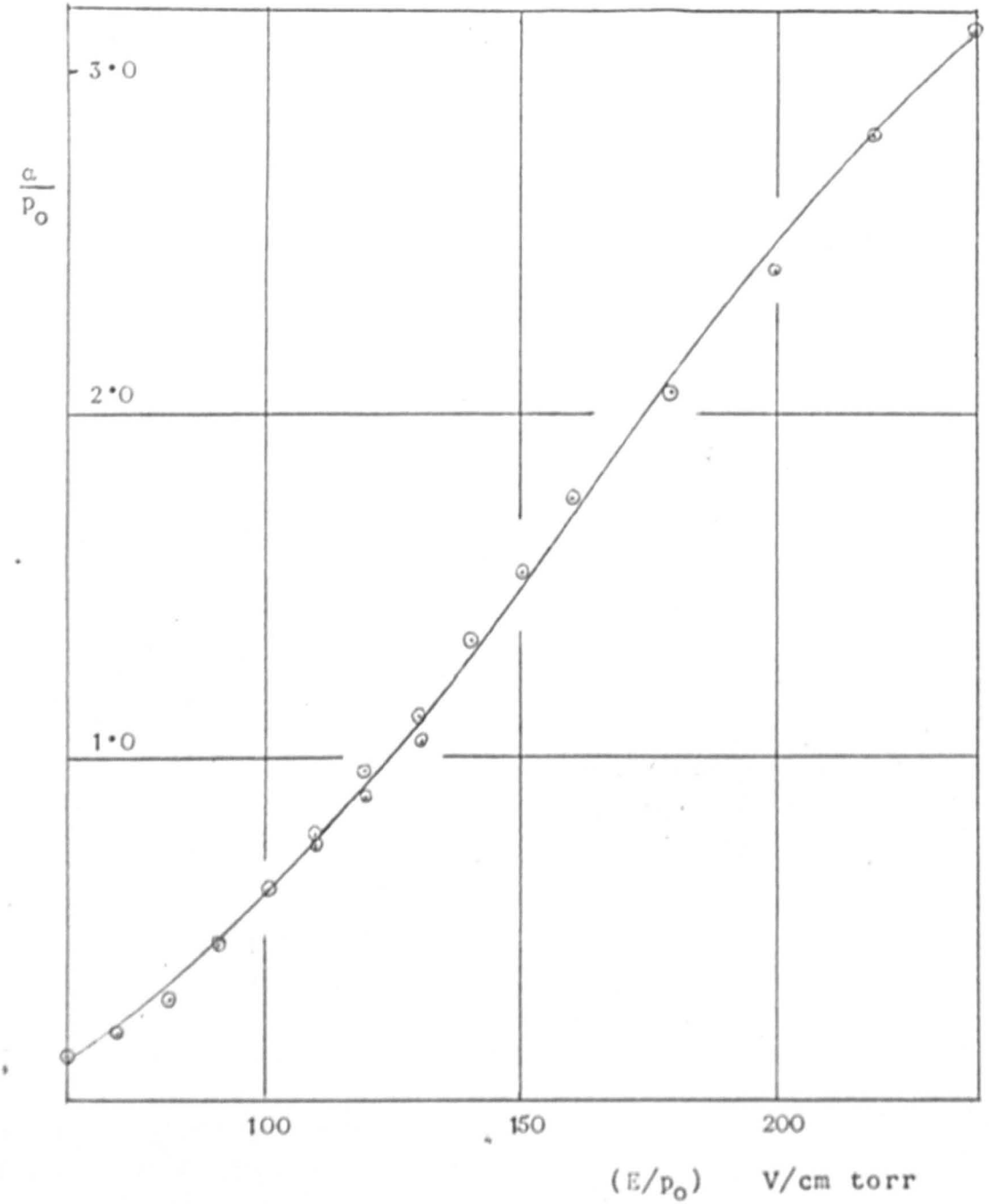

Apparent α/p_o vs E/p_o for Tube 5

Figure 28.

including secondary effects. Also, it is obvious that in the region of negative η the computed values of α cannot be very meaningful; therefore these values are not used any more.

There was also provision in the programme to print out the $(\alpha-\eta)$ values obtained in the case of each set of input points. This would be the slope of the log $\frac{dI}{dx}$ vs x curve as opposed to the slope of the log I vs x curve, which of course is normally used. (These values should be identical for the exponential growth of current in a non-attaching gas.) The computed values are plotted in fig. 26 along with the points obtained graphically. Again there is some scatter in the points, but the curve through the two sets of points is almost identical. This seems to prove the validity of the application of the analysis, and further, is indicative of the non-attaching behaviour of oxygen in the energy range concerned. However, if attachment and detachment were to occur simultaneously, both the equation and the analysis would fail to detect this.

5.5.b Tube 5

Tube 5 had solid platinum electrodes, but otherwise the construction was identical to the previous tube. The E/p range covered using the tube being $60 < E/p < 240$ V/cm torr, the analysis for α and η could not be usefully applied to the results. So the apparent α was obtained in the usual way from log I vs x curves and these are presented in figure 28.

In a preliminary analysis, it was observed that while the $(\alpha-\eta)$ values were reasonably consistent with the expected values, the individual α and η values varied by a factor of 1000 in some cases; the current growth equation 1.6

could certainly not apply to these! However, there is another factor which has to be mentioned in this context. As the x's were equally spaced in this case, the Lagrangian interpolation was not used here, $\frac{dI}{dx}$ being calculated as $10(I_1-I_2)$, where I_1 and I_2 were the currents at a separation of 1 mm. This presumably exaggerates the errors in measurement, while fitting a polynomial should smooth them out. This is probably another reason for the ridiculous α and η values obtained. However, as a comparison shows that the $\frac{\alpha-\eta}{p}$ vs E/p curve fits almost identically the curve obtained from tube 4, and the analysis cannot be expected to be valid for E/p greater than 70 V/cm torr, it does not seem worthwhile to try to do the Lagrangian interpolation on the results from tube 5. The two points corresponding to E/p 60 and 70 V/cm torr, have been corrected for η from the results of tube 4.

5.5.c General Discussion

Most of the results obtained have been presented in the previous sections and now it remains to discuss their significance and compare them with those obtained by other workers. For this, the results are considered in three parts: (i) Townsend's primary ionization coefficient (ii) the relationship between α/p and E/p (iii) the attachment coefficient.

(i) Primary Ionization Coefficient

The most important published results of α/p are those of Masch, Harrison and Geballe, Prasad and Craggs, and Schlumbohm. The maximum E/p covered by Harrison and Geballe was 70 V/cm torr and that by Prasad and Craggs was 50. So they are only on the verge of the region covered in this investigation. Masch's were the only published results till 1964 when Schlumbohm's paper came out,

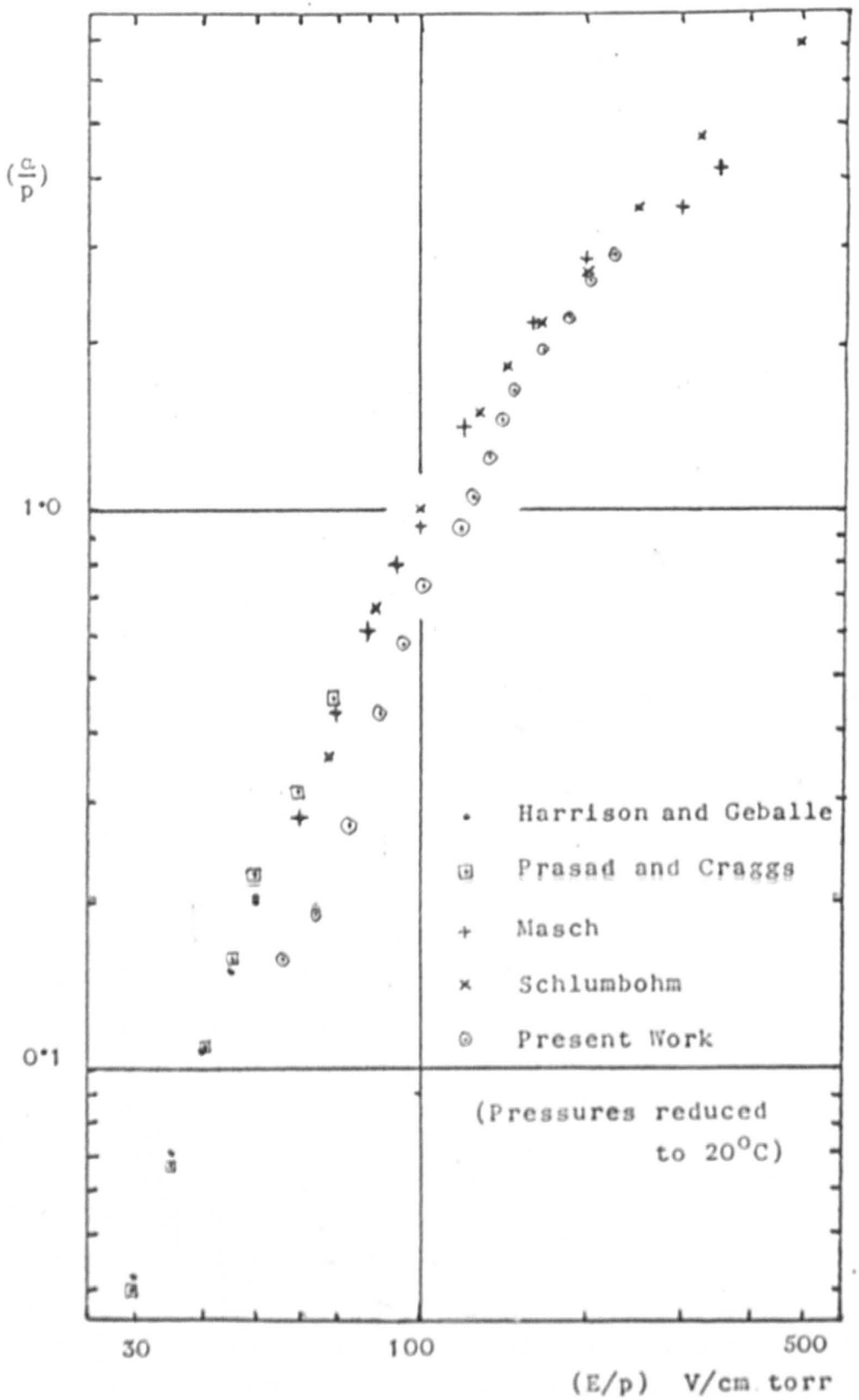

α/p vs E/p curves from Different Workers

Figure 29.

covering the higher E/p regions. These results are presented in figure 29 along with the present results. Schlumbohm's results were taken only in the region where attachment is not effective, Masch's have been limited to exclude the down-curving part and all the rest have been corrected for attachment where appropriate. The results of the present work are consistently lower than those of the others, although at the highest E/p values the present results approach those of Schlumbohm's.

The discrepancy between these results can perhaps be explained from a consideration of gas purity. Schlumbohm's curve is almost identical with that of Masch's, even though there was a time interval of more than 30 years between the two investigations. Vacuum techniques were not very advanced in 1932 so Masch's oxygen, which was obtained from a steel cylinder and used in a tube which contained large volumes of amber which could not be outgassed in any case, could not have been very pure. Schlumbohm unfortunately does not describe the vacuum techniques that he used, but as he used brass electrodes, 21 cm in diameter, it must have been virtually impossible to outgas them properly; and further, he does not mention what his background pressures were, except that "the leak rate" was "sufficiently small". The oxygen that he used in his experiments was 99·99 % pure obtained from a steel flask, but for his pressure measurements McLeod gauges were used. Thus it is possible that his gas was mercury contaminated to some extent, even though he mentions some cooling arrangements. As he used pressures down to 10^{-2} torr, even impurities which are neglibible at moderate pressures could well have had a marked effect on his results.

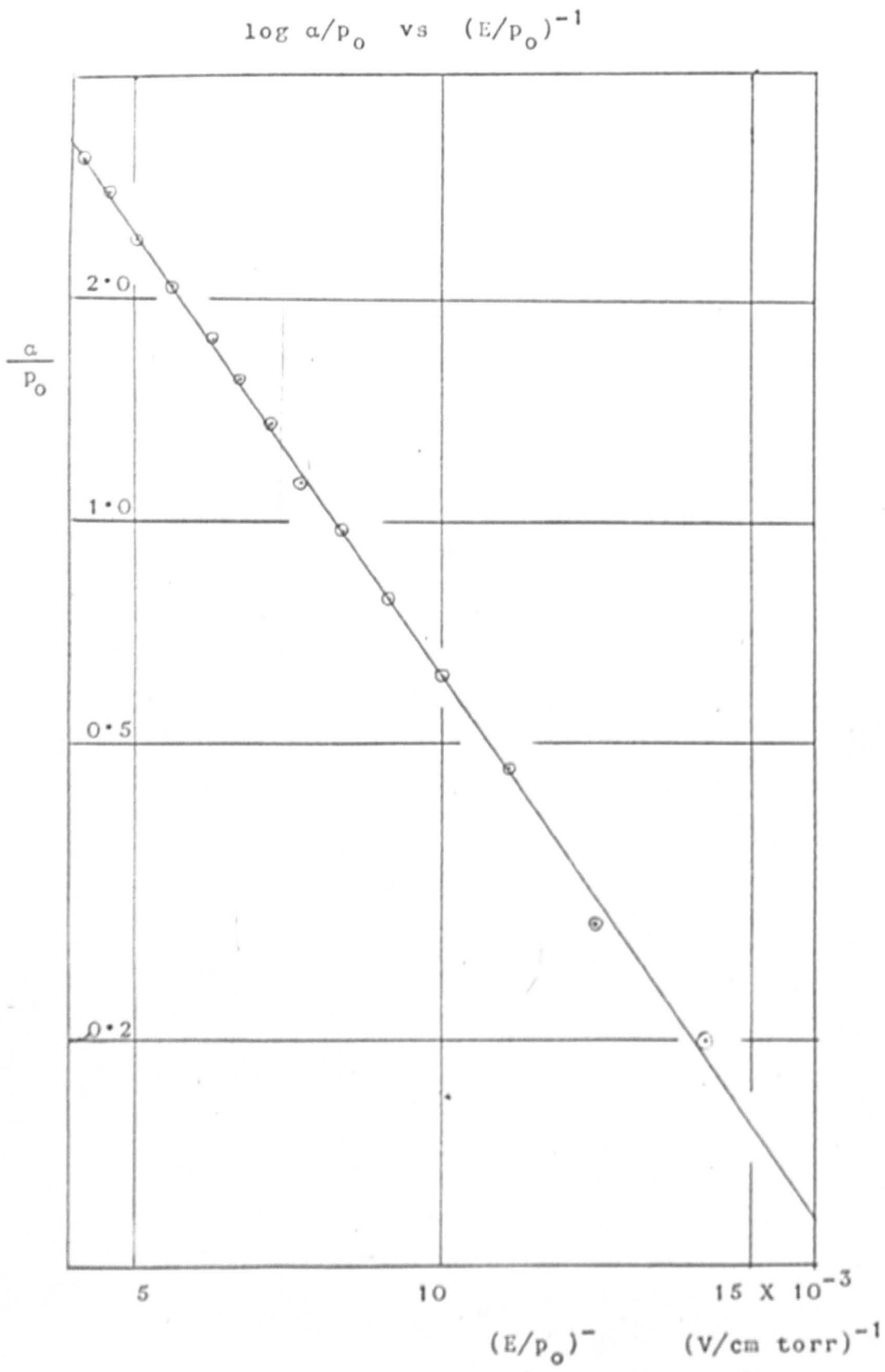

Figure 30

(ii) The Relationship Between α/p and E/p

It has already been mentioned in section 1.6.2 that α/p is a function of E/p. Townsend obtains this functional relation to be

$$\alpha/p = A\, e^{-B/(E/p)}$$

assuming the probability of ionization for electron energies greater than eV_i to be unity and assuming a distribution of free paths based on kinetic theory. While there have been more sophisticated theories since then, and while the assumptions involved in this derivation can hardly be justified, most gases have been found to obey this equation very well, at least in a limited range of E/p. Figure 30 shows a plot of log α/p vs E/p obtained from this experiment and it can be seen that over the range of E/p's used here the experimental points lie on a straight line. The slope of the line should give the constant B and the y-intercept, log A. These two constants have been calculated from the straight line and come out to be A = 18·6 and B = 350. In roughly the same region Schlumbohm quotes 7·7 for A and 203·5 for B. However, the present values seem to fit in better with the constants quoted for air and nitrogen (85): 15 and 12 for A and 365 and 342 for B respectively in the range of E/p 100 to 600 V/cm torr.

(iii) Attachment Coefficient

In this investigation, not a great deal of information has been gathered about the attachment coefficient. Unfortunately, as a result of the present tube design it does not seem possible to investigate the E/p regions where α and η are comparable in magnitude. An illustration of current growth over the whole gap distance range

($0{\cdot}2 < d < 1$ cm) for an E/p of 40 V/cm torr and pressure 5 torr will explain this:

$$\frac{I_{0{\cdot}2}}{I_1} = \frac{\alpha\, e^{0{\cdot}2(\alpha-\eta)} - \eta}{\alpha\, e^{(\alpha-\eta)} - \eta} = 70\%$$

The α/p and η/p values used here were taken from the results of Prasad and Craggs, $\alpha/p = 0{\cdot}11$ and $\eta/p = 0{\cdot}07$. Assuming the maximum error in current measurement to be $\pm$ 4%, the change in ionization current over the whole range of possible gap distances is seen to be barely outside experimental error. Thus it would appear that attempts to obtain α and η in this region (i.e. E/p less than 50 V/cm torr) with the present experimental arrangement must be rather futile. The whole range of results from tube 1 for $20 < E/p < 50$ V/cm torr bear out this fact, although there was the added complication of the correction for I_o in this case.

With tube 4, however, it has been possible to obtain a few values for η/p (see figure 27). At 60 V/cm torr η/p comes out to be 0·039 attachments/cm torr which compares very favourably with 0·041 obtained by Harrison and Geballe. While the results of Prasad and Craggs do not extend to this value, extrapolation of their curve gives $\eta/p = 0{\cdot}05$ which is again in fairly good agreement with the present results. However, at 70 V/cm torr the present value falls just below 0·001, while that of Harrison and Geballe falls only to just below 0·04; it is difficult to extrapolate the results of Prasad and Craggs, but from the curve it would appear that the value would not be smaller than 0·03. At E/p = 80 V/cm torr, the value obtained here is virtually zero (0·0016/cm torr) which is not directly evident from

either of the other investigations, though Frommhold (82) was not able to observe any stable ions above an E/p of 70 V/cm torr, which is in agreement with the present results.

All this leads one to a rather confused picture of the physical processes involved here; the confusion is only increased when one looks at the data available from beam experiments where a maximum cross section of O^- production is obtained at a mean electron energy of 6·7 eV, the cross section falling off virtually to zero at about 11 eV. In the swarm data, however, the electron energy corresponding to maximum cross section varies from 2·5 to 4 eV (Harrison and Geballe, 31), while nowhere can the cross section be seen to fall to zero except at 4·2 eV in the results of Healey and Kirkpatrick. (Extrapolating the results of Harrison and Geballe would give zero cross section at about 13 eV, but extrapolation over such large ranges cannot be taken to be valid.)

Frommhold, on the other hand, claims $\eta = 0$ for E/p less than 70 V/cm torr; while the present investigation cannot be held to prove anything conclusively, it certainly appears to support Frommhold's results, η falling off to zero at about E/p = 75 V/cm torr. Perhaps a detachment process is the explanation for this. Branscomb, Burch, Smith and Geltman (83) have measured the photodetachment cross section of O^- ions by measuring the electron current produced in a reaction between ions and photons and the threshold for detachment was found to be at 1·5 eV; the cross section rises to 6×10^{-18} cm^2 at 2 eV (roughly 6000 Å) whereafter the curve flattens out. (The maximum observed cross section for the production of O^- ions by electron

collision is about 2 X 10^{-18} cm^2.) Thus there must be considerable amounts of electron detachment in the experiments conducted in glass tubes and especially those using ultraviolet illumination. Most swarm experiments fall into this category. The beam experiments, on the other hand, use electron guns as their electron sources and as collecting electrodes completely envelope the tube, the amount of illumination inside the tube will be practically negligible.

Having said this, one must hasten to add that this is an incomplete picture. First of all it is difficult to understand why detachment is so effective above an E/p of 75 V/cm torr. One is probably justified in thinking that detachment does occur below this value also, as the maximum cross section for O^- production in swarm experiments is ten times smaller than that observed in beam experiments. Perhaps for E/p = 75 V/cm torr, the effective O^- production is so small that it is not manifest in current growth.

Another point to consider in this context is the sudden change in slope in the Paschen curve at E/p = 550 V/cm torr (mean electron energy of about 11 eV). This has already been mentioned in section 5.4.d. As this point is independent of cathode material, it is likely to be the effect of a gas process and most probably corresponds to the cessation of O^- production. However, if the production of stable ions stops at about 80 V/cm torr then this theory fails, unless one considers the process to be a series of attachments and detachments taking place in the gas volume, thus effectively retarding the growth of current; in this case, the detachment process can only be treated justifiably as a secondary process.

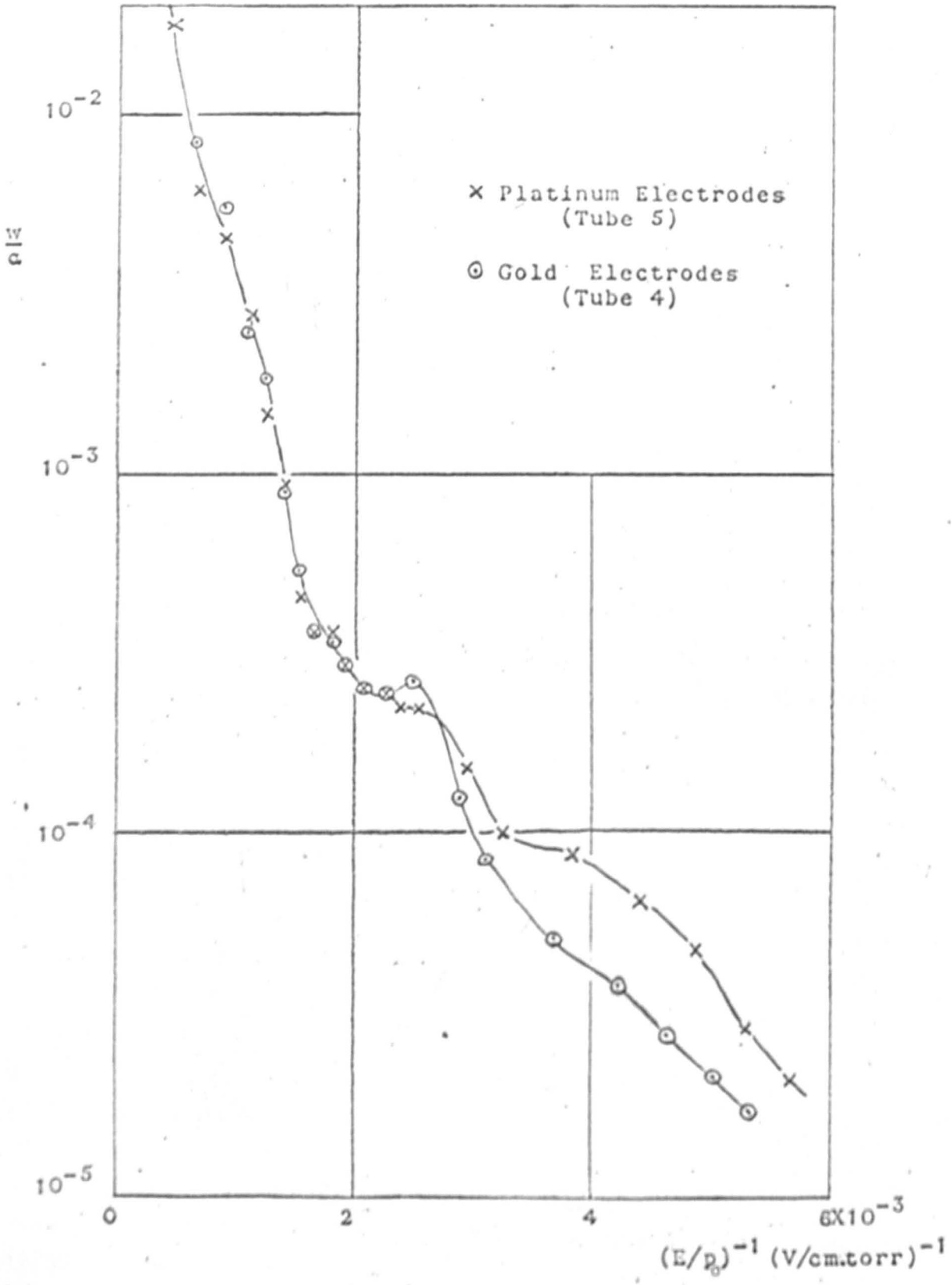

SECONDARY COEFFICIENTS vs $(E/p_o)^{-1}$

Figure 31.

5.6 Townsend's Secondary Ionization Coefficient

The generalized secondary ionization coefficient values have been obtained for gold film and platinum electrodes. They have only been calculated for tubes 4 and 5. Tube 1 has been left out as tube 4 is similar to it but better. The values have been calculated using the breakdown criterion,

$$\frac{w}{\alpha}\,(e^{\alpha d} - 1) = 1$$

at breakdown.

$$\alpha d = \left(\frac{\alpha}{p}\right)_s (pd)_s$$

can be calculated using the appropriate E/p ($=V_s/pd_s$) and therefore w/α can be obtained. The E/p range covered by the Paschen curves is roughly 150 to 2,000 V/cm torr. As the present work covers pre-breakdown current measurements, in the region $60 < E/p < 250$ V/cm torr, roughly, the values of α/p had to be obtained elsewhere to calculate w/α. Schlumbohm's (49) results have been used here because his are the most recent values covering this range and have been taken under similar conditions of gas purity, even though using a different technique.

As can be seen from fig 31, where w/α is plotted as a function of E/p, w/α depends very strongly on E/p. The features of the curves are, briefly, that they coincide in the region of E/p down to 400 V/cm torr and that thereafter they diverge, the secondary coefficients for gold being lower in this region than for platinum. Over an E/p range 2,000 to 200 V/cm torr, w/α varies almost three orders of magnitude, 2×10^{-2} to 2×10^{-5}, a significant amount. A

sharp change of slope can be noticed in this curve, as in the Paschen curves, occurring roughly at an E/p of 600 V/cm torr again.

Before one can be sure of the secondary processes that induce breakdown, one has to make a study of the formative time lags in detail. Without such a study, one can only make guesses as to the relative importance of such processes. In this experiment, however, there are one or two features that are suggestive.

The two main cathodic secondary processes are the photon process and the positive ion process (in gases where metastable states are not important). The photons obviously are not constrained to move in any particular direction in the discharge and so with random velocities at production, their paths should be evenly distributed in all directions and therefore, the fraction that reach the cathode is decided by the gap geometry. Thus for the same number of photons produced in the gap, i.e. for the same αd or (α/p)(pd), i.e. for the same pd, the smaller the gap, the larger should be the number of photons reaching the cathode, and the larger the number of secondary electrons. Therefore, as the gap distance is reduced for the same pd in any electrode arrangement, the sparking potential would be expected to decrease when the photon process is important. This was not observed with any of the three tubes. With tube-1, a reverse effect was noticed, in fact.

Positive ions on the other hand, are forced to move more or less in the field direction only. As long as the effective field E/p is the same, the effect of 'd' should be very small in a discharge with dominant positive ion

sharp change of slope can be noticed in this curve, as in the Paschen curves, occurring roughly at an E/p of 600 V/cm torr again.

Before one can be sure of the secondary processes that induce breakdown, one has to make a study of the formative time lags in detail. Without such a study, one can only make guesses as to the relative importance of such processes. In this experiment, however, there are one or two features that are suggestive.

The two main cathodic secondary processes are the photon process and the positive ion process (in gases where metastable states are not important). The photons obviously are not constrained to move in any particular direction in the discharge and so with random velocities at production, their paths should be evenly distributed in all directions and therefore, the fraction that reach the cathode is decided by the gap geometry. Thus for the same number of photons produced in the gap, i.e. for the same ad or $(\alpha/p)(pd)$, i.e. for the same pd, the smaller the gap, the larger should be the number of photons reaching the cathode, and the larger the number of secondary electrons. Therefore, as the gap distance is reduced for the same pd in any electrode arrangement, the sparking potential would be expected to decrease when the photon process is important. This was not observed with any of the three tubes. With tube-1, a reverse effect was noticed, in fact.

Positive ions on the other hand, are forced to move more or less in the field direction only. As long as the effective field E/p is the same, the effect of 'd' should be very small in a discharge with dominant positive ion

action. Diffusion cannot be ruled out completely, of course, especially when the walls are kept at the same potential as the cathode. But the chances of this were minimised in the present experimental set up with the provision of guard rings.

There are two other points which also would suggest a dominant positive ion process. The first of these is the nature of the dependence of the secondary coefficient on E/p. With a photon process it is reasonable to expect a maximum in the w/α vs E/p curve, as photon production has a peak efficiency at a particular electron energy. These curves, however, display no strong peaks though at E/p = 400 V/cm torr, there is a very small peak in each curve. (The possibility of a decline in w/α values for E/p greater than 2,000 V/cm torr exists, of course, and cannot be ruled out, though one can see no evidence of it.) On the other hand, a positive ion is produced in each primary ionizing collision and the primary ionization coefficient is a monotonically increasing function of E/p in this region, and therefore if the positive ion process was dominant, w/α would be expected to be an increasing function of E/p, too. In addition, most of the energy of the positive ions is derived from the field, and therefore would increase with E/p. Thus the nature of the functional relationship between w/α and E/p favours the positive ion secondary process. The sudden change in slope at E/p = 600 V/cm torr can also be explained qualitatively with reference to this process, since this corresponds to a mean electron energy at which the cross section for O^- production reduces to zero, virtually, and therefore there are more free electrons to

produce positive ions.

The second favourable point comes from Fisher's (84) experiments on formative time lags in oxygen. These would be expected to be of the order of d/v_e, i.e. of the order of microseconds in the case of the photon secondary process as hardly any time is lost in photons reaching the cathode once they have been produced, and this has been found to be so in other gases. Positive ions, on the other hand, have to drift across to the cathode before they can produce secondary electrons and therefore this will necessarily be a slower process involving larger formative time lags, of the order of d/v_+. Fisher reports time lags of the order of hundreds of microseconds (at about 1% overvoltage) which fits in quite well with the positive ion process. It must be acknowledged, however, that Fisher's experiments were conducted at a pressure of about 1 atmosphere which would correspond to a very much lower E/p than those mentioned here. Fisher also mentions a 'very pronounced' variation of formative time lags with pressure, which is difficult to explain on the basis of positive ion action, though perhaps electron attachment played some part under the conditions.

In conclusion, all that can be said about the mechanism of breakdown is that it appears to be predominantly due to a positive ion process. The possibility of photon action, especially of the delayed type cannot be ruled out though.

The secondary coefficients come out to be roughly the same for both platinum and gold cathodes: this is not very surprising as the work functions of the two metals are very close. Prasad and Craggs (54) quote 10^{-6} as their

value of γ for a platinum cathode at about E/p = 45 V/cm torr which is not in any disagreement with the present curve extrapolated. But Fisher's (66) 0.045 at E/p = 35.4 V/cm torr for nickel is hard to understand.

5.7 General Discussion and Suggestions for Futher Work

So far in this chapter an account of the work done for this thesis has been given and the results obtained presented wherever possible. In this section it is intended to point out some of the limititions of the techniques used, discuss some of the errors introduced and to make some suggestions which might be useful for future workers in the field.

The range of E/p has been restricted to within 50 and 250 V/cm torr in the final experiments. This was mainly a feature of the design of the apparatus. The electrodes being of about 2·5 cm diameter, it is not possible to increase d much beyond 1 cm and still have uniform fields, and gap distances below 1 mm could not be measured accurately; besides, very small gap distances also have the effect of cutting off the illumination of the cathode. The usable pressures had practical limitations too as the oil manometer could not be read to less than $\pm$ 1 mm, i.e. there was a 10 % error in a pressure difference of 1 cm of oil which corresponds to roughly 0·6 torr. The arms of the manometer were each of about 0·8 metres in length, so pressures of the order of 50 torr could be measured on the manometer if desired, although the maximum pressures used were only below 15 torr, in fact, most of the readings being obtained at a few torr pressure. The applied voltage $V = \frac{E}{p}(pd)$ was limited, of course, by the saturation voltage at the

lower 'd' end and the sparking potential at the higher 'd' end. Thus keeping $50 < V < 500$ V, the lowest accuracy of pressure measurements to about 4% and $0{\cdot}1 < d < 1$ cm, the usable E/p range is roughly between 50 and 300 V/cm torr. So to extend the E/p range to lower values, tubes with larger electrodes should be used so that the gap distance can be increased without field distortion, at higher pressures. The same reasons apply to the limits of pd values covered in the sparking potential measurements too.

The cooling trap on the gas side is virtually essential to ensure greasefree, dry gas. However one has to be extremely careful in using this, as there is evidence that this can produce unpredictable temperature variations in the experimental tube. The trap used in this work had to be manually filled up, and once on filling the trap, the sparking potential was observed to go down from 695 V to 680 V. Here the level of liquid nitrogen in the trap must have affected the temperature of the gas in the experimental tube. Thereafter, the trap was filled up half an hour before each set of readings, so that the experimental temperature would reach an equilibrium and remain fairly steady. Thus it would appear that the temperature measurements in these experiments might not have been sufficiently accurate throughout. One or more of the following suggestions should improve matters:

(i) use an automatically filling liquid nitrogen trap, where the level of the liquid stays virtually constant.

(ii) incorporate a thermometer (e.g. thermocouple) in the experimental tube, so that checks on temperature can be made if necessary while taking readings.

(iii) use a pair of bakable metal taps instead of the grease taps for the controlled introduction of gas into the tube - though unfortunately the experience in this laboratory so far has been that bakable metal taps can be extremely troublesome. Perhaps random fluctuations of temperature in the laboratory also ought to be mentioned in this context, although it can be easily seen that the error in p produced by fluctuations in room temperature of $\pm$ 2°C is negligible; ~~as~~ during any one run the temperature seldom changed by more than 2°C.

Since evaporated film and solid metal electrodes have both been used in the present work, it might be worthwhile to look at their relative merits for use in oxygen. As far as constructional details are concerned there is not very much to choose between the two, though in this case the platinum ones were less troublesome having been ordered to size and so ready to use, while the gold film electrodes had to be constructed from glass rods and gold wire! Evaporation of gold electrodes is rather a tedious process, but then outgassing solid metal electrodes is no easy job. It was feared that eddy-current heating might produce warpping of the electrodes in tube 5, or even snapping off from the supporting rods, so all the outgassing that was done was prolonged baking at 450°C. With both, it was possible to achieve ultimate pressures of the order of 10^{-8} torr. On the other hand, current measurements and sparking potential measurements were much more reproducible in the case of the platinum electrodes. It would be interesting to study the effect of O_2 ions on the gold film cathode. While the gold film would have been more than 100 Å thick, the adherence of the film to the substrate is not very strong

(81). Oxygen on the other hand, can get into the molecular interstices and get lodged there semipermanently. Whether or not this happens, and if it does, how it affects the work function of the surface, should make an interesting investigation. Gold film electrodes have, of course, been used very successfully in this laboratory for other gases, and the results from tube 4 indicate that this is probably all right for oxygen too; it is the small fluctuations in current and changes in the sparking potential, especially when the tube is new, that makes one wonder if, in fact, the surface conditions are staying perfectly constant.

It is extremely important, of course, to have an absolutely constant I_o in all the I-d measurements. The importance of measuring I accurately cannot be overemphasised because the accuracy of one's final results is so critically dependent on this. The error in I is doubled in calculating $\frac{dI}{dx}$ and it is obviously meaningless - physically, if not mathematically - trying to fit the best straight line to points which have no semblance of lying on a straight line. For the same reason, a method of interpolation proved to be much more valuable than any other in finding $\frac{dI}{dx}$. It probably would not have been quite so important, had the range of x been much larger with correspondingly larger ranges of current. This is particularly true for low E/p's where the current hardly rises above I_o.

The α's presented here have not been corrected for secondary effects: but a consideration of the magnitudes of w/α and α/p soon reveal that the correction of α/p due to w/α is very much within experimental error for oxygen in the range of E/p covered. For an E/p of 200 V/cm torr the

pressure used was typically about 2 torr. α/p is 2·4 /cm torr corresponding to this E/p from fig 29. Even at the maximum gap distance of 1 cm, the ionization current changes only by 0·2% on taking into consideration the secondary coefficient, which is well within the experimental error. As w/α appears to continue to decrease with decreasing E/p in the range of E/p covered, the correction due to w/α would be even smaller for lower E/p's and smaller gap distances.

The nature of the secondary coefficients has only been guessed at so far. It is surprising that as yet nobody has ever attempted to make a study of the formative time lags in oxygen, except Fisher (84) whose publication does not describe anything beyond some preliminary observations. A study of formative time lags in low overvoltage gaps in oxygen is being made in this laboratory at present. It would be interesting to correlate this with, and extend this to, high overvoltage breakdowns and the growth of avalanches.

5.8 Conclusion

A record of the results obtained from this investigation has been presented in this chapter. The results comprise of ionization coefficients and attachment coefficients in oxygen in the E/p range of $60 < E/p < 250$ V/cm torr and sparking potentials for low pd values, $pd < 6$ cm torr, obtained from steady-state measurements using plane parallel electrodes. The results have been critically analysed and compared with those of previous workers. Some suggestions which may be useful to future workers have been given too, for a surprising amount of work still remains to be done.

APPENDIX I

Programme for Lagrangian Interpolation

```
    DIMENSION JOVER(2), D(4,10), G(3,9), T(7)
 10 FORMAT (I3)
 11 FORMAT (F6.3)
 12 FORMAT (F3.2)
 13 FORMAT (4F6.3, 3X)
    ACCEPT TAPE 10, JOVER (1)
100 DO 101 J=1,7
101 T(J)=0.
    ACCEPT TAPE 10, JOVER(2)
    PRINT 10, JOVER(2)
102 IF (SENSE SWITCH 2) 103,104
103 NUM = 2
    GO TO 108
104 IF (SENSE SWITCH 3) 105,106
105 NUM = 3
    GO TO 108
106 IF (SENSE SWITCH 4) 107, 997
107 NUM = 4
108 DO 109 I=1,NUM
109 ACCEPT TAPE 11, D(I,1)
    T(1)=D(1,1)
110 J=2
111 DO 112 I=1,NUM
112 ACCEPT TAPE 11,D(I,J)
113 IF (D(1,J)-D(1,J-1)) 997,115,114
114 J=J+1
    GO TO 111
115 JEND=J-1
    M=2
```

```
      ACCEPT TAPE 12, T(5)
126   DO 129 J=1,JEND
      FAC=1.
      DO 128 K=1,JEND
      IF (J-K) 127,128,127
127   FAC=FAC*(D(1,J)-D(1,K))
128   CONTINUE
      DO 129 K=2,NUM
129   G(K-1,J)=D(K,J)/FAC
      IF (D(1,2)-T(1)) 146,145,130
130   DO 131 K=2,4
131   T(K) = 0.
      DO 134 J=1,JEND
      FAC=1.
      DO 133 K=1,JEND
      IF (J-K) 132,133,132
132   FAC=FAC*(T(1)-D(1,K))
133   CONTINUE
      DO 134 K=2,NUM
134   T(K)=T(K)+G(K-1,J)*FAC
135   GO TO (997,136,137,138),NUM
136   PRINT 13, T(1),T(2)
      GO TO 139
137   PRINT 13, T(1),T(2),T(3)
      GO TO 139
138   PRINT 13, T(1),T(2),T(3),T(4)
139   IF (T(1)-D(1,1)) 997,140,141
140   J=D(1,1)/T(5)
      S=J
      T(1) = S*T(5)
141   IF (D(1,JEND)-T(1)) 997,151,142
142   IF (D(1,M)-T(1)) 997,148,143
143   T(1) = T(1) + T(5)
```

```
;
144 IF (D(1,M)-T(1)) 146,145,130
145 M = M+1
    GO TO 130
146 T(6) = T(1) - T(5)
147 T(1)=D(1,M)
    GO TO 130
148 IF (D(1,M+1)-T(6)-T(5)) 149,150,150
149 M=M+1
    GO TO 147
150 T(1)=T(6)+T(5)
    T(6)=0
    M=M+1
    GO TO 144
151 IF (T(6)) 997,152,153
152 T(1)=T(1)+T(5)
    GO TO 154
153 T(1)=T(6)+T(5)
154 PRINT 11,T(1)
    JOVER (1) = JOVER(1)-1
    IF (JOVER(1)) 997,201,200
200 PAUSE
    GO TO 100
997 PAUSE
201 END
```

APPENDIX II

Programme to derive α and η from $\frac{dI}{dx}$, x and I values

```
      DIMENSION INDEX(3), X(10), DERIVX(10), Y(10), T(4),
     1    CURNT(10)
   10 FORMAT (I4)
   11 FORMAT (F7.3)
   12 FORMAT (3F9.4,3X)
      ACCEPT TAPE 10,INDEX(1)
  100 DO 101 J=1,4
  101 T(J)=0.
      ACCEPT TAPE 10, INDEX(2)
      PRINT 10, INDEX (2)
      ACCEPT TAPE 10, INDEX(3)
      PRINT 10, INDEX(3)
  102 ACCEPT TAPE 11, X(1)
      J=2
  103 ACCEPT TAPE 11, X(J)
      IF (X(J)-X(J-1)) 900,105,104
  104 J=J+1
      GO TO 103
  105 N=J-1
  106 DO 107 J=1,N
  107 ACCEPT TAPE 11, DERIVX(J)
  108 DO 109 K=1,N
  109 Y(K) = LOGF (DERIVX(K))
  110 DO 111 J=1,N
      T(1)=T(1)+X(J)
      T(2)=T(2)+Y(J)
      T(3)=T(3)+X(J)**2
  111 T(4)=T(4)+X(J)*Y(J)
      Z=N
```

```
    SLOPE=(Z*T(4)-T(1)*T(2))/(Z*T(3)-T(1)**2)
    YINT =(T(2)*T(3)-T(1)*T(4))/(Z*T(3)-T(1)**2)
    A = EXPF (YINT)
112 PRINT 12, SLOPE, YINT, A
113 DO 114 K=1,N
    ACCEPT TAPE 11, CURNT(K)
    B=A*EXPF (SLOPE*X(K))-SLOPE*CURNT(K)
    CURNTO = (A-B)/SLOPE
    ALPHA = A/CURNTO
    ETA = B/CURNTO
114 PRINT 12, CURNTO, ALPHA, ETA
    INDEX(1)=INDEX(1)-1
    IF (INDEX(1)) 900,120,100
900 PAUSE
    GO TO 100
120 END
```

LIST OF FIGURES

22 Saturation currents in tube 2.

23 Paschen curves obtained fron tube 1.

24 Paschen curves from tube 4.

25 Paschen curves from tube 5.

26 Apparent α/p_o vs E/p_o for tube 4.

27 Computed values of α/p_o and η/p_o as functions of E/p_o for tube 4.

28 Apparent α/p_o vs E/p_o for tube 5.

29 α/p vs E/p curves from various workers.

30 log α/p_o vs E/p_o.

31 Secondary coefficients as a function of E/p_o.

REFERENCES

1 Cravath A.M Phys. Rev. 36 248 1930

2 Ramsauer C Ann. Phys. 72 345 1923

3 von Engel and Steenbeck M Electrische Gasentladungen ihre Physik u. Technik Vol. 1

4 Thomson J.J. Phil. Mag. 23 449 1912

5 Varney R.N. Phys. Rev. 47 483 1935
Varney R.N. Phys. Rev. 50 159 1936

6 Kallmann and Rosen Z. Phys. 58 52 1929
Z. Phys. 61 61 1930

7 Compton A.H. Phys. Rev. 21 715 1923
Phys. Rev. 22 409 1923

9 Hagstrum H. D. Phys. Rev. 104, 309 1956

10 Kapitza L. Phil. Mag. 45 989 1923

11 Einstein A. Ann. Phys. 17 132 1905

12 Millikan R.A. Phys. Rev. 7 355 1916

13 Stebbing R. F. Proc.Roy.Soc. (Lon) A-241, 270 1957

14 Hasted J. B. J. Appl. Phys. 30, 22 1959.

15 Richardson O.W. Phil. Mag. 23 263 1912

16 de Boer J.H. Electron Emission Cambridge 1935

17 Fowler and Nordheim, Proc.Roy.Soc. a119,173,1928

18 Townsend J.S. Nature 62 340 1900

19 Townsend J.S. Phil. Mag. 3 557 1902
Phil. Mag. 5 389 1903

20 Townsend J.S. The Theory of Ionization of Gases by Collision

21 Holst G. and Oosterhuis E. Phil. Mag. 46 1117 1923

22 Dutton J.,Haydon S.C.,Llewellyn Jones F. and Davidson P.M. Proc. Roy. Soc. A 218 206 1953

23 Little F. P. Handbuch der Physik XXI 1956

24 Paschen Weid. Ann. 37 69 1889

25 Henderson and Llewellyn Jones F., Phil. Mag. 28 185 1939

26 Fricke Z. Physik 86 464 1933

27 Meyer Ann. Phys. Lpz. 58 297 1919, Ann. Phys. Lpz. 65 335 1921

28 Davies D.E. and Llewellyn Jones F. Proc. Phys. Soc. (London) B64 397, 519 1951

29 Davies D.E. and Fitch R.K. Brit. J. Appl. Phys. 10 502 1959

30 Gozna C.F. Ph.D. Thesis, University of Birmingham, 1960

31 Harrison MA.and Geballe R. Phys. Rev. 91 1 1953

32 Geballe R. and Reeves M.L. Phys. Rev. 92 867 1953

33 Crowe R.W. and Devins J.C. Annual Report, Conf. on Elect. Insul. 1955

34 Druyvestyn M. and Penning F.M. Rev. Mod. Phys. 12 87 1940

35 Bartholomeyczk W. Z. Physik. 122 437 1944

36 Davidson P.M. Phys. Rev. 99 1072 1955

37 Betts B.P. Ph. D. Thesis University of Keele 1965

38 Overton G.D.N. Ph. D. Thesis University of Keele 19[illegible]5

39 Healey R.Hand ReedJ.W.The Behaviour of Slow Electrons in Gases (Amalgamated Wireless Ltd, Sydney) 1941

40 Bailey V.A.Phil. Mag. 50 825 1925

41 Huxley L.G.H. and Crompton R.W. and Bagot C.H. Aust. J. Phys. 12 303 1959

42 Loeb L.B. Phys. Rev. 17 89 1921

43 Bradbury N.E. Phys. Rev. 44 883 1933

44 Kuffel E. Proc. Phys. Soc. 71 576 1958

45 Chatterton P.A. and Craggs J.D. J. Elect. and Controls 11 426 1961

46 Herrèng P. Cahiers Phys. 38 7 1952

47 Doehring A. Z. Naturforsch 7-a 253 1952

48 Chanin L.M., Phelps A.V. and Biondi M.A. hys. Rev. Letters 2 344 1959

49 Schlumbohm H. Z. Physik 184 494 1965

50 Masch K. Arch. Elektrotech.

51 Biondi M. A. Phys. Rev. 109 2005 1958

52 Mulcahy M.J. Sexton M.C. and Lennon J. J. Proc. Vth Intermational Conf. on Ionizn. Phen. in Gases 612, 1961

53 Chantry p.J. Whamby J.S. and Hasted J.B. Proc. Vth International Conf. on Ion. Phen. 630 1961

54 Prasad A.N. and Craggs J.D. Proc. Phys. Soc. (London) 77 385 1961

55 Prasad A.N. Proc. Phys. Soc. (London) 74 33 1959

56 Lozier W.W. Phys. Rev. 46 268 1934

57 Lozier W.W. Phys. Rev. 44 575 1933

58 Craggs J.D. Thorburn R. and Tozer B.A. Proc. Phys. Soc. (London) A-240 473 1957

59 Asundi R. Craggs J.D. and Kurepa Proc. Phys. Soc. (Lon) 82 967 1963

60 Buchel Nikova N.S. Fortschr. Physik. 8 626 1960

61 Tate J.T. and Smith P.T. Phys. Rev. 39 270 1932

62 Rapp D. and Englander-Golden P. VI th Inter. Conf. on Gases 1963

63 Massey H.S.W. and Burhop E.H.S. Electronic and Ionic Impact Phenomena (Oxford Univ. Press) 1952

64 Asundi R.K. Proc. Phys. Soc.(London) 82 372 1963

65 Schulz G.J. Phys. Rev. 128 178 1962

66 De Bitteto D.J. and Fisher L.H. Phys. Rev. 111 2 390 1958

67 Llewellyn Jones F. Dutton J. and Morgan C.G. Nature 198 680 1963

68 Lozier W.W. Phys. Rev. 45 840 1934

69 Hagstrum H.D. and Tate J.T. Phys. Rev. 55 1136 1939

70 Alpert D. J. App. Phys. 24 860 1953

Alpert D. and Buritz J. App. Phys. 25 202 1954

71 Schwarz H. Z. Phys. 122 437 1944

72 Whetten and Young Rev. Sci. Inst. 30 472 1959

73 Whetton and Young Rev. Sci. Instr. 30 472 1959

74 Fletcher J. Ph.D. Thesis (Univ. of Keele) 1963

75 Moruzzi Bri . J. App. Phys. 14 929 1963

76 Sukhum N. Brit. J. App. Phys. 15 509 1964

77 Govinda Raju G.R. Brit. J. App. Phys. 16 279 1965

78 Kaiser Kunz Numerical Analysis (McGraw Hill) 86 1957

79 Morgan C.G. Handbook of Vacuum Physics Pt. 1 Pergamon Press Ltd. Ed. by A.H. Beck

80 Myatt J. Unpublished results at Keele.

81 Holland L. Vacuum Deposition of Thin Films p.99 (Chapman and Hall Ltd) 1956

82 Frommhold L. Proc. of the III rd International Conf. on Phys. of Elec. and At. Coll. 556 1964

83 Branscomb L.M. Burch D.S. Smith S.J. and Geltman S. Phys. Rev. 111 504 1958

84 Fisher L.H. App. Sci. Res. B(The Hague) 5 281 1955

85 von Engel A. Ionized Gases 157 (Oxford University Press, London) 1955